ABSTRACT

Title of Dissertation:	MOVEMENT ECOLOGY OF THE MEXICAN FISH-EATING BAT, MYOTIS VIVESI
	Edward Risto Hurme, Doctor of Philosophy, 2020
Dissertation directed by:	Professor Gerald Wilkinson, Department of Biology

Foraging behavior is influenced by the distribution of prey in time and space and the presence of conspecifics. Echolocating bats, which advertise their behavior while vocalizing, provide a unique opportunity for understanding how an organism interacts with conspecifics and the environment to find food. Here I use GPS tracking combined with on-board recording to investigate the foraging movements of lactating Mexican fish-eating bats, *Myotis vivesi*, in the Gulf of California, Mexico, over a 5-year period. In Chapter 1, I assessed five alternative methods for behavioral state segmentation of GPS tracked foraging paths using on-board audio for validation. While most methods perform well, hidden-Markov model segmentation showed the highest accuracy at predicting foraging movement. In Chapter 2, I evaluated habitat selection across multiple scales for fish-eating bats foraging in the Midriff Islands Region in the Gulf of California. Foraging site use at large scales is most predictive and is associated with dynamic (chlorophyll concentration) and static variables (ocean

depth, sea floor slope) consistent with known tidal upwelling regions. In Chapter 3, I examine the function of in-flight social calls recorded from roughly half of all tagged individuals during their foraging flights. Calls contained spectral differences among individuals, were associated with the ends of flights as bats return to their roost, and increased in occurrence with pup age, consistent with directive calls used to communicate with mobile pups. In Chapter 4, I explore how prey distribution impacts social behavior and foraging movements. On-board audio reveals that conspecifics are present during commuting and foraging and playback experiments demonstrate an attraction to foraging call sequences. In collaboration with several colleagues I combined these findings with data from four other bat species ranging in diet and habitat type. Taken together, bat species that frequently encounter conspecifics, such as *Myotis vivesi*, have ephemeral prey and variable flights (e.g. duration and foraging site location), whereas bats that forage solitarily have predictable or non-shareable prey, such as a congener *Myotis myotis*, show less variability in their flights. Overall, these results provide new insights into the foraging dynamics and social behavior of bats.

MOVEMENT ECOLOGY OF THE MEXICAN FISH-EATING BAT, *MYOTIS VIVESI*

by

Edward Risto Hurme

Dissertation submitted to the Faculty of the Graduate School of the
University of Maryland, College Park, in partial fulfillment
of the requirements for the degree of
Doctor of Philosophy
2020

Advisory Committee:
Professor Gerald S. Wilkinson, Chair
Professor Bill Fagan
Associate Research Professor Helen Bailey
Associate Professor Yossi Yovel
Associate Professor Daniel Gruner

Preface

Chapter 1 was published in 2019 as “Acoustic evaluation of behavioral states predicted from GPS tracking: a case study of a marine fishing bat” in Movement Ecology (vol 7:21, p. 1-14). Chapters 2 and 3 are in manuscript form for future publication. Chapter 4 was previously published in 2018 as “Resource ephemerality drives social foraging in bats” in Current Biology (vol 28, p. 3667-3673.e5). K.E.-B. conceived and designed the research, carried out the data analysis, was responsible for the modeling, collected the field data, and wrote the manuscript. E.R.H. and S.G. conceived and designed the research, collected the field data, carried out the playback experiments, and wrote the manuscript. L.H. conceived and designed the research and carried out the data analysis. A.G., L.G.H.M., J.J.F.-M., A.T.V., R.A.M., D.S.J., O.E., I.B., J.R.S., G.S.W., and H.R.G. contributed to field data collection and helped write the manuscript. Y.Y. conceived and designed the research, contributed to field data collection, and wrote the manuscript. Appendix 1 is published as an online supplement to the paper published as Chapter 1. Appendix 2 and 3 are written as potential online supplements for the manuscripts corresponding to Chapters 2 and 3. Appendix 4 is published as an online supplement to the paper published as Chapter 4.

Dedication

To my sister, Kristiina Hurme, who showed me the adventure of being a scientist.

Acknowledgements

I am grateful for all the help and support I have received during my PhD. I would like to thank the members of the Wilkinson lab, starting with Dr. Jerry Wilkinson, for his guidance, critical perspective, and swift edits on my many drafts. Dr. Danielle Adams has been a friend and resource in the lab. I would also like to thank Dr. Gerry Carter, for his endless wit, Dr. Kim Paczolt, for always being a voice of reason, and the other past and present members of the Wilkinson Lab for their valuable feedback on my research.

I would also like the thank the Yovel lab. Dr. Yossi Yovel gave me an incredible opportunity to collaborate with his lab and has been a mentor from afar. Dr. Stefan Greif was instrumental with fieldwork and has always provided gracious help. Aya Goldstein, Lee Harten, and the many other members of the Yovel lab have provided valuable advice over the years.

Understanding the analysis in this dissertation would not have been possible without help from the Fagan Lab. I would like to thank Dr. Bill Fagan, the ultimate academic match maker, for bringing together a wonderful group of people and creating a collaborative environment. Dr. Eliezer Gurarie has helped immensely with understanding animal movement and increasing levity on campus.

Collection of field data would not have been possible without the help of many courageous individuals. Drs. L. Gerardo Herrera M. and José Juan Flores-Martínez, who have guided us through fieldwork on Isla Partida Norte and helped with many logistical and permitting challenges along the way. Dr. Dave Johnston, Ricardo Rodriguez, Andrea Valdez, Tenazas, Vaporub, and many others who helped

with field work under often challenging conditions. Furthermore, analysis of data was possible thanks to the help from several undergraduate students (Jash Shah, Justin Shapiro, Giovanni Tundo, Jesse Vo, Kaylee Helmbacher, Katie Geary, Saskia van Terheyden, Thomas Kinton, Josh Pertman, Haley Honegger, Samara Nehemiah, Elizabeth Touey, Holly Liposky) and one high school student (Nancy Barrett).

I would also like to thank my present and past committee members, Drs. Cynthia Moss, Helen Bailey, Daniel Gruner, and Bill Fagan, for their feedback, advice, and support along the way.

Finally, I would like to thank my friends and family for their support and interest in hearing the latest "bat facts." To my family, June, Risto, Tommi, and Kristiina Hurme, and my wife Nina Hwang, for all their love and support.

This work was supported financially by grants provided by the Department of Education GAANN fellowship, the Devra Kleiman Scholarship, National Geographic, Animal Behavior Society, the American Society of Mammalogists, the Explorers Club, and the Cosmos Club.

Table of Contents

List of Tables

List of Figures

Introduction

How do animals explore their environment and successfully locate prey? Natural selection predicts that animals are adapted to their environment and, especially in resource limited environments, should use energy efficient strategies to find resources. When resources are patchy and unpredictable, copying successful foragers or searching with conspecifics may increase foraging success. Social foraging theory suggests that an animal's use of social cues while foraging is dependent on environmental predictability, fitness benefits, and social organization (Galef and Laland 2005). Our current understanding of foraging behavior and social interactions, however, has been limited due to the difficulty of monitoring an animal's movement, interaction with conspecifics, and foraging success in the wild.

Recent advancements in biologger technology and remote sensing now allow for sophisticated monitoring of wild animals and their environment (Nathan et al. 2008, Dodge et al. 2013, Kays et al. 2015). Analysis of these data can provide a new understanding of environmental effects on movement, such as resource distribution (Dodge et al. 2013), or abiotic factors, such as temperature and wind (Sapir et al. 2014, Deppe et al. 2015). Additionally, biologgers can also provide context to movement by recording social interactions with conspecifics and heterospecifics through images (Moll et al. 2007, Rutz et al. 2007, Rutz and Hays 2009, Rutz and Troscianko 2013) and audio (Burgess 2000, Johnson and Tyack 2003, Akamatsu et al. 2005, Lynch et al. 2013, Stowell et al. 2017), in addition to GPS (Cvikel et al. 2015a, 2015b, Hooker et al. 2015, Strandburg-Peshkin et al. 2015, Greif and Yovel 2019).

There are over 1400 bat species (Tsang et al. 2015, Simmons pers. comm.) encompassing a broad range of habitats, diets, and foraging behaviors. Yet, despite being one of the most speciose mammalian orders, bat movement is poorly understood in the majority of species

(O'Mara et al. 2014). Echolocating bats constantly emit loud sound signals to navigate and capture prey. This allows nearby conspecifics to receive information on their foraging activities and success. Many bats seem to benefit from eavesdropping on conspecifics while foraging (Dechmann et al. 2009), and some species even appear to travel significant distances in pairs or groups (Howell 1979, Wilkinson 1992b, Wilkinson and Boughman 1998). However, these studies failed to quantify the resource distribution, foraging success, or foraging path of the bats. A recent study by my collaborators and I used novel GPS and ultrasonic audio biologger technology to show that bats are an ideal candidate for studying foraging behavior and social interactions (Cvikel et al. 2015a). By analyzing on-board audio recordings, we detected the presence of conspecifics and foraging attempts during flights. We estimated the density of conspecifics from the conspecific calls and flight speed, and then compared these values to simple models of social encounter rates to show that the bats encountered conspecifics more than you would expect by random chance. We found that foraging success is increased by conspecific presence, consistent with bats benefitting from public information provided by echolocation calls. Yet, the bats avoid each other when attacking prey, presumably because of constraints from collision avoidance rather than echolocation interference, also known as acoustic jamming (Cvikel et al. 2015a, 2015b). To develop a greater understanding of social foraging behavior, further work is needed to understand how different species interact with their environments and conspecifics.

This dissertation focuses on the foraging behavior of the Mexican fish-eating bat, *Myotis vivesi* (hereafter fish-eating bats). Fishing bats trawl for prey, dragging their hind limbs through the water to catch prey (Fish et al. 1991, Blood and Clark 1998). This species is unique among fishing bats in that it predominantly preys on marine fish and crustaceans (Otálora-Ardila et al.

2013). Foraging over the open ocean provides many challenges for a bat, the most basic of which is detecting foraging areas at night. While fish-eating bats are an unusual system, they offer many similarities with other echolocating bats, as well as central place foraging marine predators. In this dissertation, I investigate the movement, habitat use, vocalizations, and sociality of fish-eating bats.

As little is known about the foraging behavior of this species, my first goal was to determine how to identify foraging behavior from the GPS recordings of a flying bat. A multitude of methods exist for segmenting animal movement data into behavioral states, yet these methods are rarely validated in species that are difficult to observe. Without observations of foraging movements, it is difficult to predetermine how fish-eating bats should move during prey capture. However, most echolocating bats use a stereotyped sequence of calls immediately before prey capture known as a feeding buzz, which can be used to confirm behavioral segmentation predictions. In the first chapter, I apply five commonly used segmentation methods and use the presence of feeding buzzes as a validation set to evaluate performance.

After finding a metric for determining foraging behavior, I explored how bats select marine habitats when foraging. All animals are under selection to find adequate resources through foraging to maintain a positive energy balance. Nursing females are often under additional stress, as they must provide for themselves and their offspring. Therefore, females should attempt to forage as efficiently as possible each night. This could be achieved by foraging in areas with abundant resources. However, habitat preference can only be indirectly measured through space use data. The spatial movement of an animal should be a partial reflection of the spatial distribution of resources required by that animal (Matthiopoulos 2003). The environment shapes the distribution of resources and in a marine environment, prey may respond to the static

environment, e.g. the ocean floor, which may create consistent conditions or track dynamic covariates, such as chlorophyll abundance and sea surface temperature (Cox et al. 2018). In the second chapter, I investigate how bats respond to the environment at different scales using resource selection functions.

Acoustic recordings also provide insight into the variety of calls bats produce while flying. In analyzing recordings, a stereotyped social call was discovered in on-board audio recordings. In chapter three I explore hypotheses for the function of this call by analyzing the context and individual identity of the social calls produced. Given that all tagged bats were lactating females, I excluded the possibility that these were related to mating and explored if calls function for group formation, mother pup communication, or resource defense.

In the fourth chapter, I investigate social foraging. While social foraging increases resource competition and can create producer scrounger dynamics (Caraco and Giraldea 1991), individuals can benefit from increased detection of resources (Galef and Giraldeau 2001). If the resource is difficult to detect and not limited by competition, social foraging can be highly adaptive (Hancock & Milner-Gulland 2006). Echolocating bats broadcast their behavior through their stereotyped calls, allowing nearby individuals to eavesdrop. Given this opportunity for sociality in most echolocating bats, why do we not see social foraging in every bat species? Social foraging in bats is hypothesized to be dependent on prey distribution (Wilkinson and Boughman 1998, Dechmann et al. 2009). I analyzed on-board audio recordings for conspecific presence during foraging flights and performed playback experiments to evaluate attraction to search and foraging echolocation calls. I combined this data set with data from four other echolocating bat species with different diets and prey distributions to evaluate how resource distribution and predictability is related to social foraging behavior in bats.

My research provides important insight into the movement and social behavior of fish-eating bats. Fish-eating bats are a difficult species to study given their remote roosting locations in dynamic seas. However, their size, ease of recapture, and open foraging habitat made them an ideal species for GPS tracking. This research contributes to our understanding of bat foraging behavior as well as provides opportunities to compare how animals adapt to the marine environment.

Chapter 1: Acoustic evaluation of behavioral states predicted from GPS tracking: a case study of a marine fishing bat

Abstract

Background

Multiple methods have been developed to infer behavioral states from animal movement data, but rarely has their accuracy been assessed from independent evidence, especially for location data sampled with high temporal resolution. Here we evaluate the performance of behavioral segmentation methods using acoustic recordings that monitor prey capture attempts.

Methods

We recorded GPS locations and ultrasonic audio during the foraging trips of 11 Mexican fish-eating bats, *Myotis vivesi*, using miniature bio-loggers. We then applied five different segmentation algorithms (k-means clustering, expectation-maximization and binary clustering, first-passage time, hidden Markov models, and correlated velocity change point analysis) to infer two behavioral states, foraging and commuting, from the GPS data. To evaluate the inference, we independently identified characteristic patterns of biosonar calls ("feeding buzzes") that occur during foraging in the audio recordings. We then compared segmentation methods on how well they correctly identified the two behaviors and if their estimates of foraging movement parameters matched those for locations with buzzes.

Results

While the five methods differed in the median percentage of buzzes occurring during predicted foraging events, or true positive rate (44–75%), a two-state hidden Markov model had

the highest median balanced accuracy (67%). Hidden Markov models and first-passage time predicted foraging flight speeds and turn angles similar to those measured at locations with feeding buzzes and did not differ in the number or duration of predicted foraging events.

Conclusion

The hidden Markov model method performed best at identifying fish-eating bat foraging segments; however, first-passage time was not significantly different and gave similar parameter estimates. This is the first attempt to evaluate segmentation methodologies in echolocating bats and provides an evaluation framework that can be used on other species.

Background

Animal movement data are becoming increasingly abundant for marine and terrestrial vertebrate species at ever finer spatial and temporal resolutions, allowing researchers to address a variety of ecological questions from the point of view of the individual (Hussey et al. 2015, Kays et al. 2015, Börger 2016). However, inferring what an animal is doing from complex movements can be challenging given that different behaviors may exhibit similar movement features. For example, multiple GPS locations concentrated in a small area might indicate short tortuous movements, occurring when an animal searches for prey, or simply a resting animal with poor signal quality causing random fluctuations (De Weerd et al. 2015). Distinguishing between these alternatives is sometimes possible based on an analysis of multiple movement features. For example, an animal foraging on a productive patch often moves more slowly while turning frequently. Such area-restricted search (ARS) behavior has been predicted from optimal foraging theory and observed in several animals that exploit patchy resources (Howard 2014, Weimerskirch et al. 2017).

This example illustrates the basic approach underlying path segmentation methods, which detect patterns in movement to provide insight into underlying behavioral states and partition tracks into segments of distinct behavioral states (Edelhoff et al. 2016, Gurarie et al. 2016). These methods typically fall into three categories: pattern description, process identification, or change point detection (Edelhoff et al. 2016). *Pattern description* methods involve estimation of primary movement parameters, such as speed and turn angle, or secondary parameters derived from windows of many steps (Edelhoff et al. 2016). Parsing locations into distinct behaviors can be accomplished through simple thresholding schemes that manually separate short- and long-range movements or through unsupervised clustering, such as k-means clustering (kmC) (Van Moorter et al. 2010, Bennison et al. 2018). First-passage time (FPT), a commonly used secondary parameter, calculates the time to enter and leave a virtual circle for every location on an animal track, and is often used for revealing locations of intensive search (Fauchald and Tveraa 2003). Alternatively, *process identification* methods infer behaviors that shape the movement data (Morales et al. 2004, Patterson et al. 2008). These methods model the change in speed and turn angle through time and space to annotate the animal's movement with behavioral states. For example, Hidden Markov models (HMM) estimate a sequence of predefined states as well as the switching probabilities between states (Morales et al. 2004, Patterson et al. 2008). Expectation-maximization and binary clustering (EMbC) is a simple alternative state-space model that sequentially groups locations into clusters of high and low velocity and turn angle (Garriga et al. 2016). Finally, *change point detection* methods use a moving window to examine portions of the path to determine where local means differ from global averages of movement parameters under the assumption that these locations indicate switches in behavioral states (Gurarie et al. 2009, 2016, Edelhoff et al. 2016). Correlated velocity movement (CVM) models

use continuous time to allow for irregularly sampled data and can be combined with change point detection (CVCP) (Gurarie et al. 2017).

Despite growing interest in making inferences about behavioral states from movement patterns (Nathan et al. 2008), methods are rarely validated in wild animals that are difficult to directly observe (Webb et al. 2008, Bennison et al. 2018). Exceptions include records of foraging events captured by sensors on-board large animals, such as cameras on gannets (Tremblay et al. 2014, Goldbogen et al. 2017), time-depth recorders on elephant seals (Robinson et al. 2012), stomach temperature loggers in tuna (Bestley et al. 2008), or accelerometers on monk seals (Wilson et al. 2017), all of which provide independent validation of behavioral states.

Recent miniaturization of biologgers allows integration of ultrasonic microphones with GPS tracking to record movement and vocalizations of bats (Cvikel et al. 2015a, 2015b, Egert-Berg et al. 2018, Greif and Yovel 2019, Stidsholt et al. 2019). Many bat species use echoes from ultrasonic vocalizations to detect obstacles and prey while foraging (Griffin et al. 1960, Yovel and Greif 2018). These biosonar calls dynamically change in inter-pulse interval (IPI), frequency, and duration depending on the environment and behavioral context (Obrist 1995, Moss and Surlykke 2010, Denzinger and Schnitzler 2013). Echolocating bats that capture prey while flying emit a feeding buzz - a characteristic sequence of calls that decrease in IPI, frequency, and duration - when approaching and attempting to capture a prey item (Griffin et al. 1960, Ratcliffe et al. 2013). Feeding buzzes provide a reliable cue that indicates foraging behavior.

We used acoustic and GPS biologgers to investigate the foraging behavior of the Mexican fish-eating bat (*Myotis vivesi*, Menegaux, 1901; henceforth “fish-eating bat”), which is

endemic to the islands and coasts of the Gulf of California, Mexico (Blood and Clark 1998). *M. vivesi* eat predominantly small marine crustaceans and larval fish captured from the surface of the ocean (L.G. Herrera M., and E. Claire, personal communication; Fig. 1.1) (Otálora-Ardila et al. 2013). Piscivorous bats independently evolved in two bat genera, *Noctilio* and *Myotis* (Aizpurua and Alberdi 2018). Piscivorous bats in the genus *Myotis*, like our study species, use biosonar to detect prey that break the water surface and use feeding buzzes when capturing prey with targeted dips of their hindfeet (Schnitzler et al. 1994, Aizpurua et al. 2014, 2015, Aizpurua and Alberdi 2018) (Fig. 1.1). GPS tracking revealed that these bats often travel over 20 km to forage each night as they search for unpredictable patches of prey (Egert-Berg et al. 2018). These foraging trips often contain over a dozen short foraging bouts (9 min average) (Egert-Berg et al. 2018).

In this study, we apply and compare five segmentation methods (Table 1.1) that include pattern description (k-means clustering and first-passage time), process identification (hidden Markov models and expectation-maximization and binary clustering), and change-point detection with behavioral partitioning (correlated velocity change point analysis) to predict foraging behavior in fish-eating bat foraging trips. We use feeding buzzes in audio recordings on-board free-flying bats to confirm foraging, and then evaluate the performance of each of the methods mentioned above using true positive rate (buzzes in predicted foraging locations), true negative rate (absence of buzzes in predicted commute locations), and balanced accuracy (the average of true positive and true negative rates). To distinguish methods with similar balanced accuracy, we also compare speed and turn angles predicted for foraging by each method against speed and turn angles at locations containing feeding buzzes.

While it remains unclear how fish-eating bats decide where to initiate hunting, a high density of fish at the water surface can trigger trawling in other fishing bats (Schnitzler et al. 1994). Direct observations and preliminary movement analyses suggest that *M. vivesi*, like many other marine predators searching for unpredictable patches of prey (Weimerskirch 2007, Paiva et al. 2010), use ARS when foraging and fast straight movement when commuting (Egert-Berg et al. 2018). Therefore, we expected more feeding buzzes in areas of the trip indicative of ARS than when the animal was traveling between patches or returning to the roost. Our goals were to determine the best performing methods for this data set and provide a framework for researchers to use with independent behavioral data to evaluate segmentation methods.

Methods

Data collection

We conducted the study on Isla Partida Norte (28° 53′ 16″ N, 113 ° 02′ 30″ W), a 1.4-km2 island located in the midriff region of the Gulf of California, Mexico (Castil et al. 1980). The island holds the largest known colony of *M. vivesi* (~ 8000 individuals) (Flores-Martínez et al. 2004). Our study was conducted between May 27 and June 19, 2015, at which time females are nursing pups (permits #7668–15 and 2492–17 from Dirección General de Vida Silvestre, and permits #17–16 and 21–17 from Secretaría de Gobernación, and the University of Maryland Institutional Animal Care and Use Committee protocol FR-15-10).

Bats were captured by hand in the morning from under rocks on talus slopes along the south-east region of the island. Lactating females weighing 32.5 ± 2.8 g (mean ± SD) were selected for tagging to facilitate recapture when the bats returned to feed their pups during the day. We glued biologger tags (Robin GPS Loggers, CellGuide Ltd., Israel) with 8 GB of memory

and VHF radiotransmitters (Holohil BD-2X) weighing on average 4.6 ± 0.1 g (mean ± SD) to the back of each bat using non-toxic glue (Perma-Type Surgical Cement, Plainville, Connecticut) (Cvikel et al. 2015b). We released bats at their capture locations during midday. After 1 or 2 days, we used the transmitters to locate and recapture tagged bats. Because our tags exceed conventional recommended weight allowances for tags (see O'Mara et al. (2014) for review), we conducted a series of trials to determine the effect of the tags on the bats (see also Egert-Berg et al. (2018)). First, we confirmed that bats with a tag could fly and forage normally in a flight tent with a pool (Egert-Berg et al. 2018). We then compared trips for bats with GPS tags against bats carrying 0.5 g telemetry tags and found no difference in duration of trips (telemetry: 4.3 ± 2.1 h, GPS: 3.8 ± 1.8 h; $p = 0.4$, permutation t-test N = 20 GPS, N = 15 telemetry) and no difference in weight loss between telemetry and GPS-tagged bats after controlling for number of days tagged (ANCOVA: $F_{1,63} = 1.55$, $p = 0.22$, N = 47 GPS, N = 20 telemetry). We also found no difference in condition (weight to forearm ratio) of pups whose mothers were GPS or telemetry-tagged (ANCOVA: $F_{1,5} = 2.31$, $p = 0.20$, N = 5 GPS, N = 3 telemetry). Finally, we confirmed that conspecific vocalizations were present throughout GPS-tagged bat trips (Egert-Berg et al. 2018), indicating that bats with GPS tags traveled to the same foraging areas as bats without GPS tags.

During the night, tags recorded GPS locations every 15 s and 0.5 s of audio every 5 s (10% duty cycle at 184 kHz sampling rate). While searching for prey, on-board audio reveals that bats typically emit calls with a duration of 6 ms and with intervals of 200 ms between calls, consistent with prior call measurements (Suthers 2006). When approaching prey, the echolocation calls and intervals become progressively shorter and terminate in a feeding buzz. A feeding buzz lasts 0.2–0.25 s (Fig. 1.2); thus, a 0.5 s recording is sufficient to distinguish search phase calls from a buzz. Foraging bouts typically last 6 min (see Results) with dozens of attacks

performed during each bout. Therefore, a 10% duty cycle with a recording every 5 s almost always captures attacks in a foraging bout. To validate this assertion, in 2017 we tagged three bats with new tags (Vesper, ASC. Inc.; Table S1.2), which allow continuous audio recordings (one 50% and two 100% duty cycle) for an entire night. We then sub-sampled those recordings to mimic the 10% duty cycle data to determine how often a 10% sampling rate resulted in missing foraging bouts (we performed all possible shifts of 0.5 s out of 5 s). The analysis showed that a 10% sample rate detected 77 ± 16% of foraging bouts (mean ± SD, Fig. S1.2).

Analysis of on-board audio

On-board audio was analyzed using custom Matlab software called "Batalef," (Cvikel et al. 2015a). Calls were identified with a peak detection algorithm and manually checked. Call start and end points were determined using a 5 dB drop from the peak amplitude. Inter-pulse interval (IPI) was measured as the time between the end of one call and the start of the next. We identified buzzes by searching for calls below an IPI threshold (Geberl et al. 2015) of 10 ms that occurred in groups of at least three consecutive calls (Fig. 1.2). This was detected automatically and then validated by manual inspection. We included sequences with a terminal buzz as well as instances of aborted buzzes as both suggest that the bat was engaged in foraging behavior and attempting to capture prey (Ratcliffe et al. 2013). Because the biologger sampling schedule creates three audio recordings (before, during or after) for each GPS location, we aggregated buzzes detected in the audio files closest to a GPS fix to determine the location and movement characteristics for each buzz (Fig. 1.1b).

Analysis of location data

GPS and audio tags were deployed on eleven bats over a 10-day period resulting in fifteen trips (Table S1.1). All locations were transformed to Cartesian coordinates using a Universal Transverse Mercator (UTM) 12 N projection. GPS accuracy is ca. 8 m in the X-Y plane and ca. 11 m in the Z axis (Cvikel et al. 2015a). We excluded all GPS locations within 250 m of the island and subsequent tracks with fewer than 100 locations to remove readings while bats were in the roost or making short movements around the island. Speed, distance, and absolute value of turn angle (hereafter "turn angle") between subsequent steps were then calculated for each pair of successive locations along the path of each bat trip. Paths were segmented into either foraging or commuting states using five segmentation methods (Edelhoff et al. 2016). Below we describe how we estimated parameters associated with each of the five methods.

K-means clustering

K-means clustering (kmC) takes a set of n data points to be clustered into k clusters and finds a partition that minimizes the squared error between the mean of a cluster and the points in that cluster (Jain 2010). We applied kmC to speed and turn angles using the "kmeans" function in the R package "stats" (Hartigan and Wong 2006). To determine the optimal number of clusters, we investigated the percentage of variance explained by kmC over a range of cluster sizes to find an "elbow," or the location at which adding more clusters only marginally increased variance explained (Ketchen Jr. and Shook 2002). The elbow method showed that two clusters was the optimal number of partitions. We labeled the cluster with the lowest speed and highest turn angle as foraging (Bennison et al. 2018). After overlaying behavioral states on the parameter values, clustering produced a linear threshold at a turn angle of 75° (Fig. S1.3).

First-passage time

First-passage time (FPT) is the time it takes for an individual to enter and leave a virtual circle of fixed radius drawn around each location (Johnson et al. 1992). High FPT values are generally associated with slower and more tortuous movements, such as area-restricted searching, while low FPT values are generally associated with faster and more straight-line movements such as commuting. We used the R package "adeHabitatLT" to calculate FPT for all tracks (Fauchald and Tveraa 2003, Calenge 2006). To determine a common scale to compare FPT values between individuals, we calculated FPT for all trips over radii ranging from 100 to 5000 m in 25-m increments (Fauchald and Tveraa 2006). For each path, we calculated the variance of log-transformed first-passage time values (transformed to make variance independent of the mean) for each radius (Fig. S1.4A). The resulting peak in variances indicates the scale at which the organism is concentrating its activities; however, this scale may vary by individual. We found a common scale for analysis by selecting the radius with highest mean variance when averaged across all paths (Fauchald and Tveraa 2006).

The mean variance of log FPT peaked at a radius of 250 m (Fig. S1.4A). This value was selected as the FPT radius for all tracks. A total of 99 locations could not have FPT values calculated because they occurred too close to the beginning or end of a given trip. To determine a threshold FPT value for separating foraging from commuting, we fit a bimodal Gaussian mixture distribution with the function "normalmixEM" from the R package "mixtools" to the distribution of ln(FPT). We used the 95% upper confidence interval between bimodal peaks of ln(FPT), which occurred at 142 s (Fig. S1.4B), to set the threshold between foraging and commuting FPT values.

Hidden Markov model

A hidden Markov model (HMM) assumes an animal has more than one hidden behavioral state with characteristic speed and turn angles that can be modeled using stochastic processes (Morales et al. 2004). We used the R package "momentuHMM" to fit HMMs to all tracks (McClintock and Michelot 2018). We used linear interpolation at 15 s increments to fill in missing GPS values caused by signal loss or device malfunction to address the HMM assumption of constant sampling rate. We used a two-state model to define behavioral states.

Initial step length, or distance between sampling locations, parameters for the two-state HMM were estimated from a mixed normal distribution of the step length of all individuals using the function "normalmixEM" (state 1: mean 70.2 m, SD 27.6 m; state 2: mean 160.8 m, SD 23.0 m). The HMM estimated gamma distributions for step length parameters (state 1: mean 46.7 m, SD 26.9 m; state 2: mean 83.6 m, SD 21.1 m) and von Mises distributions for turn angles (state 1: mean 0, concentration 0.23; state 2: mean 0, concentration 11.01). State 1 has a shorter step length and uniform turn angle distribution, while state 2 has longer step lengths and a turn angle concentrated around 0. Previously, these states have been termed area restricted search and exploratory movements, respectively (Morales et al. 2004, Fryxell et al. 2008), and were assigned as foraging and commuting behaviors in this study. Transition probabilities from foraging to commuting and commuting to foraging were 3.9 and 7.2% respectively (Table S1.3). A Jarque-Bera test of normality for step length ($X2 = 301.59$, $df = 2$, $p < 0.001$) and turn angle ($X2 = 5.38$, $df = 2$, $p = 0.07$) indicated that the distribution for step length deviated from normality (Fig. S1.5, Table S1.4). We also fit a three-state HMM, which had a slightly higher median but lower mean balanced accuracy (Fig. S1.6, Table S1.5). To investigate the impact of sampling rate, we performed the same HMM analysis on subsampled data from 15 s to 10 min

intervals by 15 s increments and found that median HMM performance gradually decreased with subsampling (linear regression: slope = -5.2 × 10-5, $F(1,38) = 16.34$, $R2 = 0.3$, $p = 0.0002$; Fig. S1.7).

Expectation-maximization and binary clustering

Expectation-maximization and binary clustering (EMbC) is an unsupervised clustering algorithm that uses maximum likelihood estimation of a Gaussian mixture model (Garriga et al. 2016). EMbC is a parameter-free method that groups velocity and turn angle into low and high values, creating four clusters of intuitive biological interpretation: low velocity and low turn angle (LL - resting), low velocity and high turn angle (LH – intensive search or ARS), high velocity and low turn angle (HL – commute), and high velocity and high turn angle (HH – extensive search or possibly predator avoidance) (Garriga et al. 2016). We used the R package "EMbC" to annotate all tracks into these clusters (Fig. S8). We aggregated two search clusters, LH and HH, into foraging locations and grouped the two remaining clusters (LL and HL) into commute locations. We chose these groupings of the data because the HH category does not reach very high speeds, suggesting it is still ARS movement, and this particular grouping gave the highest performance (Fig. S1.9, Table S1.6).

Change point analysis of correlated velocity movements

Correlated velocity movement (CVM) refers to a family of continuous-time movement models where velocities follow Ornstein-Uhlenbeck processes. We used the R package "smoove" (github.com/EliGurarie/smoove) to estimate CVM and conduct likelihood-based change point analyses (Gurarie et al. 2009, 2017). We used the random movement or unbiased CVM (UCVM) model to partition each trip into behaviorally consistent segments and estimate

speed and autocorrelation for each segment. To estimate speed, autocorrelation, and potential change points, we used a 2 min window (8 location points), as increased window length would be less sensitive to detecting short foraging bouts and did not improve performance (Fig. S10). After each estimate, the window was shifted down the track 1.25 min (5 location points) and the first step was repeated. For one trip (Viv19 on 2015-06-02 UTC-7) a 2 min window length would not converge, and a window length of 2.5 min was used. The resulting peaks in log likelihood values were then used as candidate change points. Change points could not be less than 30 s apart, limiting the minimum duration of each segment. Change points were further thinned by recursively fitting CVM models to each segment with and without a final change point and then selecting the model with the lowest Bayesian Information Criterion (BIC) score.

Correlated velocity change point (CVCP) analysis determines behavioral states by refitting each segment to an advective CVM (ACVM) and choosing the model with the lower BIC score. UCVM uses a Gaussian distribution for position and velocity, with the long-term mean position equal to the initial position, whereas ACVM has a mean non-zero advective velocity. We labeled UCVM segments as foraging because they resembled ARS movement, and we labeled ACVM segments as commuting because they tend to be straight and fast. For each CVCP segment, we record the model fit as either unbiased or advective CVM, corresponding to foraging or commuting for all locations within that segment and parameter estimates of root mean squared speed and tau, a measure of time over which data are autocorrelated (Table S1.7).

Evaluation of segmentation methods

We assessed performance of each movement segmentation method using presence and absence of buzzes which were detected in the on-board audio recordings and assigned to the nearest GPS location. We expected that a good segmentation method would accurately predict

the presence of buzzes during predicted foraging and absence of buzzes during predicted commuting. We scored buzz occurrences during foraging segments as true positives and absence of buzzes in commute segments as true negatives. True positive rate (TPR), or sensitivity, is the rate of choosing the correct value when the underlying condition is true. Here, TPR is the number of matches between buzzes and predicted foraging over the total number of buzzes. True negative rate (TNR), or specificity, measures the proportion of negatives that are correctly labeled.

Since buzzes are relatively rare in our recordings, we did not use accuracy, which assumes a balanced dataset of true positives and true negatives. For example, if a method determines that all locations are "foraging" or all locations are "commuting", this would yield a 100% TPR or 100% TNR, respectively. Therefore, we used the average of TPR and TNR, referred to as "balanced accuracy", which punishes methods for selecting too many events from the same class (i.e. foraging or commuting). A balanced accuracy of 50% corresponds with a random guess, while a perfect true positive and true negative rate would yield a balanced accuracy of 100%. Furthermore, balanced accuracy is more appropriate for unbalanced data because it weights TPR and TNR equally even if the number of observations in each is different (Brodersen et al. 2010).

After computing the balanced accuracy for each method per individual, we then tested whether there were significant differences in TPR, TNR and balanced accuracy between the methods using a Friedman's test (Friedman 2006). If there were statistically significant differences between methods, we then performed Wilcoxon paired-sample tests with Bonferroni correction to determine which models differ from the model with highest balanced accuracy.

We then compared the mean speed and turn angle associated with buzzes on each bat trip to mean speed and turn angle identified for foraging by each of the five segmentation methods, as explained below, using Wilcoxon paired-sample tests with a Bonferroni correction. Finally, we compared segmentation parameters (percentage of track foraging, mean foraging segment duration, and mean number of foraging segments) between the top performing method and all other methods, to determine if methods were segmenting trips similarly to the top performing method.

All analyses were conducted using R version 3.4.3 (R Core Team 2017).

Results

Trip summary

Trip duration and number of buzzes recorded varied among individuals. After removing locations within 100 m of each bat's initial position on the island, there were 12,038 GPS locations, and 688 buzzes. The duration of trips was 3.4 ± 1.8 h (mean ± SD, range 0.9–6.4, N = 15), with total distance per trip of 42.6 ± 25.8 km (range 6.79–89.80 km, N = 15), and number of feeding buzz events per trip of 45.9 ± 32.8 (range 5–138, N = 15) (Fig. S1.1, Table S1.1). Given the 10% audio duty cycle, the actual number of feeding buzzes emitted is about ten-times greater (as we confirmed by tagging bats with 50–100% duty-cycle tags, Fig. S1.2). The distribution of times between buzzes has a long right-tail towards higher time intervals, which has an exponentially decreasing shape, indicating that most buzzes occur in clusters, i.e., in foraging bouts (Fig. S1.11).

Model performance

The performance of behavioral classification methods was assessed for each bat flight using the true positive and true negative rates (Table S1.8). Some methods over-predicted commuting behavior (e.g. EMbC and kmC), suggesting that they failed to detect or fully capture many foraging bouts. While kmC had the highest median TNR, followed by EMbC, HMM had the highest TPR and was moderately higher than FPT and CVCP (Fig. 1.4a). Balanced accuracy showed significant differences among methods (Friedman $\chi 2 = 20.69$, $df = 4$, $p < 0.001$). HMM had the highest median balanced accuracy (67.3%), followed by CVCP (64.1%), EMbC (63.2%), kmC (62.7%), and FPT (61.5%), though post-hoc tests indicated that FPT and CVCP did not significantly differ from HMM (Wilcoxon paired test with Bonferroni correction: FPT vs. HMM $p = 1$; CVCP vs. HMM, $p = 0.15$; Fig. 1.4b). Variation in balanced accuracy within methods could not be explained by distance traveled (ANCOVA: $F_{4,65} = 0.37$, $p = 0.83$) or number of buzzes during a trip (ANCOVA: $F_{4,65} = 0.38$, $p = 0.82$).

Movement parameters associated with buzz locations

All five segmentation methods identified two states: foraging with low speed and high turn angle and commuting (Table 1.2). Foraging speeds and turn angles at locations where buzzes were detected agreed with most segmentation estimates of foraging speed and turn angle; however, speed associated with buzzes (mean ± SD: 3.4 ± 0.5 m/s) differed from foraging speed estimated by kmC (Wilcoxon paired test with Bonferroni correction: $p = 0.004$) and turn angle associated with buzzes (mean ± SD: 72.5 ± 16.7°, $N = 15$) differed from turn angles estimated for foraging by kmC and EMbC ($p < 0.001$ and $p < 0.001$ respectively; Table 1.2).

Predicted foraging events

The segmentation methods also varied in how much foraging each predicted for each trip (Fig. 1.3). Percent of trip foraging, mean foraging segment duration, and number of foraging segments showed significant differences among methods (Friedman's test for percent foraging: $\chi2 = 47.41$, $df = 4$, $p < 0.001$; segment duration: $\chi2 = 53.17$, $df = 4$, $p < 0.001$; number of segments: $\chi2 = 54.03$, $df = 4$, $p < 0.001$). Post-hoc tests indicated that proportion of time spent foraging in a trip predicted by FPT and CVCP did not significantly differ from that predicted by HMM (Wilcoxon paired test with Bonferroni correction: FPT vs. HMM $p = 0.8$; CVCP vs. HMM, $p = 1$; Fig. 1.4b). FPT, HMM, and CVCP identified foraging during about 40% of each trip; whereas, EMbC predicted about 25% and kmC predicted about 20% (Fig. 1.3a). The duration and number of segments, i.e. changes in behavioral state between foraging and commuting, per trip differed substantially between most methods (Fig. 1.3b, c) with the exception of FPT and HMM which predicted very similar foraging segment duration (4–6 min) and number (35–40).

Discussion

We present the first evaluation of segmentation methodology performance in a free flying bat. Individual foraging trips varied considerably in duration and number of buzzes (Table S1.1), providing a complex set of data for each segmentation method. Our goal was to identify the best performing segmentation method for fish-eating bat foraging trips. We found that 1) HMM had the highest median balanced accuracy, 2) HMM, FPT, and CVCP foraging segments predicted speed and turn angles similar to those for buzz locations and 3) HMM segmentation was most similar to FPT in terms of percent of trip foraging, duration of segments, and number of segments in a trip. These results point to HMM as the best segmentation methodology with FPT

as a useful alternative. Overall, balanced accuracy was limited (no greater than 67% overall, and 84% for the best-identified individual trip) because buzzes are rare events during a foraging bout, so segmentation methods will inevitably identify more locations as foraging than will buzzes. Variation in accuracy of segmentation methodology may also be influenced by sampling design, which can be controlled by researchers, or by nuances of animal behavior, which can lead to biological insights.

Predicting foraging behavior

Fish-eating bat trips typically consist of an outward commute from the roost, composed of straight fast flight, followed by several foraging bouts, which can either have short transits or longer commutes connecting them, and finally a commute back to the roost (Egert-Berg et al. 2018). All methods identified commuting phases with higher speeds and lower turn angles than during foraging bouts, consistent with animals searching for unpredictable patchy resources (Hedenstrom and Johansson 2015, Aizpurua and Alberdi 2018, Egert-Berg et al. 2018). While generally robust at identifying long commute or foraging movements, segmentation methods often struggle with how finely they parse short foraging bouts and transits.

Inspection of an example trip provides insight into how each method performs (Fig. 1.5). All methods converged on a large foraging area at the furthest point from the roost and, after lining up foraging segments in time (Fig. 1.5), most methods agree on the beginning and end of some segments. However, coverage and change points for each method vary. All methods show several breaks in the foraging segment, increasing from CVCP, which only has a few foraging segments separated by a few breaks, to HMM and FPT, which have more breaks, to kmC and EMbC, which break the foraging event into over 100 brief events. Methods with high numbers of segments, such as EMbC and kmC, consistently had lower true positive rates, suggesting that

finely parsing foraging results in more missed buzzes. Yet, some of these breaks are real events in which the bat transits between small patches, such as at 2:00 (UTC-7). Other breaks in foraging segments could reflect an ARS that follows a drifting resource patch and therefore has an increased speed and more uniform direction. These identifications would then be considered "false negatives" of foraging detection and are more likely to occur with the unsupervised methods, EMbC and kmC.

Evaluating foraging with buzzes

Buzzes appear to be concentrated in foraging bouts, supporting the hypothesis that prey capture attempts increase during foraging movements (Bennison et al. 2018). However, some buzzes were clearly recorded along a straight outgoing track, which all methods classify as commuting (Fig. 1.5). There was no obvious change in speed or turn angle during these events, and they were consequently missed by all the classification algorithms, increasing the number of false negatives. It is possible that these buzzes occur during brief foraging bouts in which the bat attempted to attack prey on the water surface while commuting. Another possibility is that these brief events occur when fish-eating bats opportunistically encounter aerial prey, a behavior occasionally observed (Otálora-Ardila et al. 2013). The fact that buzzes are not exclusively limited to ARS suggests some plasticity in the foraging behavior of *M. vivesi*.

Balanced accuracy values are also likely reduced because audio was not sampled continuously, possibly leading to missed buzzes in foraging segments. Analysis of all-night continuous audio recordings revealed that a 10% duty cycle (0.5 s every 5 s) captured 77% of foraging bouts (Fig. S1.2), demonstrating that we captured most, but not all, prey capture attempts. Unfortunately, those continuous audio recordings did not include GPS sampling and therefore cannot be used to determine how each segmentation method would perform against a

more complete audio data set. Future work should aim to collect audio at a higher duty cycle in tandem with additional independent behavioral monitoring devices, such as an accelerometer, which may detect changes in wingbeat patterns, or barometric pressure, which would reveal when bats are close enough to the surface of the ocean to capture prey.

Evaluation of methods

HMM, while not significantly better than all methods, had the highest median balanced accuracy and predicted movement metrics similar to those measured at buzz locations. Where they have been independently validated with behavioral signals, HMM's have shown promise in accurately assigning behavioral states across a variety of taxa, e.g. elephant seals (Dragon et al. 2012) and gannets (Bennison et al. 2018). HMM's define both the state distribution (the distribution of input turn angle and step length) and the transition probability between states (Table S1.3). In principle, HMM's require data recorded at regular sampling intervals with negligible measurement error and can be influenced by autocorrelation in the data since there is an assumption of serial independence among turning angles and step lengths. Diagnostic plots of the HMM pseudo-residuals indicate a lack of fit because the independence of the data are often violated. Nonetheless, in our case HMM still outperformed other methods, suggesting that, in practice, model misspecification is not a fatal flaw. Timescale of autocorrelation estimates from CVCP in foraging tended to be lower than 15 s, indicating that foraging movements were independent, possibly explaining the performance of HMM in identifying foraging. Furthermore, we investigated how subsampling to coarser sampling resolutions influenced performance and found a significant but subtle decrease in median balanced accuracy, suggesting that HMM performance is generally robust to GPS sampling rate (Fig. S1.7). We also fit a three-state HMM. Despite a lower AIC and slightly higher median balanced accuracy of a three-state HMM,

a two-state HMM had a higher mean balanced accuracy and less variation than the three-state model (Fig. S1.6, Table S1.5).

Due to limited recordings per individual, all methods assumed no individual variation. Nightly differences in oceanographic conditions, weather, prey distribution, and social context could influence the way an animal commutes or forages and consequently affect method performance, especially if trips are aggregated for analysis (Cvikel et al. 2015a, Bennison et al. 2018). We limited our analyses to just movement and buzzes to simplify method comparison; however, many segmentation analyses are performed for habitat selection analysis or use environmental parameters with movement to identify behavior state changes (Fauchald and Tveraa 2003, Domalik et al. 2018, Suraci et al. 2019). While behavioral states annotation from all five methods can be used for habitat selection, HMM can include environmental covariates in the model and clearly present how those covariates influence transition probabilities, which is an additional advantage of this method. Alternatively, the transitions and parameters obtained from other methods can be analyzed with respect to environmental covariates post hoc. For example, the probability that a foraging phase might have an advective term from the CVCP could be modeled with respect to winds or currents to indirectly explore hypotheses related to drifting prey patches. As another example the frequency of extremely short foraging bouts from the clustering algorithms might be related to environmental conditions associated with less concentrated and patchier prey fish aggregations.

One of the earliest and heuristically simplest of the segmentation methods, FPT is still one of the most commonly used methods to identify foraging areas (Fauchald and Tveraa 2006, Bennison et al. 2018, Suraci et al. 2019), and – because it is explicitly spatial rather than velocity-based – can outperform more statistically complex tools (Gurarie et al. 2016). In our

study, FPT had the most variable accuracy among individual trips. FPT was most similar to HMM in performance, despite having lower median balanced accuracy, and some of the individual trips had extremely high accuracy (up to 84%). We did not explore the effect of different radii and thresholds on balanced accuracy but instead chose a radius that maximized the overall variation in FPT and a cut-off between foraging and commuting that was at the upper confidence limit for the first peak in the ln(FPT) histogram. The fact that only one radius and threshold were used likely explains much of the variability in accuracy, since both the radius and threshold may change according to individual or environmental conditions. For example, bats may be influenced by drifting prey or strong winds, which may compromise the ARS pattern and require a larger radius or threshold to separate behaviors. Replicates of trips for the same individual across environmental conditions, as well as measurements of the relevant abiotic conditions, could be combined with an FPT analysis to gain further insights into the context of fish-eating bat behavioral states.

CVCP requires a large enough analysis window to reliably estimate movement parameters and change points. By design, CVCP segments are more likely to correspond to behavioral switches than spurious changes in movement. Though less sensitive than other methods, its balanced accuracy was comparable to HMM and FPT. Furthermore, CVCP is the only method that provides a completely parameterized continuous-time movement model that is defined in terms of biologically meaningful parameters (e.g. advective and random mean speeds and characteristic time scales of auto-correlation; Gurarie et al. 2017), which makes it possible to compare the mechanistic features of larger-scaled commuting and foraging behaviors across individuals or foraging trips. Estimates of tau, which is an estimate of the time scale at which the velocity of an animal's movement is autocorrelated, are typically higher than the 15 s GPS

sampling schedule in commuting and less than 15 s for foraging locations (Table S1.7). This suggests that the 15 s sampling rate is sufficient for characterizing the commuting movements, but that the movements (and decisions) that the bat is performing while foraging occur at a faster rate, requiring an even higher location sampling rate or ancillary information (e.g. from an accelerometer) to explore the foraging behaviors in higher detail. This result does, however, suggest that the independence assumption behind the HMM is essentially satisfied, at least for the foraging state. It is further worth noting that the CVCP is perhaps best suited to distinguish between highly localized foraging and foraging for a drifting patch, since it can fit a model with advection that still has varying degrees of tortuosity and movement speeds.

The two unsupervised methods, EMbC and kmC, produced similar segmentation patterns of bat foraging trips. Pattern description methods, such as kmC, do not require a predefined length for segments and can therefore detect very brief foraging bouts (Fig. 1.3b). It is likely that EMbC is attempting to overfit the movement data and defines states that do not occur during these trips, such as resting. However, by aggregating states, we demonstrate that this method can still be useful on data that has been filtered to exclude time in the roost. While these methods identified most foraging sites, they provided unreliable estimates of parameters associated with foraging due to their lower performance.

Conclusion

Despite variation in movement statistics, performance, as measured by balanced accuracy, was not very different among methods. While performance is highest with HMM, technical constraints might lead some researchers to use simpler or faster methods, like FPT, that do not require parameter estimation, though recently developed R packages like "momentuHMM" have made the fitting of HMM models to movement data much more

accessible (McClintock and Michelot 2018). Our results do indicate that the choice of segmentation method can lead to dramatically different movement statistic estimates, such as number of foraging bouts, percentage of time spent foraging, and locations of foraging areas. It is therefore important to be aware of the assumptions and limitations of each algorithm, as well as each tool's sensitivity to sampling rate, missing locations, localization accuracy (Pinaud 2008, Dragon et al. 2012) and individual differences (Patterson et al. 2008). Ultimately, the research question should inform method selection. Evaluating biophysical parameters such as speed and time scales of movement is easier with a more realistic movement model (Gurarie et al. 2017), while identifying covariates that influence the rate of behavior switching between stereotyped behaviors will require a state space model. In many cases, important insights can be made through "triangulation" – i.e. by using several tools and comparing the outputs. As animal movement data become more readily available, it will be increasingly possible to validate behavioral annotation methods. In species that lack sufficient observational data to calibrate behavioral state estimates, such as animals with cryptic foraging behaviors, researchers must decide whether their assumptions about behavior reflect reality.

Availability of data and materials

Hurme E, Gurarie E, Greif S, Herrera M LG, Flores-Martínez JJ, Wilkinson GS, Yovel Y (2019) Data from: Acoustic evaluation of behavioral states predicted from GPS tracking: a case study of a marine fishing bat. Movebank Data Repository. https://doi.org/10.5441/001/1.kk3bg2f4

Abbreviations

AIC: Akaike Information Criterion

ARS: Area-restricted search

BIC: Bayesian Information Criterion

CVCP: Correlated velocity change point analysis

CVM: Correlated velocity movement

EMbC: Expectation maximization and binary clustering

FPT: First passage time

g: Grams

GB: Gigabyte

h: Hour

HMM: Hidden Markov models

IPI: Inter-pulse interval

kmC: k-means clustering

m: Meters

min: Minutes

s: Second

SE: Standard error

TNR: True negative rate

TPR: True positive rate

Tables

Table 1. 1 Tuned parameters and settings for each of the five segmentation methodologies.

Category	Method	Parameter	Setting
Pattern Description	k-Means clustering	–	–
	First-passage time	Radius	250 m
		Threshold	142 s
State-space modeling	Expectation Maximization and binary clustering	–	–
	Hidden Markov model	Regularization	15 s
		Initial step length (mean/SD)	State 1: 70.2/ 27.6 m
			State 2: 160.8/ 23.0 m
		Initial turn angle (mean/concentration)	State 1: 0/0.1
			State 2: 0/0.1
Behavioral Change Point Analysis	Correlated velocity movement behavioral partitioning	Window size	2 (2.5)[a] min
		Window step	1.25 min
		Minimum changepoint distance	0.5 min

[a] One bat flight did not converge with a 2 min window size and was adjusted to 2.5 min

Table 1. 2 Mean and standard deviation of flight parameters for behavioral states identified by each segmentation method.

	Foraging		**Commuting**		
Method	**Speed (m/s)**	**Turn angle |degrees|**	**Speed (m/s)**	**Turn angle |degrees|**	**Omitted points**
kmC	2.87 ± 0.20**	130.3 ± 3.1***	5.05 ± 0.40	19.2 ± 3.2	30
FPT	3.48 ± 0.46	69.0 ± 11.2	5.49 ± 0.61	21.5 ± 13.0	99
HMM	3.13 ± 0.22	83.4 ± 8.1	5.65 ± 0.42	13.9 ± 1.5	0
EMbC	3.12 ± 0.22	112.2 ± 5.9***	5.13 ± 0.39	17.3 ± 2.4	0
CVCP	3.48 ± 0.50	74.8 ± 12.2	5.33 ± 0.34	21.8 ± 7.2	0
Buzz	3.36 ± 0.54	72.5 ± 16.7	NA	NA	NA

Wilcoxon pairwise comparisons between buzz occurrence and foraging parameters for each method with Bonferroni correction (see text)

**p-value < 0.01, ***p-value < 0.001

Figures

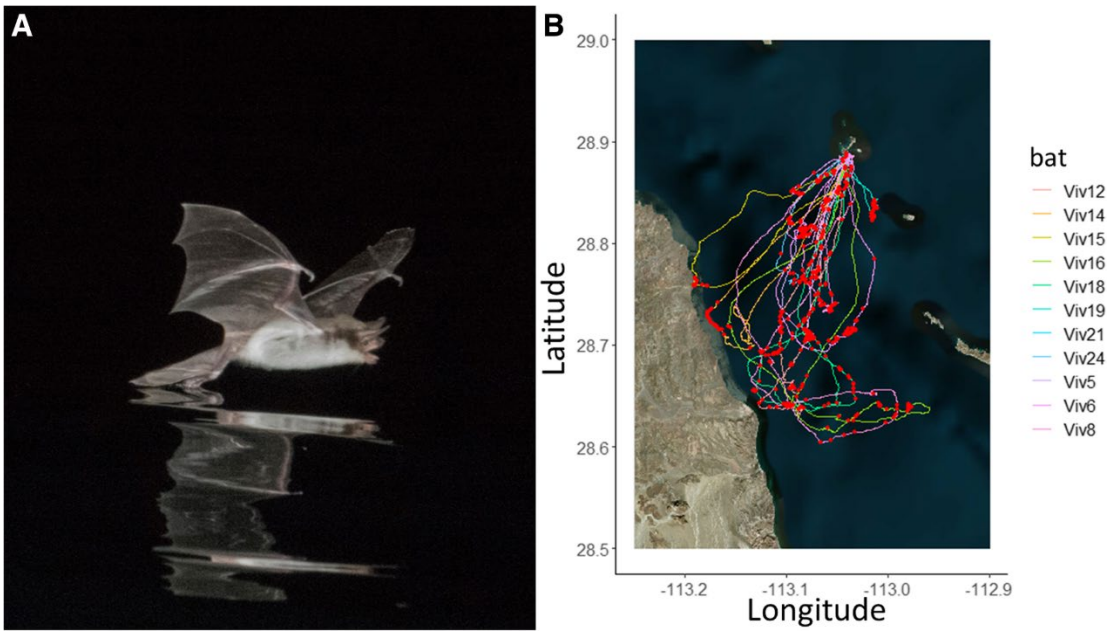

Figure 1. 1 Study species and GPS tracking.

(a) Photo of a Mexican fish-eating bat (Myotis vivesi) trawling for prey and (b) a satellite map ("Esri.WorldImagery") of the study area with GPS tracks of each foraging trip overlaid. These bats use biosonar to sense their environment, such as the ocean surface, and cue into small prey that might break the surface. Prey capture attempts, or feeding buzzes, recorded from an on-board ultrasonic microphone are overlaid on each trip. (Photo credit: Glenn Thompson)

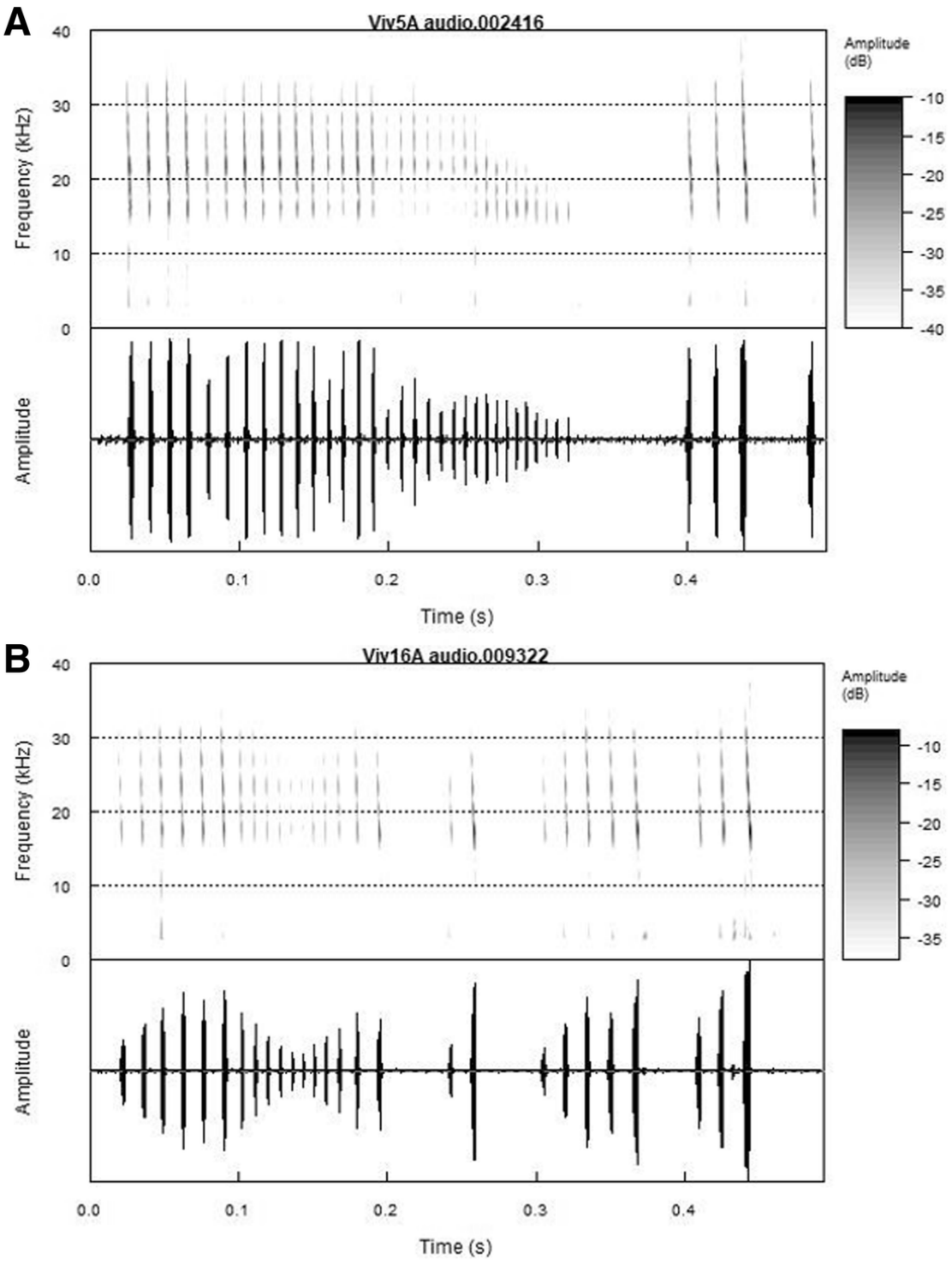

Figure 1. 2 Spectrogram (top) and waveform (bottom) of fish-eating bat echolocation calls. (**a**) Typical terminal buzz, (**b**) aborted buzz (ends at 0.2 s) followed by search phase calls.

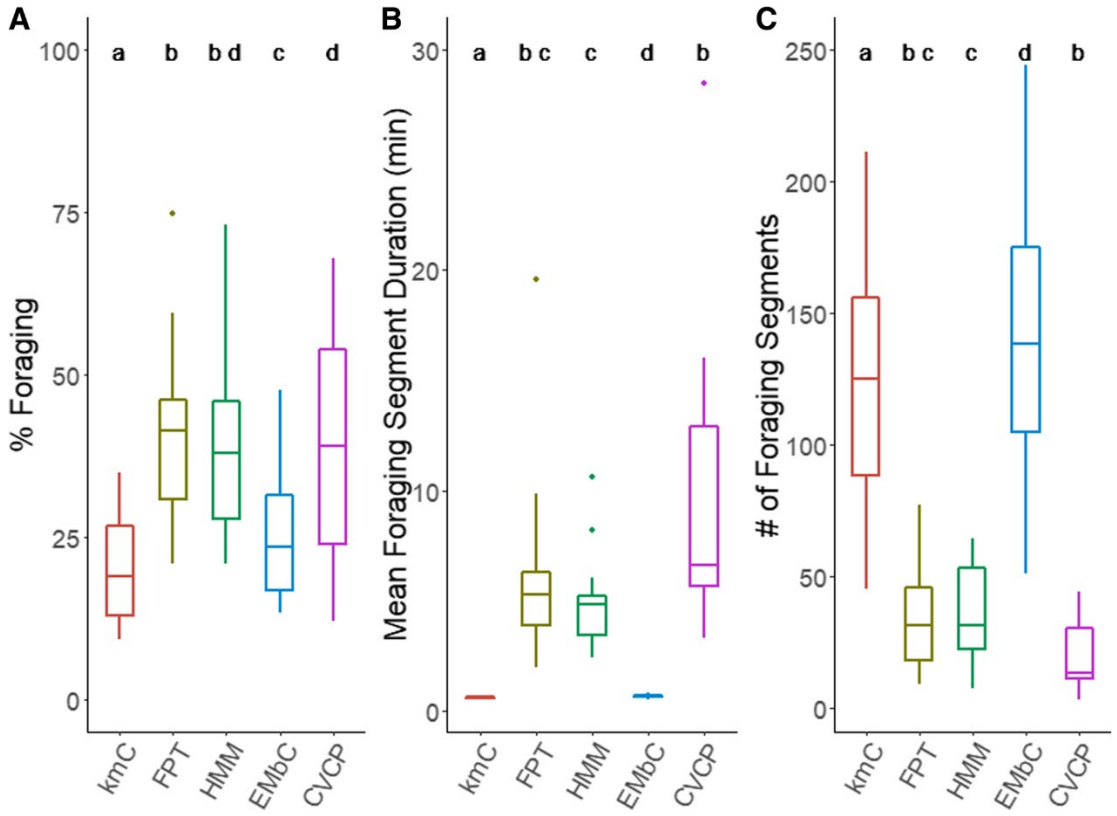

Figure 1. 3 Foraging segmentation comparison.

Box plots showing (a) the percentage of a trip in foraging behavior, (b) the number of locations in a foraging segment, and (c) the number of segments for each segmentation method (N = 15). Different letters above boxplots represent significant differences in paired Wilcoxon sign rank tests after Bonferroni correction.

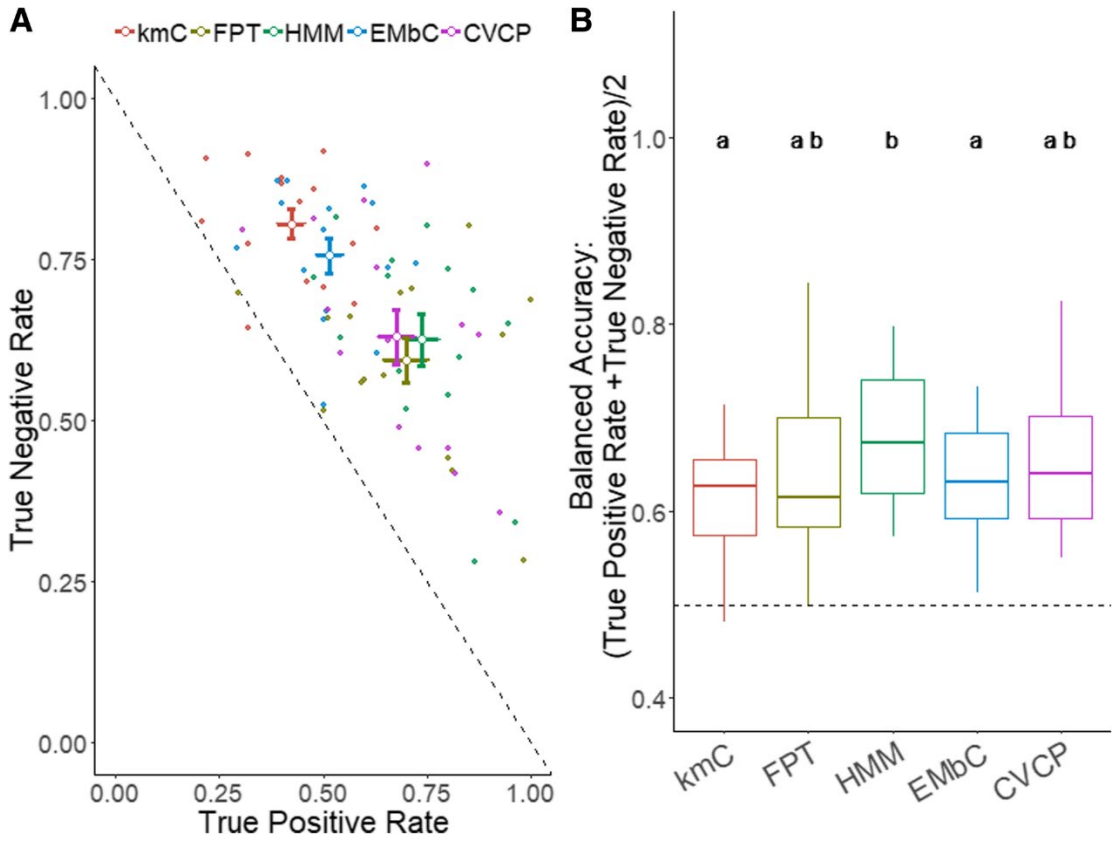

Figure 1. 4 Segmentation performance.

(a) Scatter plot of true positive rate against true negative rate (each point represents a bat flight and method combination) and (b) box plot of the balanced accuracy for each trip (N = 15). The scatter plot includes mean values of each method with standard error for true positive rate and true negative rate (a). A dashed line is included in both plots to show 50% balanced accuracy and values above the line represent good classification. Different letters above boxplots represent significant differences in paired Wilcoxon sign rank tests after Bonferroni correction (b).

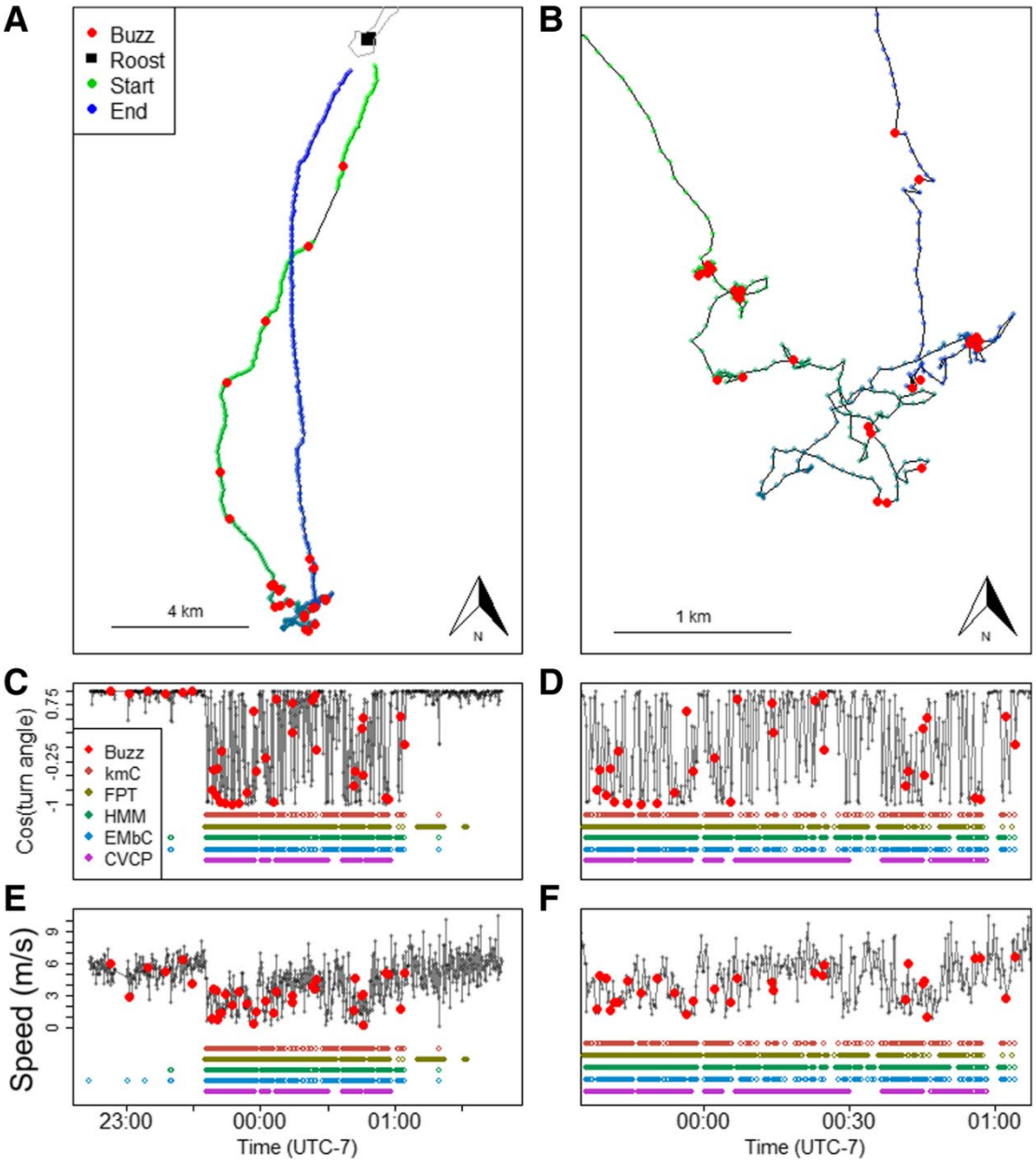

Figure 1. 5 Foraging track and segmentation.

Example trip showing (a) the flight trajectory, (c) cosine of the turn angle for the entire flight, and (d) speed for the entire flight. (b) displays a close-up of the foraging area in (a), (d) cosine of the turning angle for (b), and (f) speed for (b). Buzzes are overlaid as red circles in all plots and segmentation methodology predictions of foraging are shown in different colors below speed and

turn angle plots (c-f). The number of foraging segments identified in this trip varies between methods (kmC: 145; FPT: 80; HMM: 31; EMbC: 138; CVCP: 13).

Chapter 2: Multiscale foraging site selection from GPS telemetry in a marine foraging bat

Abstract

Habitat selection models can provide insight into how animals respond to their environment at multiple scales. The marine environment, which is shaped by interactions between the marine landscape, currents, winds and other dynamic variables, provides a challenge for animals attempting to reliably find prey. Here we utilize remote sensing data and GPS tracks of 56 Mexican fish-eating bats (*Myotis vivesi*) foraging in the open ocean over a five year period to ask if static variables (bathymetry, seafloor slope, and distance to coast) or dynamic environmental variables (chlorophyll-a concentration and sea surface temperature) predict foraging activity across multiple scales (nightly central-place foraging trips, foraging sites within the range, and foraging sites within a trip).

Selection of habitat at a large spatial scale was suggested by non-random departure directions of bats. Static features were more predictive of foraging site selection than dynamic features at all scales, though models containing both static and dynamic variables also outperformed simpler models at all scales. Deep ocean depth, steep slope, and high chlorophyll concentration were generally significant predictors in all combined models. Predictive ability also decreased at smaller scales, indicating that the location of potential prey, such as small pelagic fish, is constrained to regions identifiable by large-scale oceanographic features. Habitat selection in a marine bat provides opportunities for comparison with other marine organisms foraging in the same unpredictable environment.

Introduction

Animal movement data can provide insight into how animals perceive and respond to their environment by making decisions on where to forage. Habitat selection is defined as disproportionate use of available resources and can be characterized with resource selection functions (RSFs) to provide information on the relative probability of use of a resource (Boyce 2006, Davis et al. 2007). Preferred use of space can be detected at multiple scales: species or population range, individual home range or territory, daily travel route, feeding area, and feeding site (Johnson 1980, Schaefer and Messier 1995), and combining multiple scales in an analysis allows for a more complete picture of how animals respond to their environment (Wiens 1989, Becker and Beissinger 2003, Mayor et al. 2009). This approach has been useful for modeling species habitat and developing more strategic conservation plans (Chetkiewicz and Boyce 2009, Gerber and Northrup 2019). Furthermore, for species lacking information on diet or habitat use, multiscale selection allows for an unbiased approach to determine habitat features preferred by an organism (McGarigal et al. 2016).

In pelagic environments, prey density near the surface is generally low, patchy, and ephemeral (Russell et al. 1992, 1999, Bost et al. 2009). Marine habitats can be characterized in terms of static features (e.g. sea floor slope) and dynamic features (e.g. sea surface temperature) which can vary over space and time (Cox et al. 2013, McInnes et al. 2017). Static features have been shown to predict marine predator habitat use because they influence habitat preferences of prey (Hunt et al. 1998, Watanuki et al. 2008). Static features also interact with dynamic features, such as currents, to create favorable oceanographic conditions for marine productivity (Cox et al. 2018). For example, upwellings bring cold, nutrient-rich water to the surface, supporting plankton blooms and the organisms that feed on plankton (Genin 2004, Ainley et al. 2009,

Grecian et al. 2016). However, spatial and temporal predictability varies depending on which oceanographic processes are occurring (Cox et al. 2013). Most research on marine predator movement lacks information on the underlying oceanographic processes or the distribution and abundance of the prey. Given this complexity, it is common to investigate a small set of likely influential covariates that might accurately predict habitat use (Oppel et al. 2012, Domalik et al. 2018). Marine predator habitat use may be better explained by dynamic features because they can provide more immediate cues about marine productivity (reviewed in Hazen et al. 2013). These regions can be detected through remote sensing measurements of sea surface temperature (SST) and chlorophyll a concentration (Field et al. 1998, Ainley et al. 2009, Domalik et al. 2018).

Here we investigate the habitat preferences of female Mexican fish-eating bats (*Myotis vivesi*, hereafter fish-eating bats) during lactation on Isla Partida Norte in the Midriff Islands Region (MIR) of the Gulf of California. We used GPS tracking to investigate the foraging movements and habitat use of these bats as they forage for small fish in the open ocean. Miniature high spatio-temporal resolution GPS tags can provide insights into how foraging bats use space and interact with their environment (Cvikel et al. 2015a, Egert-Berg et al. 2018, Hurme et al. 2019). Tracking animals over several nights in a dynamic region can also allow us to determine if they assess specific environmental variables. It is currently unclear if fish-eating bats use more than size to select prey; however, diet analysis indicates they consume a variety of species of fish and crustaceans (L.G. Herrera M. and E. Claire, personal communication; Otálora-Ardila et al. 2013). Tidal dynamics in the Midriff Islands Region cause upwellings of cold subsurface water, promoting the highest chlorophyll and primary productivity levels in the gulf (Millán-Núñez and Yentsch 2000). Acoustic surveys of small pelagic fish in the MIR in

2012-2014 showed that schools were associated with low SST and high net primary productivity (NPP; Rubio-Rodríguez et al. 2018). In particular, the Ballenas-Salsipuedes Channel is known for intense mixing of the water column associated with tidal dynamics, creating conditions of consistently low SST and high NPP, leading to increased presence of small pelagic fish schools (Rubio-Rodríguez et al. 2018). However, these enriched subsurface waters are known to gradually disappear in the summer, as cold water sinks and warm water from the south moves in (Escalante-Almazán 2013, Hernández-Ayón et al. 2013).

Fish-eating bats fly up to 7 h in search of prey that they catch from the surface of the ocean (Egert-Berg et al. 2018). Analysis of GPS flight paths in combination with ultrasound recordings distinguished foraging sites, characterized by tortuous, area-restricted movements and stereotypic echolocation call series known as a feeding buzz, from commuting or travelling movements (Hurme et al. 2019). The size and spatial distribution of foraging sites across nights for the same individual is consistent with prey occurring in small, unpredictable patches, as bats typically travel 4 km between foraging sites within and between nights and spend 6 - 9 min foraging at a site (Egert-Berg et al. 2018, Hurme et al. 2019). Each night bats must decide which direction to travel away from the roost, which habitat to visit (e.g. open ocean or coastline), which area to search, and how long to stay in each patch. Given these options, bats could select where to forage at several potential scales: 1) from the available marine area within the maximum distance (45 km) to a foraging site from the roost, 2) from a subset of available sites generated by the distance and angle from the roost to all identified foraging sites, or 3) from potential sites along a foraging route. Although RSFs typically use the spatial distribution of an animal's occurrence, here we use this approach to understand the occurrence of a specific behavior (Abrahms et al. 2016, Carroll et al. 2017). We modelled the influence of static and/or

dynamic oceanographic features on the probability of foraging at a given site at four different spatial scales. We predicted that bats would select habitats with high chlorophyll abundance and low SST, which is associated with schools of small pelagic fish (Rubio-Rodríguez et al. 2018). We also predicted that they would choose locations conducive to upwellings, i.e. deep ocean, steep seafloor slope, and away from the coast.

Methods

Study Species

Mexican fish-eating bats, *Myotis vivesi*, are restricted to islands and coastal areas in the Gulf of California (Blood and Clark 1998, Herrera M. et al. 2019). As the only marine specialist bat they consume predominantly small fish and crustaceans, with a small amount of insects present in their feces during June and December (Otálora-Ardila et al. 2013). Females typically give birth to a single pup between mid-May and early June (Maya 1968, Blood and Clark 1998).

Study site

We conducted the study on Isla Partida Norte (28° 53′ 16″ N, 113 ° 02′ 30″ W), a 1.4-km^2 island located in the Gulf of California, Mexico (Castil et al. 1980). Isla Partida Norte is home to the largest known population (~8000 individuals) of Mexican fish-eating bats (Flores-Martínez et al. 2004). This island is part of the Midriff Islands archipelago in the northern half of the Gulf of California. This region is known for its high productivity year-round, caused by strong tidal mixing forces, stirring the water column down to > 500 m in depth, and creating a constant upwelling environment (Tershy et al. 1991, Álvarez-Borrego 2012). During the summer months, remote sensing measurements of ocean productivity show that most of the gulf has low

chlorophyll concentrations; however, chlorophyll concentrations in the waters around the Midriff Islands and upper gulf remain high (Kahru et al. 2004).

The elevated primary productivity in this region supports large numbers of seabirds and marine mammals (Tershy et al. 1991). Larger marine predators, such as fin whales (*Balaenoptera physalus*), forage near the Midriff islands during the summer (López et al. 2019). Isla Rasa, a neighboring island, is home to the world's largest colonies of elegant terns (*Thalasseus elegans*) and Heermann's gulls (*Larus heermanni*), which depend on this highly productive environment for raising their chicks (Velarde et al. 2004).

Oceanographic conditions during the study

The El Niño - Southern Oscillation (ENSO) is an irregular, periodic variation in the sea surface temperature (SST) of the water off the eastern tropical Pacific Ocean. While the 2018 and 2019 field seasons did not have a significant ENSO index, the majority of GPS tracking took place in 2015 and 2016, co-occurring with the start and end of an El Niño event. In the eastern Pacific Ocean, El Niño results in an increase in SST and a decrease in marine productivity. Conversely, La Niña results in a decrease in SST and an increase in marine productivity (Marinovic et al. 2002). While many species have evolved over millennia with the climatic variability of ENSO, climate change is projected to increase extreme ENSO events (Cai et al. 2015), which will likely threaten many ecosystems.

El Niño events in the Gulf of California, Mexico's largest fishery, reduce wind stress causing a reduction in upwelling and nutrient mixing (Sánchez-Velasco et al. 2017). Reduced wind stress can also reduce the depth of the oxygen minimum zone, which can limit the range and abundance of several pelagic fish (Robinson et al. 2016, Sánchez-Velasco et al. 2017).

Field methods

Our study was conducted over four field seasons, from May 27 to June 20, 2015, May 28 to June 25, 2016, May 25 to June 23, 2018, and June 6 to June 21, 2019, at which times females were nursing pups. This work was carried out under permits # 7668–15, 2492–17, and 5409-18 from Dirección General de Vida Silvestre, permits #17–16, 21–17, and 20-18 from Secretaría de Gobernación, and protocols FR-15-10 and FR-APR-18-20 from the University of Maryland Institutional Animal Care and Use Committee.

Bats were captured by hand in the morning from under rocks on talus slopes along the south-east region of the island. Lactating females weighing at least 28 g were selected for tagging to facilitate recapture when the bats returned to feed their pups during the day. Estimated pup age from tagged bats ranged from 4 to 37 days (Hurme, Ch 3). We glued biologger tags (2015 and 2016: Robin GPS Loggers, CellGuide Ltd., Israel; 2018 and 2019: Vesper GPS logger) with VHF radiotransmitters (Holohil BD-2X) to the back of each bat using non-toxic glue (Perma-Type Surgical Cement, Plainville, Connecticut; Cvikel et al. 2015a, Egert-Berg et al. 2018, Hurme et al. 2019). Total weight was 4.6 ± 0.2 g for tags in 2015 and 2016 and 4.5 ± 0.4 g in 2018 and 2019. We released bats at their capture locations during midday. We used the radio transmitters to locate and recapture tagged bats and recover the biologgers. Previous analysis of data collected in 2015-2016 demonstrated no significant effect of tagging on change in flight duration, adult mass or pup mass when compared with a radio telemetry control (see methods in Egert-Berg et al. 2018, Hurme et al. 2019).

Behavioral segmentation

Marine environments typically contain patchily distributed prey, requiring marine predators to use area-restricted search (ARS) when foraging (Charnov 1976, Bailey et al. 2019).

Behavioral segmentation methods attempt to identify behavioral states from the GPS tracks of an animal. We conducted all analyses in the R Statistical Environment (version 3.5.2 R Core Team, 2018). Validation of segmentation methods of GPS tracked fish-eating bats using on-board audio of foraging attempts revealed that hidden Markov models (HMMs) performed well at assigning behavioral states (Hurme et al. 2019). We first regularized the GPS data by resampling and interpolating all locations at 1 min intervals using the R package "adehabitatLT" and removed GPS locations within 1 km of Isla Partida Norte to eliminate the possibility of misclassifying roosting movements as foraging behavior. We then used the R package "momentuHMM" to fit HMMs to all foraging trips (Calenge 2006, McClintock and Michelot 2018).

We used a two-state model to define behavioral states. Initial step length, or distance between sampling locations, parameters for the two-state HMM were estimated from a mixed normal distribution of the step length of all individuals using the function "normalmixEM" (state 1: mean 55.1 m, SD 28.9 m; state 2: mean 280.1 m, SD 107.9 m). The HMM estimated gamma distributions for step length parameters (state 1: mean 139.4 m, SD 99.7 m; state 2: mean 327.2 m, SD 82.9 m) and von Mises distributions for turn angles (state 1: mean 0, concentration 0.71; state 2: mean 0, concentration 18.38). State 1 has a shorter step length and uniform turn angle distribution, while state 2 has longer step lengths and a turn angle concentrated around 0 (Fig. S2.2).

Foraging flight direction and duration

For each tagged bat, we calculated the following summary parameters for each night: departure direction (º), departure time (h), return time (h), flight duration (h), flight distance (km), max distance from the roost (km), and number of trips from the island (Table 2.1). We also

used behavioral segmentation to describe the number of foraging bouts, foraging bout duration (min), and percent of flight spent foraging.

We measure departure directions as the angle at 1 km from the origin and tested if yearly departure directions were randomly distributed using a Rayleigh test (Zar 1976). Additionally, we explored correlations between flight covariates and investigated if departure time or flight distance were significantly explained by pup age. Pup age was estimated from measurements of pup weight and forearm length, assuming a birth weight of 6 g and forearm length of 25 mm and a growth rate of 0.33 g/day and 0.84 mm/day (Hurme, Ch 3). We used a linear model to determine if flight duration is predicted by departure hour, pup age, or year.

Environmental data

Environmental variables were chosen for analysis based on their potential relevance to prey abundance, probability of being sensed by a bat, and data completeness. We included bathymetry (ocean depth) and seafloor slope as static habitat variables. We derived these measurements from the R package "marmap" which queries the ETOPO1 dataset host on National Oceanic and Atmospheric Administration (NOAA) servers. Oceanographic measurements were sampled at the finest resolution available, 0.0167º (ca 2.9 km^2). Nearest distance to coastline (dist2coast) and distance from the bats' roost, Isla Partida Norte, (dist2roost) were calculated from coastline vectors from large scale "Natural Earth Data" (naturalearthdata.com) and R package "raster".

We used remote sensing measurements to estimate dynamic variables. We used NOAA ERDDAP servers (https://coastwatch.pfeg.noaa.gov/erddap/griddap/) to access Aqua MODIS (Moderate Resolution Imaging Spectroradiometer) estimates of chlorophyll a concentration

(mg/m^3; dataset ID: erdMWchla1day) and sea surface temperature (dataset ID: erdMWsstd1day). Remote sensing covariates were all sampled at a resolution of 0.0125^o (ca 1.7 km^2).

We used the nearest environmental measurement in time and space for each GPS location. To adjust for missing values in daily measurements of remote sensing data, we manually averaged daily measurements into multiday composites. Composites included the nearest date measurement to the observed foraging site and 30 days previous. To approach normality, chlorophyll a concentration was log transformed.

Candidate models

We hypothesized that bats, as central place foragers under the energetic constraints of lactation, would prefer to forage close to their roost (Peery et al. 2009, Rainho and Palmeirim 2011, Domalik et al. 2018). Therefore, we included distance from the roost as a main effect in all models.

For all model covariates, first we fitted generalized additive mixed models (GAMMs; R package "mgcv"; Wood 2011) for each covariate to investigate if nonlinear terms improved model fit. We only allowed models to have two knots, equivalent to polynomial terms, to limit model complexity. We then fitted a generalized linear mixed-effect model (GLMM) using the remaining covariates and polynomial terms, where appropriate, for each model. Model covariates were centered and scaled to increase comparisons between models and determine variable importance within a model. To reduce multicollinearity between parameters we calculate variance inflation factors among variables (R package "car"; Fox and Weisberg 2019) and removed polynomial terms or covariates with variance inflation factor scores above three (Zuur et al. 2010). Finally, we included year as a fixed effect in all models. If the year effect was

significant, we also ran models for each year to determine how resource selection differed between years.

Available foraging sites

We generated available sites from a circle of available foraging habitat centered on Isla Partida Norte. Locations were regularly generated by sampling a direction from a uniform circular distribution and distance from a uniform distribution between the minimum and maximum foraging site distance. We generated 20 marine locations for every used foraging site and assigned to each location individual bat and corresponding date, allowing dynamic covariates to be sampled from the same time as the used locations. Locations over land were omitted and new available sites were generated as needed.

Simulated foraging sites

We generated 20 pseudoabsence sites for each observed foraging site by randomly selecting 20 distances and 20 angles from the distributions of distances and angles between all foraging sites and Isla Partida Norte (Stockwell and Peterson 2002). All foraging sites occurred over the ocean, so if simulated sites fell on land, these points were omitted and new available locations were generated. Simulated sites were assigned to each trip ID and corresponding date, allowing dynamic covariates to be sampled from the same time as the observed locations. This method is similar to a step selection function that uses the animal's movement to create a null set (Fortin et al. 2005). However, in this case, we assume foraging sites are independent, instead of steps along an individual's path.

Used sites

We estimated foraging and commuting sites as the median of all locations within a single HMM bout. The return commute was omitted from each trip, since bats are likely not selecting a

specific marine habitat as they fly back to the roost. Median values were calculated for all covariates of each location within a bout. Foraging site duration followed an exponentially decreasing distribution (exponential rate: 0.05; Kolmogorov-Smirnov test: $p < 0.001$; Fig. S2.3).

We fitted GLMMs with individual night as a random intercept using the R package "lme4" (Bates et al. 2015). We did not control for variability among nights within bats using random slopes due to lack of sufficient replication of individual flights across nights (Muff et al. 2020). Following the recommendations of (Fithian and Hastie 2013, Muff et al. 2020), we weighted observed points by 1 and pseudoabsences by 1000 such that the models approximately predict the spatially explicit intensity of an inhomegeneous Poisson Process (Warton and Shepherd 2010). In the foraging site vs commuting model, all points were weighted equally because unused locations were true absences, such that the model predicted actual probabilities of foraging.

Model evaluation

For each foraging site selection model, we reported marginal R^2 values, representing the relative contribution of fixed effects, and conditional R^2 values, which contain the combined contribution of fixed and random effects using "r.squaredGLMM" from the R package "MuMIn" (Table 2.5; Nakagawa and Schielzeth 2013). To further assess model fit, we evaluated the predictive ability of the top performing models through k-fold cross validation using binned calibration plots and area under the curve (AUC; Boyce et al. 2002). We randomly partitioned each dataset into five folds, with each fold containing 20% (21 or 22 of the 106 individual bat nights). We iteratively used four folds for model training and then tested model prediction on the remaining fold of withheld data. For each test, the fixed-effects output from the training data was used to predict values for both the random locations generated within each range and the

withheld GPS locations. We then partitioned the exponential of the predicted values of the test points into deciles (i.e. 10 ordinal bins containing an equal number of points) and calculated the mean value of each bin (Boyce et al. 2002). We determined the number of used locations that occurred in each bin and the expected number of used locations in each bin by multiplying the total number of used locations against each mean bin value divided by the sum of all mean bin values. We assessed model prediction by comparing the used number of locations in each bin against the expected number of used locations using Spearman's correlation coefficient (r). This process was repeated for each of the five folds to calculate a mean r, with higher mean r values indicating better predictive performance. Here we also reported the average and standard deviation of AUC scores across the five cross-validation folds.

We also created prediction maps for the top performing model of the multiscale selection using a 100 km^2 area centered on Isla Partida Norte. We created maps for each year and used dynamic covariates assigned to the median tagging day of each year. Predicted values were binned into equal sized deciles.

Results

Foraging flight direction and duration

Over the four years of the study, we recorded foraging trips of 56 lactating female fish-eating bats, resulting in 135 trips on 109 bat nights (Table 2.1). Flight directions for three years, (2015, 2016, and 2018) were not randomly distributed and instead were concentrated to the south and southwest of the island (Rayleigh test for uniformity: 2015: $p < 0.001$; 2016: $p < 0.001$; 2018: $p = 0.05$; Fig. 2.1). However, in 2019, bat departures were not significantly different from random (Rayleigh test for uniformity: $p = 0.27$). While most trips in 2019 still departed to the south and west (N = 8), one individual departed to the north east. Bats typically began foraging

at 21:13 (UTC-7), approximately 1.7 h after sunset and returned at 02:52 (UTC-7), approximately 2.6 h before sunrise. Median flight duration was 3.7 h (range: 0.4 – 7.9 h), with six foraging bouts (range: 1 – 21) that encompass ca. 43% of the flight duration (range: 13 – 100%; Table 2.1). Most bats made a single foraging trip; however, 25 bats made two foraging trips in the same night. We retrieved foraging data for 1-6 nights from each bat.

Flight duration was significantly correlated with other flight measurements, such as flight distance ($r = 0.97$, $p < 0.001$), maximum distance from the roost ($r = 0.77$, $p < 0.001$), and number of foraging sites ($r = 0.82$, $p < 0.001$). A linear model of flight duration as a function of departure hour, pup age and year indicated a significant negative effect of start hour ($\beta \pm SE = -31.5 \pm 7.6$), but no effect of pup age ($\beta \pm SE = 0.5 \pm 1.2$) or year (Fig. S2.1).

Multiscale foraging site selection

Foraging vs available sites

Individual GAMM models for foraging site vs available habitat locations indicated that all environmental covariates should be fit with polynomial terms (Fig. S2.4). The combined static and dynamic model had the lowest AIC when compared with the static model (ΔAIC: 172) and the dynamic model (ΔAIC: 205; Table 2.4). The combined model explained the most variation (50%) and k-fold cross validation demonstrated high predictive ability across all three models (Table 2.4).

The combined model suggests that foraging sites are more likely to occur in deep ocean, with high chlorophyll concentration, intermediate ocean floor slopes, close to the coast, and at an intermediate distance from Isla Partida Norte when compared with a null set of simulated foraging sites sampled from the distribution of distances and directions of all foraging sites (Table 2.3). Additionally, there were significant effects of year for 2016 and 2019.

To investigate the influence of year on resource selection, we created combined static and dynamic models by year. In general, 2015 and 2016 showed similar patterns for each covariate (Fig. 2.3). A notable exception was distance to roost, which showed differences between 2015 and 2016. In 2019, foraging site use was generally consistent, however, there was much higher variance for each parameter estimate due to small sample sizes (Fig. 2.3).

We calculated the predicted probability of foraging site use over the study area for the median used day of each year using the combined static and dynamic model fit using data from all four years (Fig. 2.4). The areas with the highest probability of foraging are along the Ballenas-Salsipuedes Channel ranging from the southwestern edge of Isla Angel de la Guarda to the Baja peninsula coast directly east of Isla Partida Norte and down to Isla San Lorenzo directly to the south. While there are fine-scale differences between years, the general pattern is consistent.

Foraging vs simulated foraging

Individual GAMM models comparing observed foraging sites to simulated foraging sites indicated that all covariates should be fit with linear terms (Fig. S2.5). The combined static and dynamic model had the lowest AIC when compared with the static model (ΔAIC: 10) and the dynamic model (ΔAIC: 29; Table 2.4). The combined and static models explained the same amount of variation (5%) and k-fold cross validation demonstrated some predictive ability across all three models (Table 2.4).

The combined model suggests that foraging sites, when compared with simulated foraging sites, were more likely to occur in areas with shallow ocean depth, high chlorophyll concentration, low ocean floor slopes, and close to the coast (Table 2.3). There was no effect of distance to roost, sea surface temperature or year on foraging site use.

Foraging vs commuting

Individual GAMM models for predicting foraging vs commuting site locations indicated that bathymetry and slope should be fit with polynomial terms (Fig. S2.6). The static model had the lowest AIC when compared with the combined dynamic and static model (ΔAIC: 3) and the dynamic model (ΔAIC: 16). The combined and static models explained the same amount of variation (3%) and k-fold cross validation demonstrated low predictive ability across all three models (Table 2.4).

The static model was the top ranked model and, consistent with the combined model, indicated that foraging bouts, when compared with commuting bouts, occur in areas with shallow or deep ocean depth and low or high sea floor slopes, avoiding intermediate values of each covariate (Table 2.3). Chlorophyll concentration, sea surface temperature, distance from the coast, distance from the roost, and year did not have significant effects on foraging site use.

Simulated and available sites showed a similar spatial pattern to observed foraging and commuting sites. Distances between foraging sites (N = 724) and commuting sites (N = 751) were on average 16.3 and 16.1 km respectively. For simulated and available foraging sites (N = 14000 each), bootstrapped means (mean distance between 1000 randomly sampled points repeated 500 times) were 14.3 ± 0.3 km and 28.9 ± 0.4 km respectively. Simulated sites follow observed foraging sites more closely because they were generated from true foraging sites, while the available foraging sites are further apart because they include sites in all directions from the island including those where the bats never foraged.

Discussion

Using GPS tracking data, our study provides insight into the fine-scale movements and habitat use patterns of lactating Mexican fish-eating bats (*Myotis vivesi*) on Isla Partida Norte,

which contains the largest known colony of this species. We found that bats generally do not depart the island randomly, but often forage to the southwest of the roost in the Ballenas-Salsipuedes Channel. Multiscale foraging site selection improved in accuracy with increased spatial scale and indicated that fish-eating bats preferred foraging sites with deep ocean and steep slopes. Our results suggest that foraging site use by lactating fish-eating bats is influenced by both static and dynamic covariates and that large-scale analysis explains considerably more of the variation in foraging site use than smaller scale analyses.

Foraging flight direction and duration

Fish-eating bats typically depart once in the night and fly for 3-4 h searching for prey over the ocean. Bats often have several foraging bouts along their flights, typically spending 10-20 min at a site (Table 2.1). We found that flight directions were generally non-random, and most flights were to the south or west of the roost (Fig. 2.1). In 2018 we recorded two individuals departing to the west and in 2019 one individual departed to the northeast, suggesting that the foraging environment or bat resource selection may be different between the first two years of tracking and the last two years. Overall, the consistency among departure directions suggests that bats actively choose which habitat to explore when they leave the roost.

As central place foragers who were also constrained by lactation, bats were limited in how far they could travel from the roost. However, foraging duration showed no significant relationship with pup age, suggesting that bats do not change their foraging strategy in relation to pup age, similar to lactating Stellar sea lions (Burkanov et al. 2011). While it is possible that pup milk requirements or feeding rates change with development (Kunz et al. 1995), we could not determine any significant impact of pup age on foraging flights. Instead, flight duration is more

strongly influenced by departure time, demonstrating that bats are limited in how far they can go by how late they leave the roost (Fig. S2.1).

Environmental predictors and habitat use

Our results suggest that foraging site use by lactating female Mexican fish-eating bats around Isla Partida Norte is influenced by both static and dynamic habitat variables. Combined models significantly outperformed simpler models in available and simulated foraging habitat models. At the largest scale, the combined model explained half of the variation in the data, followed by the dynamic model, and then the static model (Table 2.4). At smaller scales, combined and static models explained the same amount of variation and slightly outperformed the dynamic model. It is possible that bats are more likely to respond to static variables at finer scales, but this is more likely the result of a mismatch between the spatial and temporal scales of the data simulated foraging site and commuting models explained little variation in the data.

Significant polynomial terms in the models demonstrate that bats do not have linear responses to all environmental covariates. For chlorophyll concentration, distance to land, distance to the roost, sea surface temperature, and slope, bats select intermediate values. However, bats also appear to select bathymetric extremes by choosing to forage in shallow or deep areas.

Used foraging site durations ranged from 1-184 min, yet all sites were weighted equally in the models. It is possible that foraging sites with longer durations may reveal different selection parameters. However, the null model was the best performing model of foraging site duration, indicating that none of the covariates used in the models could explain why bats stayed at some sites longer than others. Therefore, we did not impose a threshold cutoff for foraging sites and included all HMM detected sites in all multiscale selection models.

Multi-scale selection

At a large scales (thousands to hundreds of kilometers), marine prey distributions are somewhat predictable; however, at mesoscale and sub-mesoscales prey is often unpredictable and patchy (Weimerskirch et al. 2005). Multiscale analyses of foraging site selection indicated that foraging sites can best be predicted at the available habitat scale (approx. 43 km radius; Table 2.4). Bats consistently fly to the southwest of Isla Partida Norte and forage in the Ballenas-Salsipuedes Channel. This region is strikingly different from much of the surrounding habitat to the north and east of the island, containing a deep channel with bathymetry up to 1.5 km deep and steep sea floor slopes (Tershy et al. 1991, Álvarez-Borrego 2012). Additionally, this region consistently has higher chlorophyll a concentration and lower sea surface temperature than the surrounding region, because tidal upwellings bring cold nutrient rich water to the surface (Millán-Núñez and Yentsch 2000, Rubio-Rodríguez et al. 2018). High site fidelity in marine predators typically occurs in regions with strong physical forcing, such as tidal upwellings or shelf edges (Weimerskirch 2007, Scales et al. 2014).

Overall, metrics of predictive ability of the models was much lower than larger spatial scale models, suggesting the RSF has limited utility in predicting the relative probability of foraging site selection by fish-eating bats. This may be a result of a lack of environmental variation at finer scales. Simulated foraging sites typically place the majority of pseudoabsence locations within the Ballenas-Salsipuedes Channel (Fig. 2.2). Additionally, the majority of foraging tracks pass through this channel, so foraging and commuting sites were very similar (Fig. 2.1; Table 2.2). This limited variability is reflected in the reduced accuracy of the selection models to distinguish between observed and simulated foraging or commuting sites.

Furthermore, we were limited to temporally coarse measurements of the dynamic environment due to cloud cover and missing data.

Fine-scale foraging site selection may use alternative cues to detect prey. Foraging site use may be influenced by conspecifics, either informing a bat of a potential prey patch through echolocation calls or decreasing a bat's willingness to join a patch that is saturated with conspecifics. Fish-eating bats are attracted to conspecific calls and likely rely on eavesdropping to find foraging sites (Egert-Berg et al. 2018). Additionally, there may be different biotic and abiotic factors or interactions between factors determining foraging site use at smaller scales. Daily measurements of remote sensing parameters, as well as ocean current and wind directions and velocities, are likely candidates for influential parameters in fine-scale foraging. However, only spatially coarse modeled measurements of these parameters have been identified which match the temporal resolution of our data (Whitaker et al. 2008, Marinone et al. 2009).

How do bats select their habitat?

It remains unclear how a bat would detect changes in the ocean depth, sea floor slope, or chlorophyll concentration. Previous work has demonstrated that Mexican fishing bats often use eavesdropping to help locate foraging sites. However, fish-eating bats do not depart at random. Instead, bats could rely on memory of good foraging habitat and perform a large scale search each night in the region with the highest probability of prey being detected. Alternatively, bats may track environmental cues, such as odors released from aggregations of fish (e.g. dimethyl sulfide; Belviso et al. 1990, Hill and Dacey 2006, Nevitt 2008) or sense temperature gradients or changes in wave patterns that may reveal strong upwellings (Russell et al. 1999, Becker and Beissinger 2003, Scales et al. 2014). Ultimately, successful bats forage where prey are located and foraging sites likely reflect the habitat selection of their prey as much as that of the bats.

More extensive sampling of the prey in tandem with tracking foraging bats will provide greater insight between predator and prey associations and the environment in this region. Experimental work should further explore potential marine cues bats use to find prey.

Interannual variation

Larger climatic trends may shape yearly difference in foraging site selection. In 2018 and 2019, bat foraging tracks were not consistently in the Ballenas-Salsipuedes Channel. Furthermore, foraging site selection in the available model suggests that bats may be responding to the environment differently in 2019 (Fig. 2.3). These differences in foraging direction and habitat selection may be linked to a weakened El Niño during these years. El Niños reduce the productivity of the entire gulf, except for the Ballenas-Salsipuedes Channel. The Ballenas-Salsipuedes Channel is a known refugia for cetaceans and seabirds during El Niño (Tershy et al. 1991) and may fill this role for fish-eating bats as well. Furthermore, non-El Niño conditions typically have lower phytoplankton biomass in the Ballenas-Salsipuedes Channel (Santamaria-del-Angel et al. 1994), which may explain the different foraging directions in 2018 and 2019. Unfortunately, logistical challenges with biologgers prevented recording foraging flight from as many bats in 2018 and 2019 as in the first two years. We do not have a sufficient number of GPS-tracked bats from weak El Niño years to determine if these differences are widespread or simply the result of a few unusual individuals. Further research should be conducted to investigate if and how foraging site selection parameters change during a strong La Niña season. Additionally, monitoring of the population dynamics and pup survival would be essential to determine if ENSO has a significant impact on the fish-eating bats.

Marine predators can serve an important role as ecosystem sentinels (Moore 2008). In this region, elegant tern (*Thalasseus elegans*) and Heermann's gull (*Larus heermanni*) nesting

success is a clear indicator of fishery health (Velarde et al. 1994). Sea surface temperature anomalies (SSTA) originally linked with the El Niño - Southern Oscillation were strongly linked to elegant tern chick survival on Isla Rasa (Velarde et al. 2015). However, since 2000, SSTA has become uncoupled from ENSO and is a more accurate predictor of chick survival. Warm oceanographic anomalies drive the thermocline down and decrease the intensity of upwellings, decreasing fish availability for seabirds. There is a need for multiyear monitoring of population and birth rate in conjunction with analysis of movement patterns to determine how this vulnerable and unusual bat species interacts with its changing environment.

This study was not an exhaustive investigation of all of the possible environmental covariates that may influence bat foraging site habitat as this is the first investigation of the habitat selection of this species and little is known about the mechanisms these bats use to detect prey. Additionally, investigation of covariates that may be related to ENSO or upwellings as well as complex interactions between parameters was outside the scope of this study. Furthermore, this study focuses exclusively on bats from Isla Partida Norte; it is unclear how bats in other regions in the Gulf of California may select their environment. These models can be used to predict where bats would likely forage in an average El Niño year (Fig. 2.4), applied to a new habitat, or to compare with other marine species.

Tables

Table 2. 1 Summary data for GPS tracks obtained from 56 individual lactating female Mexican fish-eating bats totaling 109 bat nights (N = 41 for 2015, N = 58 for 2016, N = 3 for 2018, and N = 7 for 2019).

Foraging trip descriptor	*Median*	*IQR*	*Range*
Departure time (local time: UTC - 7)	21:13	20:40 – 22:39	20:25 – 3:38
Max distance from roost (km)	16.6	10.6 – 23.2	1 – 43
No. foraging bouts	6	3 – 9	1 – 21
Foraging bout duration (min)	9	4 – 20	1 – 184
Duration of foraging (h)	1.3	0.8 – 2.1	0.3 – 4.4
Percentage of flight foraging	43.3 %	31.3 – 54.5 %	13 – 100 %
Duration of flight (h)	3.7	2.5 – 4.8	0.4 – 7.9
Return time (local time: UTC - 7)	2:52	1:10 – 3:45	21:34 – 4:56
Total distance traveled (km)	53.5	33.8 – 71.2	3.8 – 129.3
Number of trips	1	1 – 1	1 – 2
Days tagged	1	1 – 3	1 – 6
Pup age (days)	19	11 – 29	4-37
Day of the year	153	151 – 163	147 – 175

Table 2. 2 Median and interquartile values of all model covariate values for foraging sites, commuting sites, simulated foraging sites, and available sites.

	Parameter	*Abbreviation*	*Foraging*	*Commuting*	*Simulated*	*Available*
Dynamic remote sensing	log(Chlorophyll a concentration) (30-day composite, mg/m^3)	chla	1.75 (1.29 – 2.19)	1.7 (1.2 – 2.16)	1.57 (1.19 – 1.95)	1.14 (0.85 – 1.71)
	Sea surface temperature (30-day composite, º)	SST	21.77 (21.08 – 22.29)	21.77 (21.09 – 22.25)	21.78 (21.18 – 22.3)	22.06 (21.28 – 22.82)
Static	Distance from Isla Partida Norte (km)	D_{roost}	15.5 (8.79 – 21.35)	14.52 (7.51 – 20.9)	12.85 (7.11 – 18.36)	18.27 (9.34 – 29.1)
	Distance from nearest coast (km)	D_{land}	7.76 (3.93 – 12.37)	8.53 (4.17 – 12.81)	10.23 (6.16 – 13.5)	11.07 (6.74 – 16.54)
	Ocean depth (m)	bath	-374 (-910 – -112)	-378 (-834 – -113)	-557 (-1052 – -217)	-360 (-484 – -150)
	Ocean floor slope (º)	slope	0.1 (0.05 – 0.16)	0.11 (0.06 – 0.16)	0.13 (0.07 – 0.17)	0.04 (0.02 – 0.1)

Table 2. 3 Parameter estimates for combined static and dynamic hypothesis models across all scales.

Covariates are all scaled and centered before model fit. Estimates and standard errors are presented for parameters used in each model. Significant parameters ($p < 0.05$) are shown in bold.

Parameters	***Commuting***	***Simulated***	***Available***
Intercept	**-0.87 (0.2)**	**-10.01 (0.08)**	**-10.27 (0.14)**
bath	0.11 (0.12)	**0.09 (0.04)**	**0.28 (0.08)**
$bath^2$	**0.39 (0.13)**	-	**0.25 (0.04)**
chla	0.09 (0.11)	**0.2 (0.06)**	**1.0 (0.1)**
$chla^2$	-	-	**-0.14 (0.04)**
D_{land}	0.09 (0.11)	**-0.23 (0.06)**	**-0.32 (0.08)**
D_{land}^2	-	-	-0.06 (0.08)
D_{roost}	0.08 (0.11)	-0.11 (0.06)	**-0.62 (0.07)**
D_{roost}^2	-	-	**-0.17 (0.06)**
slope	0.14 (0.12)	**-0.12 (0.04)**	**0.82 (0.08)**
$slope^2$	**0.2 (0.07)**	-	**-0.23 (0.04)**
SST	-0.01 (0.1)	-0.02 (0.05)	**0.19 (0.07)**
SST^2	-	-	**-0.14 (0.05)**
year2016	0.1 (0.19)	0.02 (0.11)	**-0.32 (0.11)**
year2019	0.34 (0.42)	0.25 (0.23)	**0.54 (0.22)**

Table 2. 4 Models of Mexican fish-eating bat foraging site use during lactation on Isla Partida Norte in 2015, 2016, and 2019.

Model	Parameters	K	AIC	ΔAIC	Marginal R^2	Conditional R^2	CV cor (SE)	CV AUC (SE)
Foraging vs available								
Combined	~ $bath^2$ + $chla^2$ + D_{land}^2 + D_{roost}^2 + $slope^2$ + SST^2 + year	16	14174	0	0.50	0.50	0.96 (0.02)	0.81 (0.01)
Static	~ $bath^2$ + D_{land}^2 + D_{roost}^2 + $slope^2$ + year	12	14346	172	0.38	0.38	0.92 (0.03)	0.79 (0.01)
Dynamic	~ $chla^2$ + D_{roost}^2 + SST^2 + year	10	14379	205	0.45	0.45	0.97 (0.02)	0.79 (0.01)
Null	~ 1	2	15142	959	0	0	-	-
Foraging vs simulated foraging								
Combined	~ bath + chla + D_{land} + D_{roost} + slope + SST + year	10	15029	0	0.05	0.05	0.68 (0.11)	0.58 (0.02)
Static	~ bath + D_{land} + D_{roost} + slope + year	8	15039	10	0.05	0.05	0.70 (0.12)	0.58 (0.03)
Dynamic	~ chla + SST + year	7	15058	29	0.04	0.04	0.65 (0.12)	0.58 (0.02)
Null	~ 1	2	15147	118	0	0	-	-
Foraging vs commuting								
Static	~ $bath^2$ + D_{land} + D_{roost} + $slope^2$ + year	10	1390	0	0.03	0.03	0.43 (0.07)	0.55 (0.01)
Combined	~ $bath^2$ + chla + D_{land} + D_{roost} + $slope^2$ + SST + year	12	1393	3	0.03	0.03	0.44 (0.08)	0.56 (0.01)
Null	~ 1	2	1400	10	0	0	-	-
Dynamic	~ chla + SST^2 + year	6	1406	16	0	0	0.24 (0.07)	0.52 (0.00)

The full models for each hypothesis are reported as well as the null model for analysis of each scale. All models include individual night as a random effect. Distance from Isla Partida Norte (dist2roost) is also included in all models except for nulls. We report: K = number of parameters estimated, AIC = Akaike's Information Criterion, ΔAIC = the differences between the AIC of each model and the model with the lowest AIC score, marginal R^2 = marginal pseudo-R^2, and conditional R^2 = conditional pseudo-R^2 (Nakagawa and Schielzeth 2013), CV cor = cross validation average of the correlation of binned predicted values against expected used values, CV AUC = cross validation average of the area under the curve of predicted against true used values (Boyce et al. 2002).

Figures

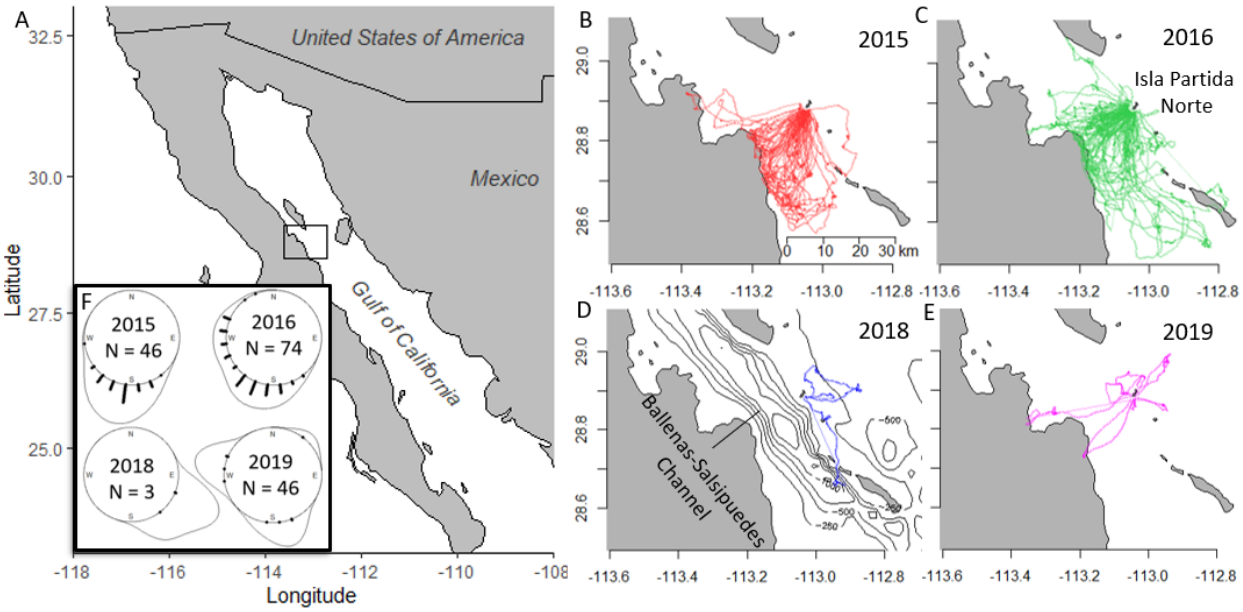

Figure 2. 1 Foraging paths of individual Mexican fish-eating bats.

Locations in 2015 (red, *n* = 19), 2016 (green, *n* = 29), 2018 (blue, *n* = 3), and 2019 (purple, *n* = 7) were recorded via GPS logger **B-E**. Depth contour lines are shown in black for the fine scale map around Isla Partida Norte in the map for 2018. **F.** Departure directions of foraging flights measured at 1 km from the roost are shown in radial histograms (bottom left corner). Number of trips per year is shown within each circle.

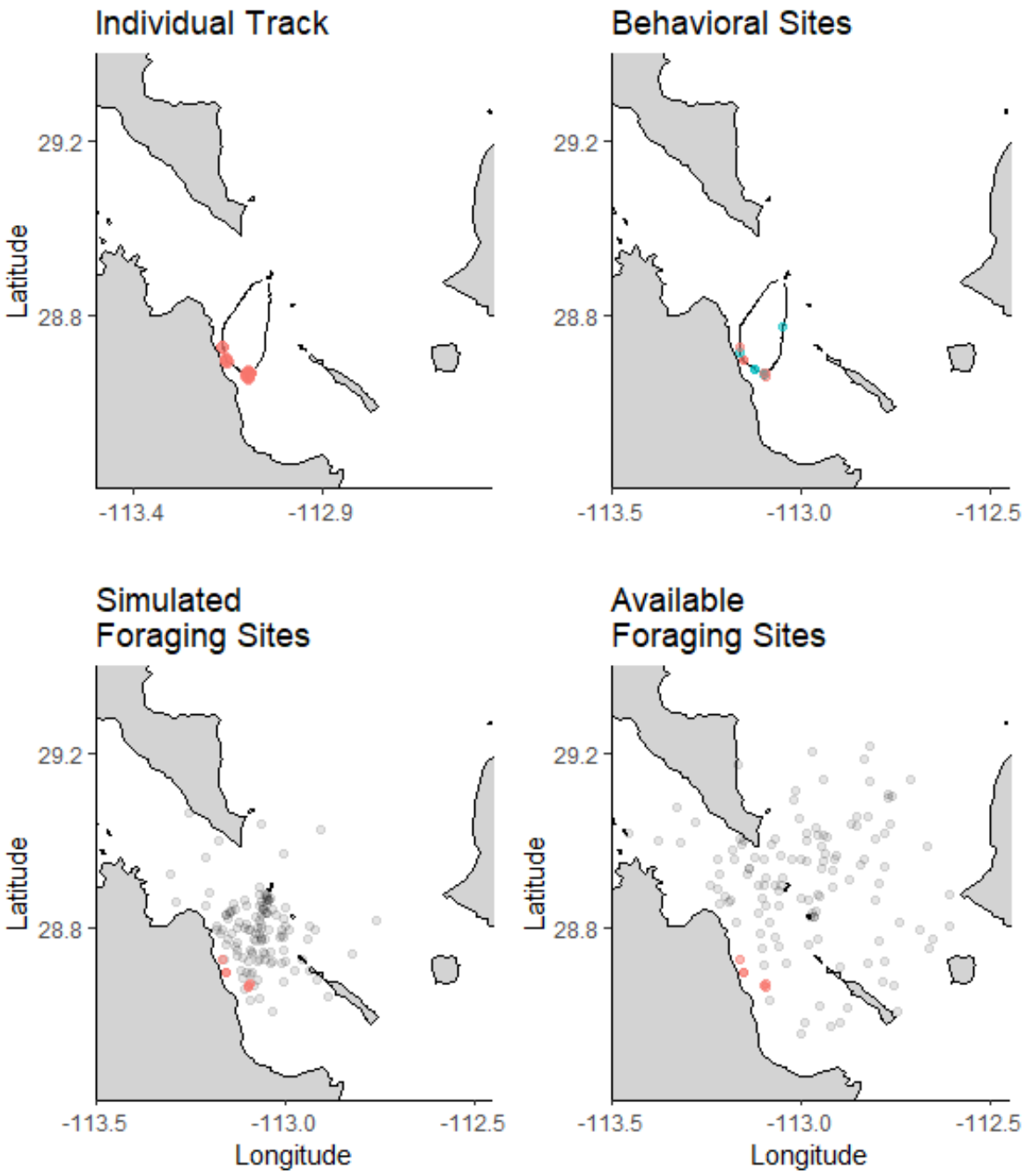

Figure 2. 2 Multi-scale habitat selection for a typical bat.

In the top right, the entire flight track (Mviv15_08 on 2015-05-31) is shown, with hidden-Markov-model-assigned foraging locations in red. The median locations of behavioral bout, i.e. foraging and commuting, are plotted on the track in red and blue

respectively. Pseudoabsences, predicted either by simulating foraging sites from sampling the angle and distance from origin of all foraging locations, or by sampling available foraging sites selected from a uniform direction and a uniform distribution between the minimum and maximum foraging site distances, are shown in grey circles. The ratio of pseudoabsence sites to recorded foraging sites is 20 to 1.

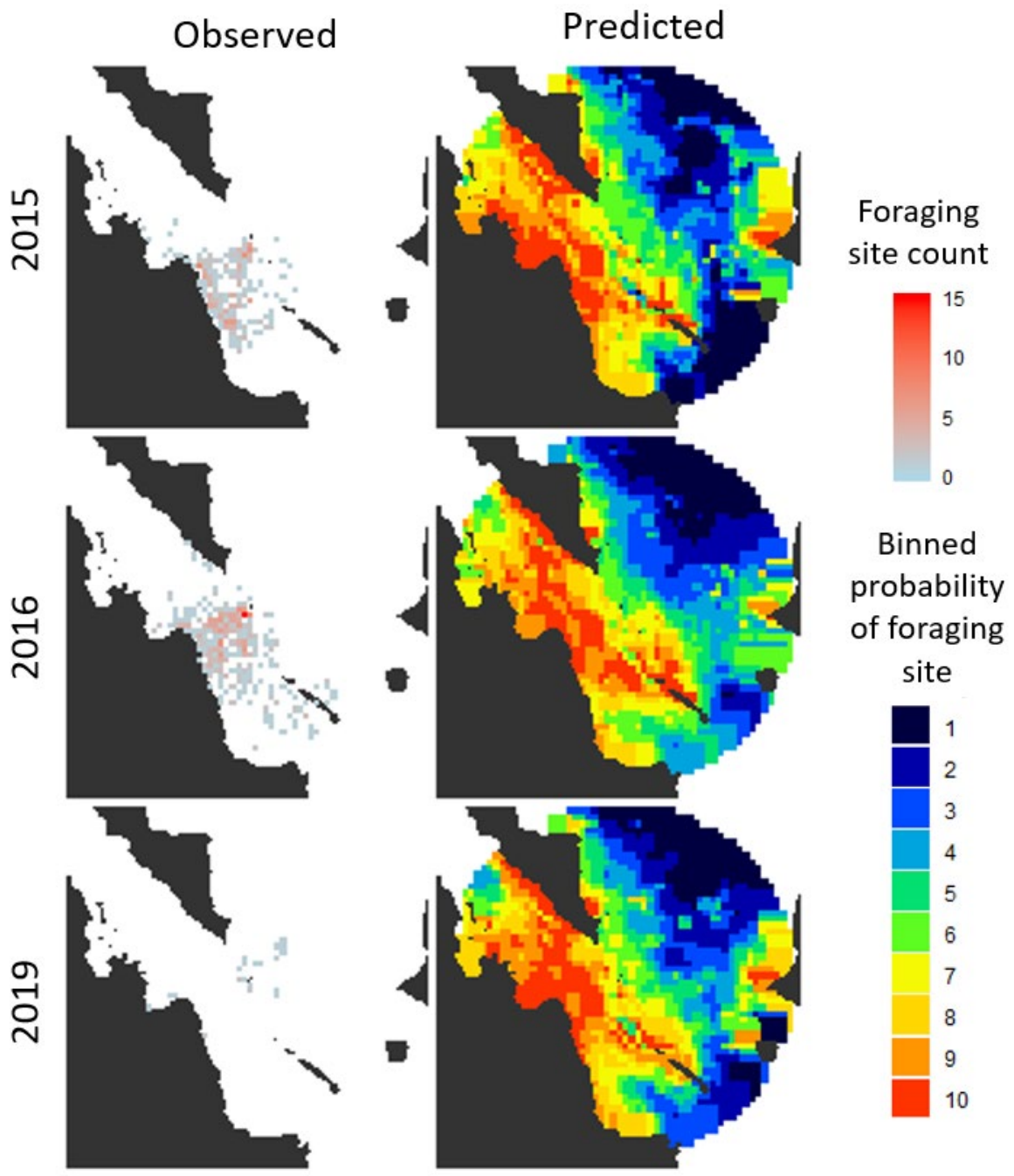

Figure 2. 3 Used and predicted foraging site use.

Predictions were generated from the combined dynamic and static model of foraging site use against available habitat. Available habitat for predicted maps was limited to within 50 km from Isla Partida Norte. Dynamic variables were sampled from the

median tracked day of each year (2015-06-02; 2016-06-06; 2019-06-14). Observed foraging site use is rasterized to the same grid scale as the environmental covariates. Predicted probability of use was binned into 10 groups of equal area.

Chapter 3: Function of in-flight social calls emitted by a marine foraging bat

Abstract

The function of social calls emitted in flight has received little study for the majority of bat species. Here we utilize playbacks and automated ultrasound recordings from off-shore stations and on-board data loggers carried by free-flying Mexican fish-eating bats, *Myotis vivesi*, to determine the function of a variable frequency-modulated social call. We identified in-flight social calls made by 17 of 31 lactating females carrying audio recording units and evaluated call context, impact on behavior, and information capacity to understand if these calls might be related to pup discovery, group formation or resource defense. While some social calls occur several kilometers from the roost before pups are volant, we find that most social calls occur late at night as bats return from foraging and approach roost sites. Social call occurrence increases with pup age and number of trips from the roost and calls contain highly repeatable elements that carry information on sender identity. In two trips, social calls were recorded in on-board recordings from nearby conspecifics in flight; however, the identity of the caller was unknown. Similar social calls are also produced within the roost, yet conspecific caller identification in roosts is also challenging. Our results are consistent with the hypothesis that social calls function primarily as directive calls to aid in pup localization by mothers as pups become old enough to move among roosts. Additional research on mother-pup interactions and vocal repertoires of pups is needed to confirm this hypothesis.

Introduction

Bats are highly social acoustic specialists capable of extensive vocal repertoires (Obrist 1995). While bat echolocation can convey information on species (Fenton and Bell 1981), sex (Neuweiler et al. 1987), age (Jones et al. 1993), individual identity (Brigham et al. 1989, Masters et al. 1995, Yovel et al. 2009), and behavior (reviewed in Bohn & Gillam, 2018; Chaverri, Ancillotto, & Russo, 2018), in-flight social calls (hereafter social calls) are not constrained to function for ranging or obstacle detection. Social calls are generally lower in frequency, longer in duration, and frequency modulated (FM) to allow for increased receiver detection (Wiley and Richards 1978, Bradbury and Vehrencamp 2011).

The function of most bat social calls falls into three main categories: social integration, conflict resolution, and courtship (reviewed in Bohn & Gillam, 2018). Social integration calls facilitate reunions and can enable recognition of individuals or groups. The most common call type, referred to as an isolation call, is emitted by young pups and is involved in parent-offspring reunions. This call type likely occurs in all bats (Gould et al. 1973), contains more information in species that form large colonies (Wilkinson 2003), and is heritable (Scherrer and Wilkinson 1993). In Egyptian fruit bats, these pup social calls can also be shaped by the conspecific calls around them (Prat et al. 2015, 2017). In some species (e.g. *Tadarida brasiliensis*, *Phyllostomus discolor*), females produce directive calls that elicit isolation calls from pups (Esser and Schmidt 1989, Balcombe 1990). Some species use contact calls to coordinate individuals within a group, typically around foraging sites, e.g. group-specific screech calls used by *Phyllostomus hastatus,* (Wilkinson & Boughman,

1998), or during roost site selection, e.g. Spix's disc-winged bats, *Thyroptera tricolor* (Chaverri, Gillam, & Vonhof, 2010) and pallid bats, *Antrozous pallidus* (Arnold and Wilkinson 2011). Bats also use social calls in instances of resource competition and conflict resolution. Captive big brown bats, *Eptesicus fuscus*, produce social calls in tandem flights that appear to claim prey (Wright et al. 2014). Wild lesser bulldog bats, *Noctilio albiventris*, will give honks to unfamiliar conspecifics, consistent with the "dear enemy" hypothesis (Voigt-Heucke et al. 2010). Mexican free-tailed bats, *Tadarida brasiliensis*, emit sinusoidal FM calls to mask buzzes of conspecifics to interfere with prey capture (Corcoran and Conner 2014). Bat social calls have also been described in courtship displays, functioning as songs and territorial displays to attract females and defend territories (reviewed in Smotherman et al. 2016b)

However, the function of in-flight social calls in wild bats is rarely determined (Corcoran & Conner 2014) due to the difficulty of monitoring individuals for extended periods of time. Most studies on in-flight social calls have used playback experiments (Barlow and Jones 1997, Boughman and Wilkinson 1998, Wilkinson and Boughman 1998, Arnold and Wilkinson 2011, Carter et al. 2012) or automated recordings (Bohn and Gillam 2018, Springall et al. 2019). Therefore, the behavioral context of the social call can remain elusive.

Here we combine playback experiments and automated recordings with data loggers which record GPS location and ultrasonic audio from individual Mexican fish-eating bats, *Myotis vivesi*, to provide information on the context of social call production. The Mexican fish-eating bat is found on islands throughout the Gulf of California, Mexico (Blood and Clark 1998, Flores-Martínez et al. 2004, Herrera M. et

al. 2019) and forages predominantly on schools of small fish and shrimp in the ocean at night (Otálora-Ardila et al. 2013). Data from GPS and ultrasonic audio loggers have revealed that these bats often forage near conspecifics, which allows them to eavesdrop on the foraging calls of neighbors to find ephemeral prey patches (Egert-Berg et al. 2018). While screening recordings for conspecific echolocation calls, in-flight social calls were detected in the audio recordings of several tagged bats (Fig. 3.1; Fig. S3.1).

In this study we aim to determine the function of these in-flight social calls by evaluating testable predictions about the context in which they are given, how individuals respond to playbacks, and the amount of information they contain (Table 3.1). This study was conducted on lactating females; therefore, we dismiss the possibility that social calls are used for courtship. We consider if social calls are used in three different scenarios: 1) parent-offspring communication, 2) group formation while foraging, or 3) conflict resolution. If social calls are used for social integration, we would expect calls to occur primarily around roosts and contain either individual or group level information. Directive calls used to communicate with pups and contact calls used to advertise a roost site to conspecifics would be expected to occur near roosts; however, directive calls should become more common as pups become volant, while contact calls used to coordinate roosting should occur near the roost independent of pup age. Furthermore, if in-flight social calls function as directive calls, we would anticipate their structure to remain similar within the roost when interacting with their pups. Both conflict resolution calls and foraging recruitment calls would be expected to occur near feeding buzzes, a stereotypic sequence of calls

given immediately before prey capture; however, we would expect conflict resolution calls to reduce the number of conspecifics, whereas recruitment calls should increase them. Using recordings from stationary microphones and tagged individuals, we examine whether time of night, day of year, duration of foraging, percentage of flight foraging vs commuting, conspecific presence, and pup age predict social call production.

Methods

Study site and animals

Sound recordings, playbacks, and bat measurements took place over four field seasons (late May to late June 2015 – 2018) on Isla Partida Norte, Gulf of California, Mexico (28° 53′ 16″ N, 113 ° 02′ 30″ W), a 1.4 km^2 island. The work was conducted under permits #7668–15 and 2492–17 from Dirección General de Vida Silvestre, permits #17–16 and 21–17 from Secretaría de Gobernación, and the University of Maryland Institutional Animal Care and Use Committee protocols, FR-15-10 and FR-APR-18-20. This island contains the largest known population of *M. vivesi.* Our work occurred just after pups were born and we worked predominantly with lactating females and their pups. Because of the demands of lactation (Millar 1977, Gittleman and Thompson 1988) females should be under constraints to forage as efficiently as possible and quickly return to their pups in the roost, although foraging success and pup age may influence this pattern (Wilkinson 1992).

Pup age estimation

To determine pup age, we calculated average postnatal growth rates and estimated birthdates based on pup size at initial capture. Early in pup development,

weight and forearm growth are linear in bats (Kunz 1974, Tuttle and Stevenson 1982). In a similar-sized congener, *Myotis myotis*, this linear growth occurs for the first 30 days, at which time the pup is approximately 80% of adult weight and 95% of adult forearm length (De Paz 1986). After capture, adult and juvenile bats were weighed to the nearest 0.1 g (Weighmax Classic 3805 Series Digital Scale) and forearm length was measured to the nearest 0.5 mm (Neiko 01407A Digital Calipers). Recaptured pups increased in weight by an average (± SE) of 0.33 ± 0.003 g/day and forearm length by 0.83 ± 0.002 mm/day. Newborn pups weigh ca. 6 g (Maya 1968; Blood & Clark 1998), which we validated with measurements from pups with attached umbilical cords (mean weight: 6.6 g, mean forearm length: 24.7 mm, N = 2). Weight and forearm length were linearly related in the pups we measured (linear regression, $R^2 = 0.88$, $p < 0.001$). Using this relationship, we estimated the average pup forearm size at birth (assuming birth weight: 6 g and forearm length: 25 mm). From these growth rates and average birth sizes, we calculated approximate birthdates for each pup. In 2015, only mass was measured, so age estimates are solely based on mass. In all other years, pup age is an average of estimates from mass and forearm length. We do not have measurements of the fourth-finger metacarpus-phalangeal joint, preventing us from estimating pup age beyond the linear phase of growth (Kunz 1982). Therefore, we likely underestimate the age of large pups by a few days.

Measurements of pup flight ability in *Myotis myotis*, a similar-sized congener, indicate that pups start flying when they have reached 96% of adult size, which is typically around 30 days (De Paz 1986). Mass of an adult fish-eating bat is typically 30 g and forearm length is 62 mm (Maya 1968; Fish & Clark 1998). Using this

threshold of adult size, we estimated that pups could be volant around 40 days of age. Previous studies estimate volancy at 45 to 50 days of age (Maya 1968, Blood and Clark 1998).

Context of social call production

Off-shore recordings

To record vocalizations from foraging bats, six buoys were anchored at approximately 100 m depth, roughly 600 m from the southern coast of Isla Partida Norte. Buoys were placed ca 600 m apart, although the exact position of each buoy changed with the tides (SD of buoy position: 100 m). Buoys were equipped with a Wildlife Acoustics SM2 Ultrasonic recorder, which was programmed to record audio continuously with 16-bit sampling at 192,000 Hz between 19:00 and 06:00 (local time: UTC - 7). Microphones were fixed atop a wooden pole 2 m above sea level to reduce echoes and noise from water. Recordings occurred from June 3 – 21, 2016, which corresponded with an average pup age of 19 – 36 days. Because of mechanical issues with microphones at some buoys and lack of bat presence at others, recordings from only two buoys were analyzed.

Audio files were saved as WAC (wave audio compressed format) and then converted to .wav files using WAC2WAV Wildlife Acoustics Audio Converter (Wildlife Acoustics, Concord, MA). Converted .wav files were typically around five seconds long. The first hundred files of each hour were manually checked for bat echolocation pulses and scored for feeding buzzes, social calls, and the presence of more than one bat as indicated by overlapping pulses or calls of multiple amplitudes (e.g. O'Farrell, Miller, & Gannon, 1999).

GPS and acoustic tagging

Bats were captured by hand in the morning from talus slopes. Lactating females weighing at least 28g were selected for tagging. Females do not fly with pups and typically return to capture locations to nurse pups after foraging, regardless of tagging. In 2015 and 2016, Robin GPS loggers (CellGuide Ltd., Israel) were attached to bats and in 2017 and 2018, Vesper GPS loggers (A.S.D., Israel) were used. Previous analysis of tagged bats revealed no significant difference in adult and pup weight change after tagging vs recapture when compared with radio telemetry controls (see Egert-Berg et al., 2018 and Hurme et al., 2019 for evaluations of tag weight on adult and pup weight change).

The percent of time audio was recorded, i.e. the duty cycle, varied between years, based on battery and storage capabilities of the tags, from 8% to 100%. The recording schedule of the tags for each year was as follows - 2015: 0.5 s recording every 5 s (N = 12), 2016: 5 s recording every 30 s (N = 2) and 5 s recording every 60 s, (N = 3) 2017: 7.5 s recording every 15 s (N = 7) and 35 s recording every 35s (N = 3), 2018: 7.5 s recording every 15 s (N = 4).

Response to social calls

Playback experiment

To test bat responses to social calls, we conducted playback experiments using social calls, feeding buzzes, or silence. For playbacks, we used an ultrasonic loudspeaker, (Ultrasonic Dynamic Speaker Vifa, Avisoft Bioacoustics, Germany) that was pointed to the sky. We used an Echometer Touch 1 (Wildlife Acoustics, Concord, MA) connected to an iPod Touch (6th Generation, Apple, Cupertino, CA)

to record bat activity. The microphone was placed 5 m from the speaker. The playback files were obtained from acoustic recordings on the bat (see GPS and Acoustic Tagging).

Playbacks were conducted on a western beach of Isla Partida Norte, approximately 200 m from the nearest roost. Trials began at 21:30 to avoid the peak in activity just after sundown. All three treatments were played back twice on each night, but their order varied randomly between nights. Each treatment playback lasted 5 min before a 1 min break and then the next treatment playback was played. Playbacks were performed on five nights (22 – 24 and 26 – 27, June 2017). These dates corresponded to estimated average pup ages from 28-33 days.

We analyzed recordings in Avisoft SASLab Pro (version 5.2.14, Avisoft, Germany) to identify and count individual bat vocalizations per trial. We used a highpass filter of 55 kHz and a -40 dB threshold with a 3 ms hold to capture only the high frequency harmonics of the echolocations calls. Because high frequencies are directional, this procedure assures that only bats approaching the speaker/microphone system are detected.

Distinctiveness of in-flight social calls

Acoustic measurements

On-board audio files were divided into 0.5 s segments and spectrograms of each recording were manually sorted into different call types. Social calls were defined as any call that showed increased duration or an upward modulation not characteristic of FM echolocation calls (Fig. 3.1; Fig. S3.1). Following Bohn et al. (2008), we define elements of the call as “syllables” and a call as a group of syllables

separated by less than 30 ms. Calls typically had two distinct syllables, with the first syllable often in a U-shape, followed by a break and then a downward sweeping syllable that is similar to an echolocation call (Fig. 3.1; Fig. S3.1). Feeding buzzes were distinguished by a short sequence of calls with increasingly shorter intervals and decreasing amplitudes (Schnitzler et al. 2003). Conspecific echolocation calls were identified as echolocation pulses occurring at a lower amplitude than the calls of the tagged bat (see Fig. S3.3). Calls occurring within the roost were characterized by higher background noise, presumably caused by the microphone scraping against rocks, and lower call amplitude resulting in a characteristically fuzzy signal (Fig. 3.1). For further analyses of similarity between roost and in-flight social calls we used bats for which we had recordings of at least eight in-flight social calls. We selected roost social calls that were the most distinct from the background noise; however, multiple bats often roost together so it is possible that a bat other than the tagged individual gave social calls recorded in the roost.

We analyzed vocalizations with Avisoft SASLab Pro (version 5.2.14, Germany). Measurements were taken from spectrograms generated using a 512-point fast Fourier transform and a FlatTop window with 87.5% overlap, which resulted in a frequency resolution of 195 Hz and a time resolution of 0.64 ms. To characterize in-flight social calls produced from tagged bats we measured seven parameters (Table 3.3). The start and end of syllables were measured from 20 dB below the peak amplitude of the entire call. Syllables were usually separated by a short silent period; however, in a few cases this break was absent and syllables appeared connected while remaining above the 20 dB threshold. To maintain consistent acoustic measurements,

we manually separated syllables at the lowest amplitude between syllables where breaks typically occur and assigned break values of 0.

Statistical Analysis

Context of social call production

We evaluated the context of social call production by fitting models to predict social call rate or occurrence using recordings either from stationary buoys or free-flying tagged bats. To predict the presence of social calls per hour of buoy recording we used a binomial logistic regression. Predictions of social call function require information on when calls are given, such as time of night, season, foraging activity, and social context (Table 3.1). Social calls related to foraging should occur near buzzes and conspecifics. Contact calls are expected at the beginning or end of the night. Directive calls are expected at the end of the night and during early pup volancy. If social calls correspond with pup development, we might expect a peak, as opposed to a linear increase, in social call activity per day, possibly corresponding to when pups are most likely to be volant. Accordingly, we model the presence of social calls per hour as a function of a quadratic term for day of year, hour of night in which the recording occurred, percentage of buzzes that occur in that hour, and percentage of recordings in an hour containing more than one bat.

To predict the presence of social calls recorded from tagged bats, we used a binomial generalized linear model to test for effects of estimated pup age, foraging duration, proportion of buzzes in a trip, and number of trips in a night on the presence or absence of social calls for each tagged bat night. A trip is defined as the sequence of recordings bracketed between departing and reentering a roost in a night. Flight

duration, or total time in a night spent away from the roost, may influence directive call occurrence as uncertainty of pup location is expected to increase with increased time away from the roost. Furthermore, we would expect pup age to influence social call production, as older pups are more likely moving around and require mothers to search for pups as they return to roosts. Increased number of trips in a night may also indicate bats searching for pups during the night. As with automated buoy recordings, close association of social calls with buzzes could indicate conflict resolution, such as bats defending a resource, or recruitment in which calls attract individuals to a resource. Number of buzzes in a flight was divided by total number of buzzes to create a variable that measured buzz activity independent of flight duration. Day of year and year effects did not significantly improve the model and so were removed from the final model.

Social call location in time and space

To investigate when social calls occur during flight, we measured the time between social calls and buzz sequences, conspecific calls, and arriving at the roost. To understand where in a foraging trip social calls occur, we calculated the median percentage in a flight in which social calls occurred (0% being the beginning and 100% the end of the flight) for all individual foraging trips. We then tested this distribution against a uniform distribution using a Kolmogorov-Smirnov test.

To test if social calls are associated with foraging or activities around the roost, we measured the time and distance (for tracks with GPS information) between social calls and the nearest buzz and roost visits. For individuals with GPS and audio recordings with social calls present (N = 8), we measured the Euclidean distance

between locations where social calls were emitted and the nearest buzz and roost visit. We tested if there was a significant difference between these times and distances using a Wilcoxon signed-rank test.

To test if social calls are related to conspecific presence, we used a two-minute interval before and after social calls to allow for multiple audio recordings from all programmed duty cycles and used a Wilcoxon signed-rank test to determine if conspecific presence changes with social call production.

For all analyses of social call context, time of night (UTC-7) was measured as hours from midnight, where before midnight is negative and after midnight is positive.

Playback experiments

We used a Wilcoxon sign-rank test to investigate pairwise comparisons between treatments with a Bonferroni correction. We also used a generalized linear model to investigate the effects of treatment, order, date, and time on the number of calls recorded. To normalize response values and account for trials with zero bat calls, we added one and then log transformed all counts.

Individuality and repeatability of call parameters

To test for individual distinctiveness of social calls, we performed discriminant function analyses (DFAs), using the R package "MASS" (Ripley et al. 2019), on all acoustic measurements to separate individuals in a multidimensional signal space defined by the acoustic parameters. For eight individuals, we selected between 6 and 39 calls. We randomly divided the calls per individual into training

and test sets (50% per set) and used the training set to calculate the discriminant function with which the test set was then classified.

To test for call stability and identify which components may be most important in individual recognition, we calculated the repeatability of each call parameter using the formula: $r = s^2_A/(s^2 + s^2_A)$, where s^2_A is the variance among individuals and s^2 is the variance within individuals over time (Lessells and Boag 1987, Bell et al. 2009).

To test for similarity between in-flight and roost social calls within an individual, we performed a DFA on roost social calls. Roost social calls were manually selected as social calls that resembled the frequency-modulated pattern of in-flight social calls and had a high signal to noise ratio (Fig. 3.1). We only included roost calls from individuals that were selected for in-flight call DFA. We evaluated the accuracy of the model for each individual and then used the model to predict the identity of the caller (as given by the in-flight social calls). Additionally, we calculated the spectrogram correlation coefficient between in-flight and roost social calls for each individual using Avisoft CORRELATOR (Avisoft Bioacoustics, Germany). For each individual correlations between social calls were grouped by all in-flight social calls, all roost social calls, and finally correlations between each in-flight and roost social call pair. We compared the median values of these three comparisons using a Kruskal-Wallis test for differences among the groups and then, if significant differences are supported, pairwise comparisons between all groups using a Wilcoxon-signed rank test.

All statistical analyses were conducted in R (R Core Team, 2019).

Results

Context of social call production

Social calls mostly appear at the end of the night

We manually screened all buoy recordings made during 20 consecutive days in June 2016 for bat activity and social call presence. Bats were present in 63% of recordings. In 17.6% of recordings only one bat could be discerned while in 45% of recordings more than one bat was present. Buzzes were detected in 3.4% of recordings and social calls in 1.5% of recordings. Social calls occurred in 15 of the 20 days with recordings.

Presence of social calls at offshore buoys significantly increases with hour of night and presence of multiple bats (Table 3.2). The model suggests that social calls are most likely to occur later in the night as bats are returning to the roost. The linear and quadratic terms for day of year were significant revealing a peak in social call activity over the recording period (Fig. S3.2). The proportion of recordings containing buzzes was not associated with the presence of social calls.

Occurrence of social calls increases with pup age

We manually scrutinized 73.5 h of audio recordings from tagged bats divided into 0.5 s files by behavioral context. We identified 41.4% recordings as roost and 58.6% recordings as in-flight, of which 2.2% contained buzzes and 0.1% contained in-flight social calls. Numbers of social calls identified per bat ranged from 1 to 197, with more social calls identified in recordings made with higher duty cycle ($r(29) = 0.42$, $p = 0.02$). Consequently, to compare the number of calls across years we adjusted the number of social calls by dividing total counts to the lowest recording

duty cycle (e.g. the number of calls detected in the 100% recordings were divided by 12.5 to normalize them to the 8% duty cycle). In-flight social calls from conspecifics were detected in two bats (Mviv15_24 and Mviv17_60), which were the latest bats tagged in the field seasons of each respective year and had pups that could have begun flying (estimated pup age for Mviv15_24: 29 days and population pup average for Mviv17_60: 29 days, Fig. S3.2).

A binomial linear model of presence of social calls per day for each bat revealed that social calls are more likely to occur with older pups and more trips from the roost (Table 3.2). Duration of flight and percentage of buzzes in the flight were not significantly related to presence of social calls.

Median social call time for each individual flight revealed that the majority of calls occur at the end of a flight (Kolmogorov-Smirnov test for uniformity, $N = 40$, $p < 0.001$, Fig. S3.4). Social calls occur closer to the roost than to buzzes, when measured in time (average of the median time difference in a flight from social calls to buzz: 51.9 min, social calls to roost: 3.3 min, $N = 40$, Mann Whitney U: $W = 157$, $p < 0.001$, Fig. 3.3A) and distance (average of the median distance in a flight from social calls to buzz: 11.3 km, social calls to roost: 1.2 km, $N = 9$, Mann Whitney U: $W = 46$, $p = 0.04$, Fig. 3.3B).

Response to social calls

Playback of social calls do not attract conspecifics

Response to playbacks as measured by call production was significantly different between buzz and social call treatments (Fig. 3.4). Call production in response to buzz playbacks was highest (mean ± SE, 249.7 ± 80.6 calls/trial) whereas

the response to social calls was significantly lower (32.0 ± 7.5 calls/trial) than the response to buzz calls but not significantly different from the control (silence: 14.1 ± 4.7 calls/trial).

Conspecific presence does not increase in response to social calls

Conspecific calls were present within 2 min of a social call in 110 of 190 calls inspected (58%); however, only 6 of the 32 individuals inspected had conspecifics present. Of those 110 calls, 26 social calls only had conspecifics present before the call was produced, 30 social calls only had conspecific calls after the social call was produced, and 54 social calls had conspecifics present both before and after the social call was produced. There was no significant difference in the number of conspecific calls before a social call versus after a social call by individual (paired Wilcoxon-signed rank test: $V = 28.5$, $p = 0.16$).

In-flight social calls are individually distinctive

To determine if calls contain information on individual identity, a DFA was trained on half of the social calls for eight individuals (N = 75; Fig. 3.5A). This model classified 85.5% of test set calls (N = 69) to the correct individual (individual accuracy: mean 82.9%, SD 20.1%), which was significantly higher than chance alone (Wilcoxon signed-rank test for matched pairs: N = 8, exact P = 0.007). Repeatability was significant for all measured acoustic parameters of social calls; however, some variables appear to carry more information about caller identity (Table S3.2). Frequency variables (peak frequency of first and second syllables) and duration of the first syllable had the highest repeatability, while other parameters were considerably lower.

Roost social calls were not as predictable as in-flight social calls. A DFA trained on half of the roost social calls for eight individuals classified 62.8% of test set calls (N = 86) to the correct individual (individual accuracy: mean 52.2%, SD 25.4%, range 0.2-0.88), which was also significantly higher than chance alone (Wilcoxon signed-rank test for matched pairs: N = 8, exact P = 0.007).

To determine if in-flight social calls were similar to roost social calls, we trained a DFA on roost social calls (N = 149), and predicted 53.4% of in-flight social calls (N = 144) to the correct individual (individual accuracy: mean 36.2%, SD 38.6%, range 0-97.4%). However, this prediction was not significantly higher than chance alone (Wilcoxon signed-rank test for matched pairs: N = 8, exact P = 0.14). Three individuals (Mviv15_06, Mviv17_34, and Mviv17_49) had no calls correctly assigned, while three other individuals (Mviv16_32, Mviv17_60, and Mviv18_02) had between 66.7 and 97.4% calls correctly assigned. Furthermore, spectrogram correlations across calls within individuals were significantly higher for in-flight social calls than for roost social calls or between inflight and roost social calls (Fig. 3.5B).

Discussion

Taken together, our results are consistent with in-flight social calls functioning primarily as directive calls emitted by adult females as they approach a roost. Buoy recordings reveal that social calls typically occur late in the night and recordings from tagged bats show that social calls are more likely to occur once pups are capable of moving in or between roost sites. Discriminant function analysis and repeatability estimates indicate that social calls contain information about individual

identity and resemble roost social calls, which often appear to occur in association with conspecific social calls, possibly from pups or another nearby adult (Fig. S3.6). Playback experiments and on-board recordings show that social calls do not elicit a strong response from nearby conspecifics, which is in agreement with the hypothesis that these social calls facilitate mother-pup reunions. These social calls are unlikely to influence conflict resolution as they did not occur near or during foraging events. In both passive and biologger recordings, buzzes were not significantly associated with social calls. Furthermore, it is unlikely that these social calls function as contact calls as we did not record them from all tagged bats and we rarely found conspecific social calls in on-board recordings. Direct observations of mother-pup reunions are, therefore, needed to verify that these calls are used as directive calls.

Seasonal context

Effective mother-pup communication facilitates localization, avoids non-intentional allosuckling, or aggression from other adults (Bohn et al. 2009). Mothers returning to roosts after foraging must navigate to their pups, which may be a daunting task when group sizes are large (Wilkinson 2003) or pups are beginning to fly. Mothers may use spatial memory (McCracken 1993) and olfactory cues (Gustin and McCracken 1987, Loughry and McCracken 1991, De Fanis and Jones 1995) to localize pups over short distances, but acoustic communication is more directional and travels longer distances (Bradbury and Vehrencamp 2011). Mothers consistently show attraction to pup isolation calls (Bohn et al. 2007), yet pups do not always discriminate among adult social calls (Balcombe 1990, Knörnschild and von Helversen 2008, Mayberry and Faure 2015). In these instances of unidirectional

recognition, mother echolocation or directive calls may still encode individual identity that is recognized by other adults (Brigham et al. 1989, Masters et al. 1995).

Pup age appears to influence in-flight social call production. In-flight mother-pup communication calls are expected to peak in activity when pups begin their foraging flights, likely because mothers may need to guide pups back to the roost (Wilkinson 1992; Bohn and Gillam 2018; Ripperger et al. 2019). Likelihood of in-flight social calls increased with pup age in tagged bats. Additionally, social calls from offshore recording reveal a peak in social call activity during buoy recordings in 2016. However, the population estimate of pup age during these recordings ranges from 19-36 days, which is likely too young for sustained flight. While this may be consistent with the first week of pup volancy for many of the bats on Isla Partida Norte, we lack observations of volant pups and recordings from different time periods to confirm this interpretation.

Flight context

In addition to pup age, number of trips, or departures from the roost, predicted in-flight social call production further supports the inference that directive calls function to help localize pups. Within a given night, social call production occurred predominantly at the end of flights when bats are returning to the roost and when making multiple trips in a night (Fig. 3.2). However, we did not find a significant relationship between duration of flight and social call production. It appears that number of trips better captures the variation in social call production. If females find their pup upon their first return from a foraging trip, they may not need to make in-flight calls or multiple trips. However, if a female is unable to locate her pup after

returning from a foraging trip, we would expect social calls and trips to increase as bats must leave the roost to locate their pup. Before pups achieve true powered flight, they often engage in wing flapping and fluttering flights within two weeks of birth (Powers et al. 1991, Mayberry and Faure 2015). Pre-volant fish-eating bat pups have been found crawling outside of roosts (Maya 1968) and these exploratory movements would increase the uncertainty in pup location. We would also expect that time away from roost and time of night should increase this uncertainty, as pups will have had more time to move around. Furthermore, a mother that is unsuccessful in searching for a pup may make several trips from the roost in an attempt to find her pup.

It remains unclear why social calls occur so far from the roost (Fig. 3.3). The median distances of social calls for some bats occur 2-3 km from the roost and in rare cases social calls are produced up to 20 km from the roost, clearly out of range of pre-volant pups. One possibility is that these calls are emitted toward pups that are flying near their mothers (Brown et al. 1983). It is also possible that social calls have more than one function and may be given to serve another as yet to be determined function.

Social context

In-flight social calls produced from nearby conspecifics may reflect an adult also searching for their pup or possibly in-flight mother-pup communication. In a few cases, we recorded conspecific social calls from on-board audio recordings which were given near social calls produced from the tagged individual (Fig. S3.3). While we did not knowingly tag bats with pups large enough for sustained flight, based on estimates from forearm measurements, it is possible that some individuals lacking pup measurements, such as Mviv17_60, had volant pups. Because we captured bats

by lifting stones in talus slopes, older pups could crawl away, which made identification of mother-pup pairs at capture difficult. While suggestive of in-flight mother-pup interactions, more data are needed to determine if newly volant pups emit in-flight social calls.

Social reaction

We observed little response from free-flying conspecifics to playbacks of social calls (Fig. 3.4). Additionally, only a small percentage of tagged-bat recordings containing social calls contained conspecific echolocation calls and of those with conspecifics, their presence appeared to occur evenly before and after the social call. Yet, in offshore recordings we do find a significant relationship between presence of social calls and recordings with multiple bats. This result may be the result of ascertainment bias if social calls are being detected simply because more bats are present rather than being associated with a particular social context. Automated recordings lack the contextual information provided by tagged bats or by playback experiments, so determining cause and effect is difficult.

Information content

The discriminability and repeatability of in-flight social calls are consistent with them acting as individual signatures, which is a prerequisite with mother-pup communication calls. On-board recordings provided many instances of multiple in-flight social call vocalizations from the same individual, which are rarely obtained in field conditions (Arnold and Wilkinson 2011). Accuracy of assigning a call to the correct individual was high (85% for all calls and on average, 82% by individual),

given that all social call recordings were opportunistic, and we were limited in the number of social call replicates per individual. As is common with DFA, classification success decreases with increasing number of individuals and increases with increasing numbers of vocalizations per individual and acoustic parameters measured per syllable (Beecher 1989). Roost social calls appear similar in structure to in-flight social calls; however, individual discriminability was more variable and correlations between calls was low within roost calls. We suspect this is due to the difficulty in distinguishing calls from the focal bat and a conspecific roosting together. Despite possible caller confusion for roost calls, three individuals had very similar roost and in-flight calls (accuracy between 66 and 97%). It is also possible that the acoustic environment of the roost affects the call structure. While tagged bat audio is suggestive of roost social calls being used during mother pup reunions (Fig. S3.6), we cannot confirm caller identity in roosts.

Mexican fish-eating bats can use eavesdropping on conspecific calls to locate foraging sites during foraging flights (Egert-Berg et al. 2018), yet little is known about their social behavior with relatives or near the roost. Indeed, little is known about social calls for the vast majority of bat species because it is difficult to observe the context of social calls in the wild (Arnold and Wilkinson 2011, Corcoran and Conner 2014). We found that social calls are mostly emitted when returning to the roost and are likely involved in mother-pup communication. This inference is further supported by the individual specificity of the social calls. Incorporating on-board recordings with a behavioral context and testing our hypothesis in a multifaceted way,

allows for a unique and comprehensive approach for understanding bat social call function.

Tables

Table 3. 1 Predictions for information, features, context, and impact of in-flight social calls (adapted from Bohn & Gillam, 2018)

Social Call Type	Information	Features	Social Context	Social Reaction	Flight Context	Seasonal Context
Parent-offspring	Identity	Long duration, vFM	Few bats present	↑bats	Returning to roost	Early pup volancy
Group formation	Identity – group/individual	Long duration, vFM	Few bats present	↑bats	Leaving or returning to roost; Near feeding	Continually
Conflict resolution	Resource holding potential, intent	Buzz, broad spectrum	Many bats present	↓bats	Near feeding	Continually

Table 3. 2 Estimated regression parameters, standard errors, z values, and p values for the logistic regression of in-flight social calls per hour of automated recordings and tagged individuals.

Variable	*Estimate*	*Std. Error*	*z value*	*P-value*
Offshore buoy recordings				
Intercept	-3.40	0.59	-5.73	> 0.001***
Hour of night	0.25	0.07	3.82	> 0.001***
Day of year	6.83	3.04	2.25	0.02*
Day of year^2	-10.27	3.23	-3.18	0.001**
Log(Percentage of recordings with more than one bat+1)	0.68	0.16	4.36	> 0.001***
Tagged bat recordings				
Intercept	-5.06	1.47	-3.44	> 0.001*
Pup age (days)	0.14	0.05	2.78	0.005*
Duration	0.00	0.00	0.94	0.35
Number of trips	0.39	0.18	2.22	0.026*
Percentage of flight time with buzzes	-5.10	18.10	-0.28	0.78

Table 3. 3 Acoustic variables used for discriminant function and repeatability analyses.

Acoustic Parameter	*Description*
Duration 1st Syllable (ms)	Duration from the start to the end of the first syllable of the
Peak Frequency 1st Syllable (kHz)	Frequency with the maximum energy density in the mean spectrum of the first syllable
Peak Frequency 2nd Syllable (kHz)	Frequency with the maximum energy density in the mean spectrum of the second syllable
Break between Syllables (ms)	Duration from the end of the first syllable and start of the second syllable
Difference in amplitude between syllables (dB)	Difference in peak amplitude between the first and second syllables
Slope of start frequency to peak frequency of 1st syllable (kHz/s)	Frequency over time measurements taken from the start to peak amplitude of the first syllable
Slope of peak frequency to end frequency of 1st syllable (kHz/s)	Frequency over time measurements taken from the peak amplitude to the end of the first syllable

Figures

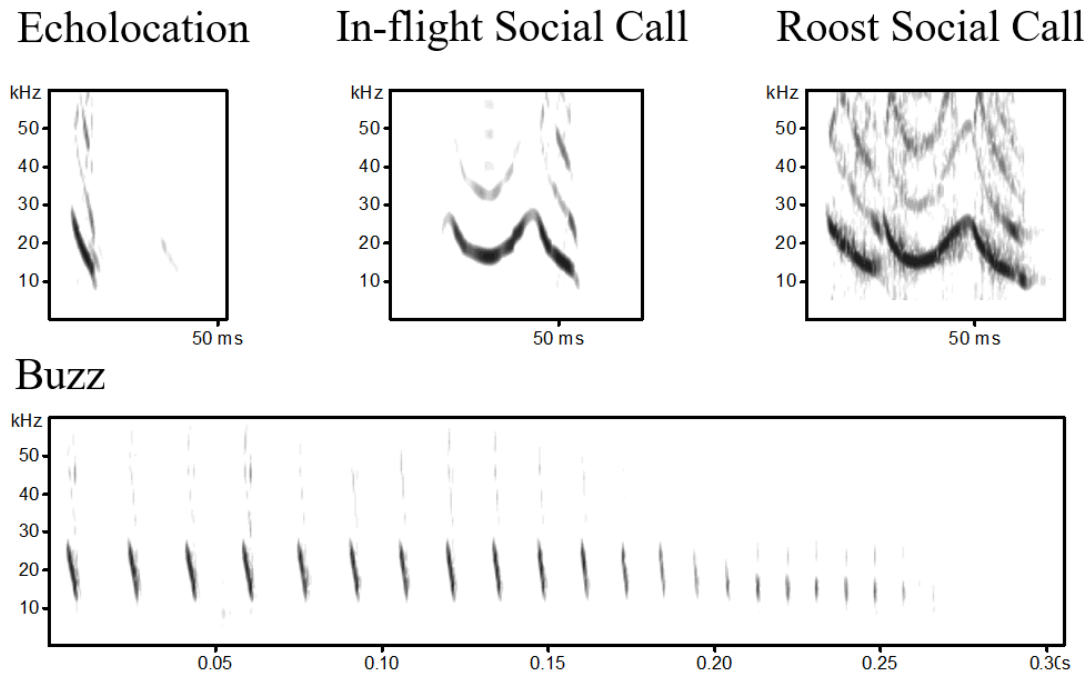

Figure 3. 1 Representative spectrograms of echolocation, in-flight and roost social, and buzz calls.

Echolocation and roost social call spectrograms include conspecific calls (defined by lower amplitudes) that follow and precede the calls from the focal bat respectively.

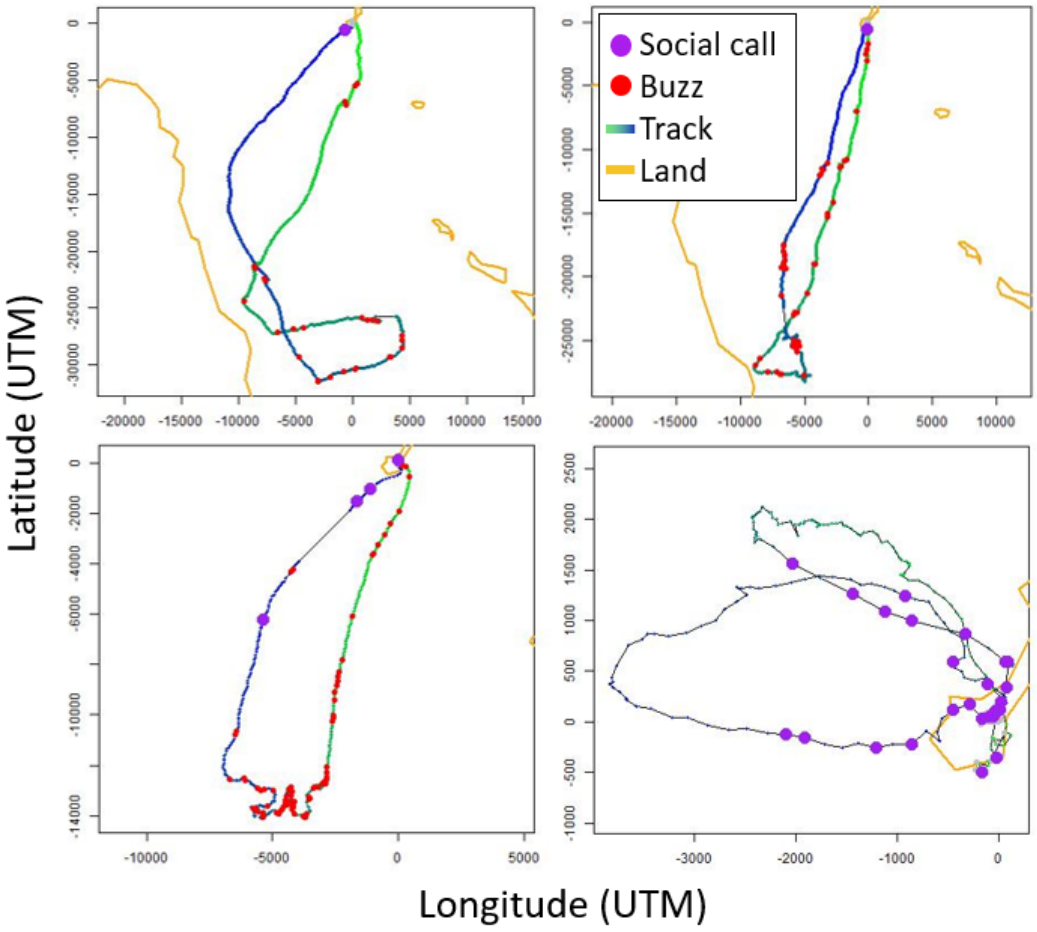

Figure 3. 2 Example tracks with in-flight social calls.

From top right to bottom left: Mviv15_08, Mviv15_12, Mviv15_24, and Mviv16_32. GPS fixes are color coded from transitioning from green to blue from start to finish. Purple circles reflect locations of social calls. Map coordinates are centered on the roost on Isla Partida Norte and orange lines reflects the extent of the surrounding land.

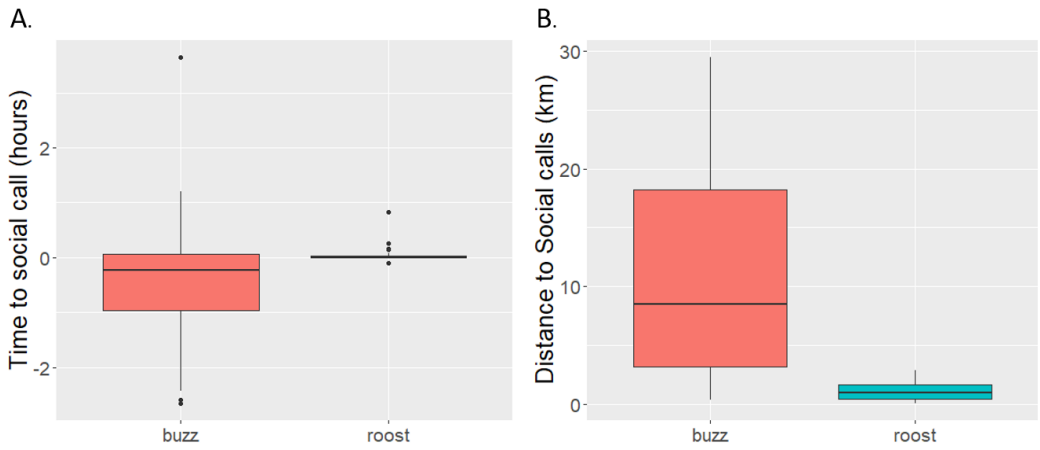

Figure 3. 3 Time and distance to social calls.

Box plots of the median A. time (N = 40) and B. distance (N = 8) from social call production to the nearest buzz or roost event per individual.

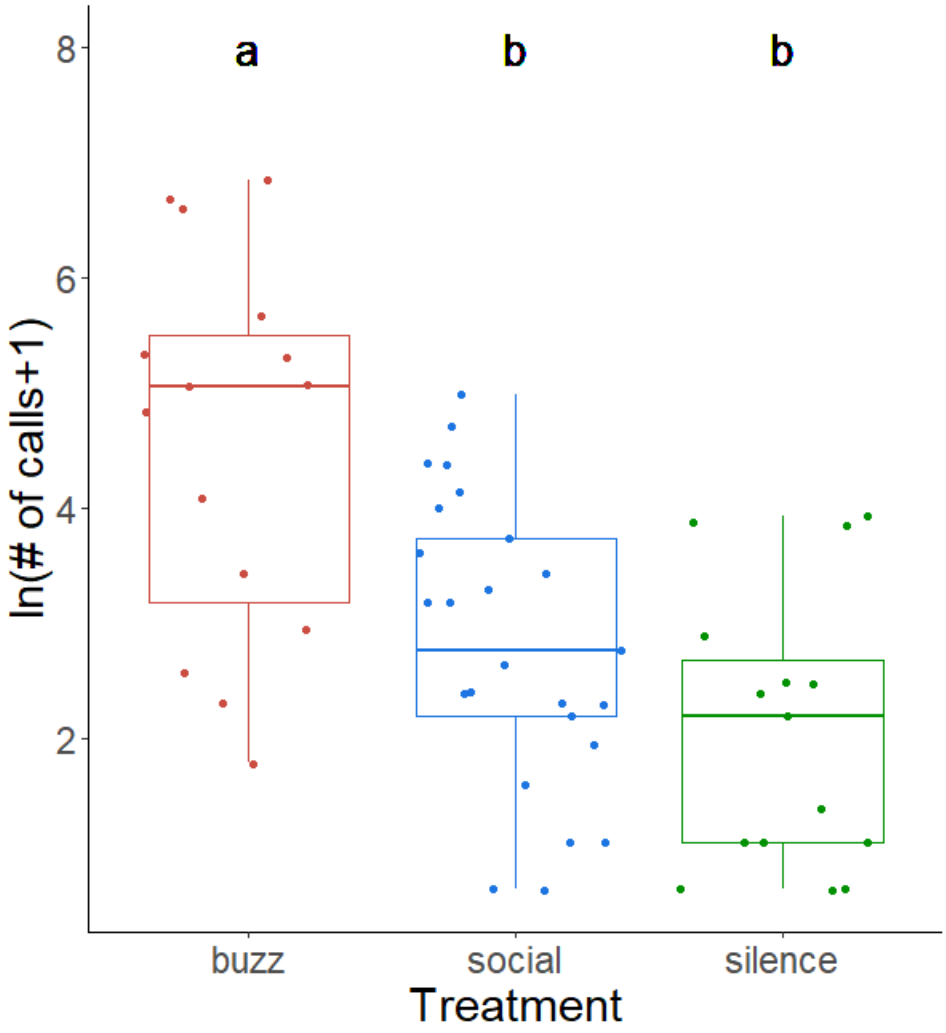

Figure 3. 4 Response to playbacks.

Boxplot of number of calls recorded during each ultrasonic playback by treatment. Number of calls is increased by 1 to adjust for zeros and then log transformed. Letters demonstrate significant differences in Wilcoxon signed-rank tests between

treatments.

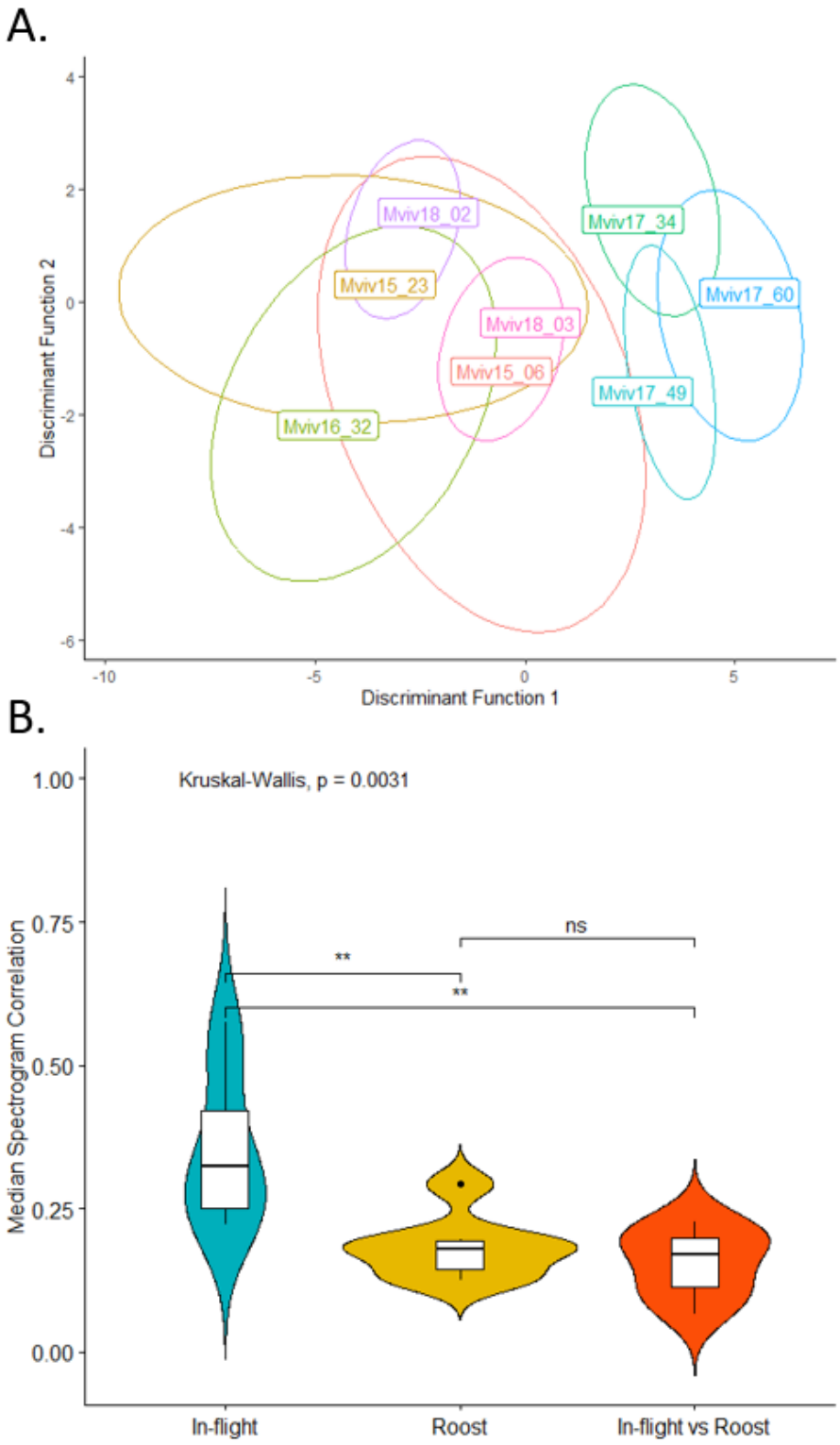
A.
Discriminant Function 2
Discriminant Function 1
Mviv18_02
Mviv15_23
Mviv18_03
Mviv15_06
Mviv16_32
Mviv17_34
Mviv17_60
Mviv17_49
B.
Kruskal-Wallis, p = 0.0031
Median Spectrogram Correlation
ns
**
**
In-flight
Roost
In-flight vs Roost

Figure 3. 5 Discriminability of social calls.

A. Centroids with 95% confidence intervals plotted for the first two discriminate functions from a linear discriminant function analysis of in-flight social calls (N = 8). B. Violin and boxplots of the median spectrogram correlation between social calls recorded in-flight, within a roost, or all in-flight and roost combinations for each individual. Wilcoxon-signed rank test comparison of groups showed a significant difference between median correlations between in-flight social calls and both roost social calls and in-flight and roost social call comparisons.

Chapter 4: Resource Ephemerality Drives Social Foraging in Bats

Summary

Observations of animals feeding in aggregations are often interpreted as events of social foraging, but it can be difficult to determine whether the animals arrived at the foraging sites after collective search (Krebs 1974, Clark and Mangel 1986, Wilkinson 1992a, Giraldeau and Caraco 2010) or whether they found the sites by following a leader (Flemming et al. 1992, Bumann and Krause 1993) or even independently, aggregating as an artifact of food availability (Barclay 1982, Grünbaum and Veit 2003). Distinguishing between these explanations is important, because functionally, they might have very different consequences. In the first case, the animals could benefit from the presence of conspecifics, whereas in the second and third, they often suffer from increased competition (Danchin et al. 2004, Dall et al. 2005, Hancock et al. 2006, Codling et al. 2007, Giraldeau and Caraco 2010, Sumpter 2010). Using novel miniature sensors, we recorded GPS tracks and audio of five species of bats, monitoring their movement and interactions with conspecifics, which could be inferred from the audio recordings. We examined the hypothesis that food distribution plays a key role in determining social foraging patterns (Wilkinson and Boughman 1999, Dechmann et al. 2009, 2010). Specifically, this hypothesis predicts that searching for an ephemeral resource (whose distribution in time or space is hard to predict) is more likely to favor social foraging (Danchin et al. 2004, Hancock et al. 2006, Dechmann et al. 2009, 2010) than searching for a predictable

resource. The movement and social interactions differed between bats foraging on ephemeral versus predictable resources. Ephemeral species changed foraging sites and showed large temporal variation nightly. They aggregated with conspecifics as was supported by playback experiments and computer simulations. In contrast, predictable species were never observed near conspecifics and showed high spatial fidelity to the same foraging sites over multiple nights. Our results suggest that resource (un)predictability influences the costs and benefits of social foraging.

Results and Discussion

We compared the movement and social foraging behavior of five bat species (representing four families), which cover a wide range of foraging styles and exploit different resources (see Table 4.1). Two species rely on ephemeral resources (henceforth the "ephemeral foragers"): (1) the greater mouse-tailed bat (*Rhinopoma microphyllum*, Rhinopomatidae), an open-space insectivorous bat that preys on ephemeral insect swarms (Levin et al. 2013), and (2) the Mexican fish-eating bat (*Myotis vivesi*, Vespertilionidae), which forages primarily over marine waters (Flores-Martínez et al. 2004, Otálora-Ardila et al. 2013), where it feeds on local upwellings of fish and crustaceans (Flores-Martínez et al. 2004, Otálora-Ardila et al. 2013) whose exact location is difficult to predict on any given night. Indeed, our analysis of the spatial distribution of marine chlorophyll (a proxy of marine food availability (Paiva et al. 2009, Péron et al. 2010)) indicates low predictability of food spatial distribution over consecutive nights (Fig. S4.1). Two additional species rely on plants which provide predictable stationary food resources (henceforth the "predictable foragers"): (1) the lesser long-nosed bat (*Leptonycteris yerbabuenae*, Phyllostomidae), a

nectarivorous (and occasionally frugivorous) bat foraging on cactus pollen and nectar, which are predictably available at the same plants during our monitoring periods (Fleming et al. 1996), and (2) the Egyptian fruit bat (*Rousettus aegyptiacus*, Pteropodidae), which feeds at trees that offer fruit continuously for weeks (Korine et al. 1999). Our fifth species, the greater mouse-eared bat (*Myotis myotis*), gleans terrestrial insects (e.g., beetles and crickets) from the ground (Arlettaz 1999) and can therefore also be considered a predictable forager because these insects commonly occur in large numbers in the same patches over many consecutive nights (Rodríguez-Muñoz et al. 2010). We first use GPS data to compare the movement of these five species and then use on-board audio recordings to test the hypothesis that ephemeral foragers use group searching whereas predictable foragers do not. For further support, we model the foraging behavior of the ephemeral forager (*M. vivesi*) and the predictable forager (*M. myotis*) with the most data and use playback experiments to determine whether these two species differ with regard to conspecific attraction (Gillam 2007, Knörnschild et al. 2012).

Food Predictability Shapes Foraging Patterns

Individuals of all five species flew many kilometers each night, spending several hours foraging outside the roost (Table 4.2), but several movement patterns varied in accordance with their reliance on ephemeral or predictable resources (Fig. 4.1 and S4.2):

(1) The spatial fidelity—the distance between the two closest foraging sites visited on consecutive nights—was large (>1 km) in bats relying on ephemeral food and small (<50 m) in bats relying on predictable food (Fig.

4.1B; $F_{1,4} = 22.1$, $p = 0.01$, nested ANOVA with species nested within foraging style and defined as a random effect; see STAR Methods for how foraging sites were inferred). Whereas ephemeral foragers had to search nightly for feeding sites, predictable foragers returned to the same sites night after night. For example, a mouse-eared bat returned to the same site on seven consecutive nights (Fig. S4.3), and an Egyptian fruit bat returned to the same tree 20 nights in a row.

(2) Predictable and ephemeral foragers also differed in temporal variability, estimated as the coefficient of variation (CV) of activity time (total time spent away from the roost) on consecutive nights. We calculated the CV of the activity time, that is, the SD of the activity time over all nights divided by the mean activity time. Ephemeral foragers exhibited a substantial CV, ≥50%, whereas predictable foragers were significantly more consistent, spending very similar amounts of time on the wing night after night (mean CV < 15%, $F_{1,4} = 22.7$, $p < 0.01$, nested ANOVA; Fig. 4.1C). In a previous study, we used audio recordings on board *Rhinopoma* to show that the number of attacks on prey often varies between nights and does not correlate with searching time, thus demonstrating the uncertainty faced by ephemeral foragers (Cvikel et al. 2015a).

(3) Predictable foragers visited fewer foraging sites per night than ephemeral foragers (Table 4.2; fewer than six versus more than eight sites per night, respectively; $F_{1,4} = 9.0$, $p < 0.06$, nested ANOVA).

Although predictable foragers repeatedly visited the same foraging sites, they still flew as far as ephemeral foragers in order to obtain food (Fig. 4.1 and Table 4.2). Even mouse-eared bats never started foraging near the cave. Instead, they flew far, often passing above foraging grounds that seemed suitable. The median distance to foraging sites in this species was 14.8 km (n = 15 bats), with one bat flying ~32 km to a site. In contrast to ephemeral foragers, however, fidelity to a foraging site over several nights was high for mouse-eared bats (Fig. S4.3), with some bats repeatedly foraging in a 100 m radius area (Fig. S4.3). Relying on a predictable resource thus does not necessarily mean commuting less. When good roosting sites are rare, predictable foragers will often prefer to roost together and commute far.

Bats that Rely on an Ephemeral Resource Searched in a Group

Because the studied species all roost in colonies with hundreds to thousands of individuals (Table 4.2), the chances of tracking two bats that moved together was very low. On-board audio recording offered a unique window into the sociality of these species, as we could detect when bats encountered conspecifics from their calls. There was a clear difference in the social foraging behavior of the ephemeral and the predictable foragers. In brief, ephemeral foragers moved in groups, and predictable foragers did not (all results below are based on data from all bats from which we had audio; Table 4.1). Fish-eating bats commuted with conspecifics during the entire night (cf. Video S4.1, which presents the encounters for several bats). They commuted very close to conspecifics at least 6.5% of the time (median; quartiles 4.2%–8.2%; conspecific percentage was defined as the percentage of audio files with conspecific calls, and we did not differentiate between files with few or many

conspecific calls). Note that due to the limited sensitivity of our on-board microphone, we could only record conspecifics when they came as close as 12 m to the bat carrying a microphone (Cvikel et al. 2015b). Because the bats' hearing range for conspecific calls is far larger (can reach up to 185 m), there were most likely many more conspecifics within eavesdropping range that we did not detect. Indeed, when using a new tag version (Vesper) with better audio sensitivity (and a detection range of ~50 m), we estimated a conspecific encounter rate of 55% (n = 1 bat). Moreover, as we recorded a 0.5 s sound file every 5 s, an encounter rate of 6.5% means that on average there was a nearby conspecific every 1.25 min, suggesting that there were many more conspecifics beyond the reach of our microphone. We observed a similar encounter rate (~8%) in the second ephemeral forager (Rhinopoma microphyllum) in a previous study (Cvikel et al. 2015a). For comparison, in all three predictable species, we detected no conspecific calls during commutes (absolute zero). To make sure that this was not due to technical limitations, such as the different sensitivity of our microphone at different frequencies used by the predictable species, we recorded bats from these three species with our new and more sensitive Vesper tag, thus assuring that the detection range of conspecifics was higher for the three predictable species than for the two ephemeral species (see STAR Methods). Even with these more sensitive tags, we never recorded any conspecifics near the predictable species. Moreover, because Rousettus bats do not always echolocate while commuting, we used the movement data of bats in our colony, including 3,605 GPS tracks collected from 96 individuals and 15,551 events of bats entering and leaving the colony (collected from 150 individuals), to determine

whether bats ever depart or travel together. Analysis of this immense dataset strongly suggests that Rousettus do not leave the colony in groups and do not commute in groups when searching for food (see STAR Methods).

Foraging Patterns Deviate from Random

For the two species with the most tracking data (39 fish-eating bats and 18 mouse-eared bats; Table 4.1), we simulated independently moving bats with random conspecific encounters to test whether the observed conspecific encounter rates could be explained purely by the bats' density and movement patterns. We used observed data to characterize the movement patterns and the foraging areas of these two species (Fig. S4.2C and S4.2D). In fish-eating bats (ephemeral foragers), the observed conspecific encounter rate was four times higher than expected by chance during commuting (medians: 6.5% versus 1.6%, $p < 0.0001$; permutation test on the median, n = 100 simulations of 10,000 bats), supporting the hypothesis that fishing bats intentionally search in groups (Fig. 4.2A and 4.2B). The observed conspecific encounter rate at foraging sites was more than two times higher than expected by chance (medians: 27.5% versus 12.8%, $p < 0.0001$; permutation tests on the median, n = 100 simulations of 10,000 bats), which further supports our inference that these bats move in groups because distant unpredictable feeding sites would not be found by multiple bats simultaneously unless they commuted together. In mouse-eared bats (predictable foragers), conspecific encounter rate was significantly smaller both during commuting and foraging than expected by a random process (medians: 0.0% versus 0.1%, quartiles 0%–0% and 0%–0.2%, $p = 0.001$; and 0.0% versus 0.2%, quartiles 0%–0% and 0.3%–0.5%, $p = 0.0001$, respectively; permutation tests on the

median, n = 100 simulations of 4,000 bats). Unlike the ephemeral forager, mouse-eared bats thus do not aggregate, and in contrast, most likely actively avoid conspecifics.

For the fish-eating bat, we also compared the temporal variation in conspecific encounter rate (i.e., how encounter rate changes over time during a night) between observed and simulated data. Observed bats encountered conspecifics at a constant rate during the entire night (Fig. 4.2C, gray line), as would be expected if the bats intentionally moved together. Because bats often foraged while returning to the island, as evidenced by recorded echolocation attack sequences, it is reasonable that the conspecific encounter rate remained high when heading home (Fig. 2C, gray line). In contrast, the conspecific encounter rate for simulated flights was greatest early in the evening (when bats emerge from their roost) and decayed to nearly zero within ~1.5 hr, as the bats dispersed (Fig. 4.2C, black line).

Eavesdropping Is Limited to Social Foragers

Finally, we performed a playback experiment with the two species that we modeled to confirm that ephemeral foragers eavesdrop and follow a searching conspecific, whereas predictable foragers do not. We placed an ultrasonic speaker at locations where we previously observed individuals commuting to foraging sites. We measured attraction to the playback speaker using echolocation sequences of flying bats to score approaches and passes (see STAR Methods). We compared attraction to three playback treatments: (1) conspecific search calls, or recordings of calls emitted by conspecifics that are searching for prey; (2) conspecific feeding buzzes, or recordings of calls emitted by conspecifics that have found prey and are attacking it;

and (3) noise, or pulses of noise with the same duration, rate, and bandwidth as the search calls of each species.

The two species clearly differed in their responses to the playbacks (Fig. 4.2D and S4.4). Fish-eating bats were significantly more attracted to playbacks of conspecific search and buzz calls in comparison to noise (~5 and ~15 times more, $p < 0.04$, for the comparisons of search versus noise and buzz versus noise, respectively; Wilcoxon signed-rank test, after Bonferroni correction). Likewise, we have previously shown that *R. microphyllum* (the other ephemeral species) is also attracted to conspecific search and buzz calls to a similar degree (Cvikel et al. 2015a). In both cases, many bats flew close to inspect the speaker. In contrast, mouse-eared bats did not approach any playback ($p > 0.1$ for all comparisons, Wilcoxon signed-rank test).

Conclusions

Our data indicate that resource predictability correlates with foraging style. Of the five bat species that we studied, the two species relying on ephemeral resources intentionally aggregated while searching for food, whereas the three that rely on predictable resources were never observed near conspecifics during search. Neither body mass nor colony size could explain these differences in social foraging (Table 4.2). Why should ephemeral bats search in groups? In a previous study, we used a computer simulation to show that group foraging bats can gain information about the location of prey by remaining within eavesdropping range of conspecifics (Cvikel et al. 2015a). Interestingly, the terminal frequency of the fish-eating bat's echolocation signal (~18 kHz) is surprisingly low for a *Myotis* bat. Because low frequencies

attenuate less, this should enable conspecific eavesdropping up to ~185 m (assuming a dynamic range of 120 dB between the emitter's intensity and the receiver's detection threshold).

Importantly, the advantage of group searching as described above would hold for any animal that can estimate the positions of neighboring conspecifics (to some degree) using any sensory system. Bats' reliance on sound is not a prerequisite, and visual animals could benefit from similar behavior. For example, scavenging birds of prey (Jackson et al. 2008, Harel et al. 2017) can visually detect a conspecific circling a carcass from many kilometers, and marine birds can spot diving neighbors (Wilkinson and Boughman 1999). Likewise, a bird searching for seeds can observe pecking behavior of a conspecific from a greater distance than it can detect an individual seed. This can sometimes also lead to producer-scrounger dynamics (Katsnelson et al. 2008).

The relationship that we found between resource ephemerality and foraging sociality does not demonstrate causation. In addition to the unpredictability of the resource (in time and or space), several additional conditions (which often, but not always, correlate with resource ephemerality) should influence social foraging patterns. These include (1) patch abundance, i.e., a patchy resource with food that it is sufficient to provide food for many foragers once found, and (2) sparseness, which means that the resource is rare and necessitates exhaustive searching. Note that in theory, a resource could be ephemeral but not sparse. In the case of the fish-eating bat, not only is the resource patchily distributed and hard to predict in space, but it is also time limited, as it appears at the surface for a short time and then can quickly

dive beyond the bat's reach. Perhaps this is why bats spent 9 min, on average, in a patch before departing. Such a short-lasting resource might also encourage social foraging because a single individual only has time to consume a portion of the patch before it disappears, so competition between individuals should be reduced (Clark and Mangel 1986). Nevertheless, even when all of these conditions are met, social foraging may not occur. Moreover, other forms of social interactions can influence foraging. For example, mouse-eared bats were solitary both when flying to foraging sites and when searching for prey at foraging sites. Field researchers have reported observing individuals of this species actively defending foraging sites (C. Dietz, personal communication). Such behavior is only economically beneficial when the resource is defendable. In comparison, the nectarivorous and frugivorous species that we monitored exhibited different forms of social foraging. These two species did not search for food collectively, but they were observed at foraging sites in groups, occasionally interacting on a fruit tree (*Rousettus*) or chasing each other around a cactus (*Leptonycteris*). Such social interactions do not influence searching, but they could enable information transfer (Ward and Zahavi 1973, Wilkinson and Boughman 1998) or result in competition (Schoeman and Jacobs 2008). Social foraging can have different causes and more field data are required in order to reveal its origin and underlying functions. This study illustrates how new technologies can shed new light onto fundamental questions in behavioral ecology, such as social foraging, and how bat diversity can serve as a comparative and representative toolbox for mammals in general.

STAR Methods

Contact for Reagent and Resource Sharing

Further information and requests for resources should be directed to and will be fulfilled by the Lead Contact, Yossi Yovel (yossiyovel@gmail.com).

Experimental Model and Subject Details

Data acquisition and analysis

Animal capture and experiments in Bulgaria, Mexico and Israel were conducted under permits of the responsible authorities (Bulgaria: MOEW-Sofia and RIOSV-Ruse, permit # 465/29.06.2012 and 639/28.05.2015. Mexico (*M. vivesi*): permits # 7668-15 and 2492-17 from Dirección General de Vida Silvestre, and permits # 17-16 and 21-17 from Secretaría de Gobernación, and the University of Maryland Institutional Animal Care and Use Committee protocol FR-15-10; Mexico (*L. yerbabuenae*): permit # 04019/15, 03946/15 14509/16 from Dirección General de Vida Silvestre. Israel: (*R. microphyllum* and *R. aegyptiacus*): permits # 2011/38346 and 2012/38346 from the NPA, and # L-11-054 from the Tel-Aviv University IACUC.

Method Details

Animal Monitoring

M. vivesi data acquisition in Mexico took place during May and June of 2015-2016 in Partida Norte Island, Mexico (28°52′30”N, 113°02′17”W). Lactating females that had pups were tagged. Moreover, the pups did not lose weight over this short period (pup weight increased (non-significantly) by 0.02 r, on average, $p > 0.9$,

Wilcoxon signed rank test, n = 10 pups). All bats were captured in their roost in the morning (around 10.00AM), mounted with the devices within an hour from capture, and released where they were caught. Data acquisition for *L. yerbabuenae* bats was performed in El Pinacate y Gran Desierto de Altar Biosphere Reserve, Sonoran Desert, Mexico, during May-June 2015-2017 where we tracked post-lactating females. In Bulgaria, post-lactating females of *M. myotis* were tracked between July and August of 2013 and 2015. They were caught with a harp trap at Orlova Chuka cave in northeastern Bulgaria when exiting the cave in the evening, tagged at the site and released. We collected data for *R. microphyllum* bats in northern Israel during the summers of 2012-2013 (see ref Cvikel et al. 2015a). The *R. aegyptiacus* bats that we tracked were males captured in two caves in central Israel (Beit Govrin and Herzelia). We collected data for this species during February-June 2012-2015. All bats were processed and tagged within 2 hr and released at the cave. Additional bats from all species were tagged with light telemetry tags for comparison (see details below). Tags in all sites were retrieved by recapturing the bats after several days or by retrieving them from the ground after they fell off the animals.

In Mexico, Bulgaria and Israel the microphone and tracking device (30 × 20 × 4 mm) consisted of a GPS data-logger (Lucid Ltd., Israel) and a synchronized ultrasonic microphone (FG-23329, Knowles). The device's total weight (including battery, coating and a telemetry unit—LB-2X 0.3 g, Holohil Systems Ltd. Carp, Ontario, Canada) was 4.3 g on average (see discussion of weight effects below). The telemetry unit was attached to the device helping the experimenters to locate it. The devices were wrapped in colored balloons for water proofing and were attached to the

bats using medical cement glue (Perma-Type Surgical Cement, AC103000, McKesson Patient Care Solutions, Inc., Moon Township, PA, USA). After gluing, bats were held for about 5 min to allow the glue to dry, and then placed in a cloth bag for another 15 min before releasing (see ref (Cvikel et al. 2015a, 2015b) for full details). In case of recapture, the device was gently removed from the recaptured bats by cutting the fur that was attached to the tag. The tags remained on the animals for < 4 days on average (and up to 9 days at most). The microphone was positioned on the bat's back in between the shoulders, ca. 2 cm behind the bat's mouth, thus ensuring very high signal-to-noise ratio. Audio was sampled at 192 kHz. Due to the limited battery life and memory capacity when operating the microphone, we recorded a 0.5 s audio window every 5 s (10% recording duty cycle). GPS points were sampled at 15 s intervals. One *L. yerbabuenae* and one *M. vivesi* were sampled with a new tag (Vesper, ASD inc. Israel) with audio recorded at 200 kHz (using an on-board microphone, FG-23329, Knowles) in segments of 20 s every 30 s.

Because Rousettus bats do not always echolocate while commuting, we also analyzed GPS tracking data collected over 14 months in our in-house wild colony of fruit-bats. Bats in this colony (N = 30-50 individuals) roost in Tel-Aviv University and fly out to forage in the wild. They behave like bats in the nearby wild colonies. They fly similar distances, visit nearby colonies and occasionally switch roosts (Kolodny et al. 2017). Similarly, bats from nearby colonies visit and join our colony. Each of the bats was tracked over dozens of nights with many tracked simultaneously on the same nights. We analyzed a total of 3605 tracks collected from 96 individuals (bats come and go and thus we have a total of more than 50 bats). On average, we

tracked 5 bats simultaneously on a given night, but we often tracked 10 on the same night. Despite this huge dataset, we never observed two bats flying together – not when emerging, not during foraging and not when returning. Moreover, we monitored the exit times of all individuals in the colony over a period of 14 months (in total we monitored the exit of 150 individuals, while we only had GPS data for 96 individuals). Of the 15,551 events of bats exiting or entering the colony only in 48 cases (~0.3%) did another bat follow within a time-period of 5 min which might suggest following behavior.

The definition of foraging versus commuting

We used a union of two movement indices, the Straightness index (Postlethwaite et al. 2013) and the First passage time (Fauchald and Tveraa 2003), to detect foraging events and separate them from commuting periods. In brief, the Straightness index is the ratio between the distance from the starting point to an end-point and the actual path length traveled between these two points (a value of 1 means moving straight). The straightness index was calculated at each point along the trajectory with a window of 15 min (and an almost complete overlap – a 1 point shift). An index value of max 0.5 was set for foraging following manual scrutiny of part of the data. The First passage time is a measure of the time an animal spends within a given radius along the path. The First passage time was estimated for each location along the trajectory with a radius of interest of 60 m. The minimum First passage time for defining foraging was set to 50 s. Any point along the trajectory that crossed one of the two thresholds (had a straightness index of less than 0.5 or a first passage time of more than 50 s) was defined as a moment of foraging. After

identifying all potential foraging sites (i.e., connecting all locations in which foraging occurred), we omitted sites in which bats spent less than 30 s in total, and we merged sites that were less than 60 m apart. We only performed this analysis on bats that were farther than 100 m from their roost. We used the on-board audio recordings where we could detect echolocation attack sequences to confirm that this algorithm was performing well (this could only be done in *M. vivesi* as *M. myotis* is a gleaner and does not emit attack sequences).

Simulation of independently moving bats

In the simulations of both species, the bats moved according to the movement parameters of the real bats, that is, with the same average speed and the same distribution of turning angles, but as independent individuals without any intention to aggregate in groups. We used a permutation test to compare the simulated data to the real data. To this end, 10,000 random samples of 10 bats were drawn from each model and the median of the real data (e.g., conspecific rate median) was compared to these 10,000 simulated groups.

Fish-eating bat model

The aim of the simulations was to examine whether the rate of encountering conspecifics observed in the fish-eating bat could be explained by random encounters of conspecifics when moving independently in the foraging areas (i.e., due to the number of bats moving through the area). We simulated 10,000 bats independently flying in a rectangle area of 34 × 17 km2 - the area was estimated by taking the convex hull of the areas covered by all 39 searching bats (90 nights in total) which were tracked in the study. This area was probably an underestimation of the actual

area covered by the bats – the more bats we followed the more the area increased. The number of bats we used was a maximum estimate of the number of bats on Isla Partida Norte which is by far the largest colony in the area (Harel et al. 2017). The simulated bats left the island dueing 30 min (like the real bats) flying toward the same range of angles relative to the Island as the real bats (165-245 degrees, relative to north defined as 0). The simulated island was positioned at the same position relative to the foraging rectangle as the real island – this means that the simulated bats spread a triangular area within the foraging sites (like the real bats) while the complete rectangle only defined their maximal borders – they never crossed these borders (see turning heuristics below). The simulated bats flew for 3.5 hr (the average observed flight duration of the real bats) at a constant velocity of 5.9 m/s (the average speed of searching bats according to the real data). They stopped at foraging sites for 9 ± 2 min on average (see details below).

Simulated bats that were farther than 1 km from the borders of the foraging area performed a correlated walk movement, changing their direction relative to the previous heading every 5 s, according to a (zero-centered) normal distribution of possible angles with a standard deviation of 0.1 rad. This distribution was estimated based on the turning angles of the real 39 bats (over all 90 nights). When a simulated bat came as close as 1 km to the borders of the foraging area, it altered its turning behavior by adding a bias to the angle-distribution turning it back into the area. The bias aimed to turn the bats back into the foraging area (as the real bats did). The bias was randomly negative or positive, and it was added as follows:

a) Between 1 to 0.68 km from the borders, the bat turned based on the same distribution above but with a bias of 12 degrees thus turning back into the foraging area.
b) Between 0.68 to 0.36 km from the borders, the bat turned based on the same distribution above but with a bias of 21 degrees.
c) Bats that still reached one of the borders of the area turned back (according to a physical reflection model).

In all cases a-c the bat either turned like in the general search model or it turned as defined in a-c with increasing probabilities (40-70%–80% in a-c respectively). A bat that reached the border without turning bounced back in with the impinging angle equal to reflected angle. These parameters were chosen such that the turning angle distribution of the simulated bats will resemble the distribution of the real bats (Fig. S4.4). The overall movement of the simulated bats captured the essence of that of the real bats crossing through the foraging areas in an ellipse-like trajectory (compare Fig. 4.2A and Fig. 4.2B).

Because we did not want to assume anything about the distribution of the resource that might influence our results, we used the bats' behavior to model the resource. The probability of finding a foraging site at a given time-point was a Poisson process with an average Lambda of 0.045 sites per minute (based on the observed data). When a simulated bat detected a foraging site, based on this probability, this was now a foraging site for all bats encountering it. The bats remained within the site for 9 ± 2 min (the exact time was drawn from a normal distribution with a mean and standard deviation based on the real data). We used the

estimated detection range (185 m) to model the attraction of other bats to this discovered site. When a bat passed within 185 m from a bat that found a foraging site, it was immediately attracted to the site. This assumption aimed to model the aggregation of (independently moving) bats at foraging sites, a process which could have influenced the encounter rate of conspecifics right after leaving the site. Indeed even independent bats aggregated at foraging sites (but to a much lesser degree than the real bats, see main text). The bat's movement inside the foraging site was modeled as a random walk (see below). The simulation stopped after 3.5 hr wherever the bat was – we did not simulate the final return to the island, because we only aimed to examine the encounter-rate of conspecifics. Importantly, all of the simulation assumptions intended to increase the encounter-rate of conspecifics in the simulation. We used the maximum number of bats roosting on the island, and we assumed that they all left every night flying in the same direction (in reality bats occasionally did not leave the island). We probably underestimated the foraging area (see above), and we used the maximum range (185 m) for detecting foraging conspecifics (which in the real bats is only achieved when the bat is facing the center of the beam of another bat and is otherwise shorter). This approach of increasing the encounter-rate of conspecifics in the simulations aimed to set an upper-bound on the potential encounter-rate of bats that were moving independently. If the real bats encountered conspecifics more than this upper-bound, they were probably intentionally aggregating.

The analysis of the simulated bats was identical to that of the real bats to allow a fair comparison. To this end, during the commute periods of each simulated

bat, we measured its distance from all other simulated bats. We registered every distance to another bat that was smaller than 12 m as an encounter event, as we would have recorded by our microphone in reality (because our microphone could only record bats from up to 12 m). This was also an over-estimation because of the directionality of the echolocation beam (see above). We only quantified interactions occurring more than 1 km from the island (in both the real and simulated bats) in order to avoid overestimations due to the synchronized emergence.

We also modeled the encounter rate within foraging sites. The number of bats arriving at the foraging sites was determined based on the model of independently moving bats and the attraction between them (see above). The sites themselves were modeled as 210 m-radius circles (the average size of the foraging sites estimated based on a convex-hull of foraging bats). The first bat arriving at the site left after 9 ± 2 min (see above) and the other bats left within 1 min after the first one. Bats moved through the foraging site in a Brownian movement and their encounter rate was calculated as above.

Mouse-eared bat model

The model for *M. myotis* was similar with a few adaptations to the behavior of this species. Four thousand bats emerged from a central location (their cave) flying in straight lines in all directions (as we observed in the data, Fig. S4.2). The bats stopped at a distance from the cave, which was sampled from the distribution of the distances of the real foraging sites. We did not model the behavior in the foraging sites in this case as these bats showed no tendency to aggregate. For this species, we assumed a detection range of a conspecific by our microphone as 8 m – according to the

emission level of these bats and the sensitivity of the microphone at the most intense frequency of the bats' signal.

Validation of conspecific recordings

The fact that we did not detect conspecifics in the three predictable foragers did not result from a technical artifact for two main reasons. First, for the predictable foragers we also used recordings from our new and much more sensitive device (Vesper, ASD Inc. Israel). We used Vesper recordings of 4 *M. myotis*, 4 *L. yerbabuenae* and 10 *R. aegyptiacus*. We calibrated the Vesper's microphone estimating the recording range for these species at ca. 30 m, 20 m and 25 m respectively. In all cases, this is much more than the 12 m recording range for the two ephemeral species (with the old device). We therefore strongly biased our recordings in favor of the predictable species and still found that they do not encounter conspecifics. Second, in the models of independently moving bats (above) we took into account the exact detection range of our microphone (which was 12 m for *M. vivesi* but only 8 m for *M. myotis* with the old device). The comparison was therefore fair and we found that *M. myotis* encountered conspecifics in reality less than expected by chance.

Playback Experiments

To test if bats are attracted to foraging conspecifics, we performed playbacks of *M. vivesi* and *M. myotis* search and attack echolocation calls (using the Avisoft UltraSoundGate Player D/A converter connected to a Vifa speaker, Vifa, Copenhagen, Denmark). The sequences we used (i.e., a search sequence and an

approach sequence which ended with a buzz) were composed of signals that were recorded on-board wild bats using our miniature sensors. A third white noise control-treatment included a train of noise pulses. As our main comparison was between the search and the noise treatments, these two playbacks had the same pulse duration, pulse interval and bandwidth. The amplitude for all playbacks was normalized so that the peak intensity of all treatments was identical (the total energy was higher in the approach sequence because the calls were more frequent). In the case of *M. vivesi*, the playbacks were performed from an anchored boat roughly 100 m off Isla Partida Norte while in *M. myotis* it was ca. 10 m from the entrance of the cave (in the past, we used a similar position near the cave of *R. microphyllum* which showed clear attraction to the playback of searching conspecifics even at such a short distances (Korine et al. 1999)). Playbacks were made when the bats were emerging from their roosts, but after the majority of bats have already left so that mostly single bats were passing by to ease the analysis of the behavior. Playbacks were performed along 6 consecutive nights in Mexico and 5 consecutive nights in Bulgaria. All three treatments were played back twice on each night but their order varied haphazardly between nights. Each treatment-playback lasted 5 min before the next treatment-playback was played.

Playback recordings were analyzed using "Batalef," a custom-made in-house MATLAB program for sound analysis. Calls were automatically detected using a peak detection filter based on the local noise in the channel. Signals were bandpass-filtered between 30 - 50 kHz to ensure that only loud high frequency calls will be detected. This allowed automatic recognition of bats, which approached the

microphone and distinguishing them from passing bats and from our own playback (Fig. S4.4). High frequencies are more directional and attenuate more rapidly and thus they will be picked up by the microphone only when the bat points its emission toward it. A total of ~29,000 and ~9,000 calls were analyzed in Mexico and Bulgaria respectively. At least 30% of the data (of each species) were scrutinized manually to confirm high performance of the automatic algorithm. Because individual bats were hard to identify, we quantified the number of calls per session (night) per treatment (search, buzz, noise) and we ran a non-parametric paired test on the search versus noise and buzz versus noise comparisons (and corrected the p values for multiple comparisons using the conservative Bonferroni correction).

Controlling for the effects of the extra-loading on the bats

The extra-weight loaded on the bats reached a maximum of 15% of body mass (14 ± 0.5% In *M. myotis* and 14 ± 1.0% in *M. vivesi*). The analyzed GPS-tagged bats from both species left their roosts as usual together with the non-tagged individuals. Tagged individuals flew directly to their foraging sites and engaged in foraging, suggesting that they behaved as usual. To validate that the bats could forage with this extra weight we performed several controls for both species:

(1) We trained bats to forage in a room / tent to confirm that they could do so with the extra-weight. *M. vivesi* bats successfully learned to rake a small artificial pool and catch food items that were on the water (e.g., beetles) while *M. myotis* quickly learned to glean mealworms from a plate positioned on the floor in a flight room when carrying the extra-weight.

(2) Light telemetry tags (ca. 1% of the bats body mass) were mounted on bats of both species and the time they spent foraging (out of the roost) was compared to that of the GPS bats. For a fair comparison we used a telemetry logger (DataSika, Biotrack, New Market, Ontario, Canada) that was placed in the roost of each species and thus picked up the telemetry signals of the bats when they were in the roost (the logger checked the presence of each tag on average once every minute). The GPS bats also had telemetry tags so we used an identical method for both treatments. Foraging flights were defined as events in which a bat was not detected by the logger for at least 20 min (between 20:00 and 7:00 local time). The amount of time that the *M. myotis* control bats, tagged with light tags, spent out of the roost did not differ from the amount of time spent by bats tagged with the GPS tags (5.8 ± 0.9 versus 5.5 ± 1.0 hr respectively, $p = 0.37$, permutation t test; $n = 15$ GPS bats and $n = 8$ telemetry tags). The same result was obtained for *M. vivesi* where control bats, tagged with light tags, flew for 4.3 ± 2.1 hr on average while the GPS tagged bats flew 3.8 ± 1.8 hr ($p = 0.4$, permutation t test $n = 20$ GPS bats and $n = 15$ telemetry tags).

(3) When we had a chance to recapture bats, we compared the weight loss of bats that were tagged with GPS to that of bats tagged with light telemetry tags. In *M. myotis*, both GPS-tagged bats and bats tagged with light telemetry tags lost weight, but there was no significant difference between the two treatments (on

average the GPS and telemetry bats lost 1.3 ± 1.3 versus 0.9 ± 0.5 g, mean ± SD respectively, p = 0.5, permutation t test; n = 8 GPS bats and n = 6 telemetry tags). There was also no difference when accounting for the time period of the tagging (ANCOVA hypothesis of parallel slopes: *M. myotis* adults – $F_{1,44} = 0.005$, p = 0.95, N = 28 and 20 Telemetry bats). In *M. vivesi* weight loss was slightly higher in GPS bats in comparison to the telemetry tagged bats (bats lost 1.8 ± 1.3 versus 0.9 ± 0.9 gr, mean ± SD respectively, p = 0.05, permutation t test; n = 12 GPS bats and n = 10 telemetry tags). However, when time since first capture was taken into account and the loss of weight per day was estimated, we found no significant difference between telemetry and GPS tagged bats (ANCOVA hypothesis of parallel slopes: *M. myotis* adults – $F_{1,7} = 3.866$, p = 0.09, N = 7 GPS and 4 telemetry bats; *M. vivesi* adults – $F_{1,63} = 1.549$, p = 0.218, N = 47 GPS and 20 telemetry bats). This suggest that the difference resulted from the capture of GPS bats after more nights than the telemetry bats (GPS bats were tagged for significantly more time than telemetry bats – 2.5 versus 1.6 days; p = 0.0001, Wilcoxon rank sum test, N = 47 GPS and 20 telemetry bats).

In both species, both GPS and telemetry bats lost weight over the period of the few days that they carried the tags. Telemetry units were tiny, adding only ~1% to the body mass, so it was probably not the weight of the tags that caused the bats' weight loss. One possibility is that the nuisance of carrying a foreign body stressed the bats. Another explanation is regression to the mean as we always tried to select

the heaviest bats for tagging, so these bats could have been above their typical average weight. Loss of weight could also be a result of the normal seasonal trend, because we had tagged (currently or recently) lactating bats that probably lose weight during this time of the season (after reaching a peak weight during pregnancy).

In terms of the pups' health, there was no significant difference in the weight to forearm ratio between M vivesi pups whose mothers were GPS or telemetry tagged (ANCOVA hypothesis of parallel slopes: $F = 2.306$, $p = 0.204$, $N = 8$, 5 GPS and 3 telemetry pups).

Importantly, the tags stayed on the animals for an average period of < 3days (in the most extreme case 9 days) so their effect of the animals' welfare was extremely limited in time. Note that as we are comparing two species in this work, even if the bats behavior was somewhat affected by the tags' weight (e.g., their foraging success declined), the comparison of foraging and social behavior between the two species is still valid as it is hard to imagine that the huge differences that we observed between the two species could be an artifact of the extra loading – it is hard to imagine that the weight made a social bat suddenly solitary in such a short time. For similar controls in Rhinopoma see Cvikel, Egert Berg, et al. (2015).

Quantification and Statistical Analysis

For analyzing the differences in movement between ephemeral and predictable foragers, we ran a nested ANOVA test with species nested within foraging style (i.e., ephemeral versus predictable) and species defined as a random effect. This test was run for each movement parameter separately.

The comparison of the model to the real bats (the conspecific encounter rate), we used a permutation test because the sample size of the model (i.e., the number of simulations) was a parameter we could control, thus influencing the power of our analysis.

We used a non-parametric Wilcoxon rank sum test to examine the attraction of bats to playbacks because of the small sample size and because the tests were run within the species, (so there was no need for an ANOVA structure). All statistical analyses were done in MATLAB.

Acknowledgments

This work was supported by European Research Council (ERC) grant number ERC-2015-StG - 679186_GPS-Bat and ONRG grant number N62909-16-1-2133 to Y.Y.; by Consejo Nacional de Ciencia y Tecnología (National Council of Science and Technology) grant number 237774 to L.G.H.M.; by National Geographic Society Young Explorer Grant 9705-15, The Explorers Club Exploration Fund—Mamont Scholars Program, and an Animal Behaviour Society Student Research Grant to E.R.H.; and by a Helen Johnson Grant through Tower Foundation grant number 034-1500-0508 to D.S.J. We are grateful to the Mexican (Dirección General de Vida Silvestre, Comisión Nacional de Areas Naturales Protegidas, and Secretaría de Gobernación) authorities for granting us permission to conduct this research. H.R.G. and the Siemers Bat Research Station in Bulgaria were funded by the German Research Foundation (Emmy Noether Program GO2091/2-1 to H.R.G.). S.G. was supported by the Minerva Foundation and by Tel-Aviv University. Transportation to the island was provided by Secretaría de Marina-Armada de México. The Prescott

College Kino Bay Center, the Area de Protección de Flora y Fauna Islas del Golfo de California—Baja California, Lorayne Meltzer, Martin Ziebell, Leonel Moreno, and Vaporrúb provided logistic support during our work in Mexico. Ricardo Rodríguez M., Jorge E. García V., Ricardo Rodríguez, and Esteban Gross helped with field work in Mexico. We are grateful to the Directorate of the Rusenski Lom Nature Park (Director Tsonka Hristova) for cooperation and support. We thank the responsible Bulgarian (MOEW-Sofia and RIOSV-Ruse) and the Arizona Game and Fish Department.

Author Contributions

K.E.-B. conceived and designed the research, carried out the data analysis, was responsible for the modeling, collected the field data, and wrote the manuscript. E.R.H. and S.G. conceived and designed the research, collected the field data, carried out the playback experiments, and wrote the manuscript. L.H. conceived and designed the research and carried out the data analysis. A.G., L.G.H.M., J.J.F.-M., A.T.V., R.A.M., D.S.J., O.E., I.B., J.R.S., G.S.W., and H.R.G. contributed to field data collection and helped write the manuscript. Y.Y. conceived and designed the research, contributed to field data collection, and wrote the manuscript.

Tables

Table 4. 1 Number of Bats per Analysis

Species	Resource Predictability	Bats with Movement Data (No.)	Mean Number of Nights (No.)	Bats with Movement Data of More Than Two Nights (No.)	Bats with Audio (No.)
Myotis vivesi	ephemeral	39	2.9	15	10
Rhinopoma microphyllum	ephemeral	12	1.7	6	8
Myotis myotis	predictable	18	2.7	15	14
Rousettus aegyptiacus	predictable	15[a]	2.6	15	10
Leptonycteris yerbabuenae	predictable	10	2.5	7	7

a

We also used data of additional 150 *Rousettus* bats for which we either had GPS data or colony emerging times (STAR Methods) .

Table 4. 2 Movement and Ecological Characteristics of Five Bat Species

Species	Average Colony Size (N)	Body Mass (g)	Main Food	Food Predictability	Maximum Distance (km)	Activity Time (hr)
Myotis vivesi	5–1,000[a]	30	fish and crustaceans	ephemeral	25.1 (21.1–29.9)	3.7 (3.1–4.3)
Rhinopoma microphyllum	1,000	30	flying insects	ephemeral	9.8 (8.3–13.5)	5.5 (2.8–6.8)
Myotis myotis	4,000	30	terrestrial arthropods	predictable	20.9 (12.7–25.4)	5.4 (5.0–5.8)
Rousettus aegyptiacus	500	130	fruit	predictable	12.6 (7.3–22.8)	5.8 (5.4–6.8)
Leptonycteris yerbabuenae	100,000	25	nectar (and fruit)	predictable	53.5 (46.7–59.0)	6.6 (4.8–7.6)

Medians and quartiles are presented for all parameters. Colony size is typical for the areas where we worked. The maximal distance was defined as the distance to the farthest foraging site. Activity time was defined as the period during which the animal was away from its daytime roost. Hundreds of small groups of approximately five individuals can be found under neighboring rocks.

Figures

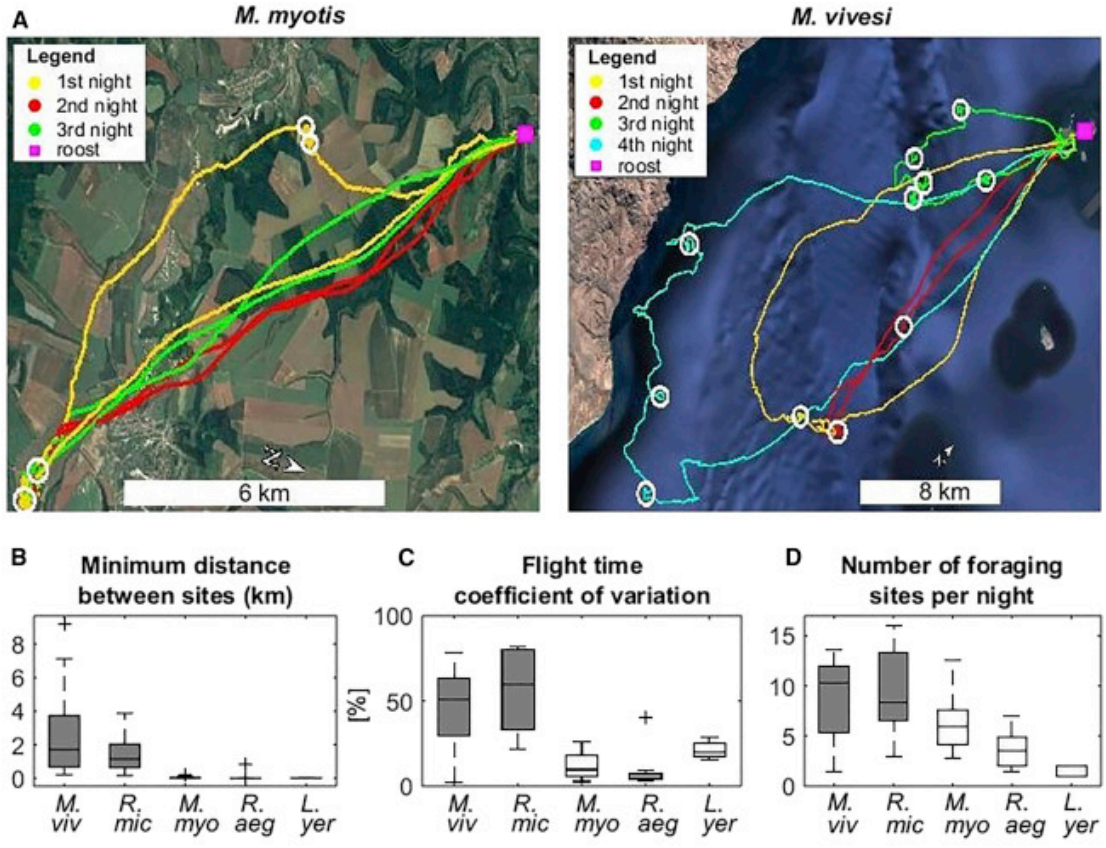

Figure 4. 1 Foraging Movement Patterns of Five Bat Species

(A) The complete foraging movement of two individual bats over several consecutive nights. The mouse-eared bat (left) used a few foraging sites per night (white circles) and returned to the same foraging sites on consecutive nights, whereas the Mexican fish-eating bat (right) covered large areas and switched foraging sites nightly. (B–D) Movement parameters of five bat species (only individuals with at least two nights were used in the analysis; Table 1) relying on ephemeral (gray bars) or predictable (white bars) resources.

(B) Spatial fidelity—the distance between the closest foraging patches visited on consecutive nights.

(C) Temporal variability—the coefficient of variation of the activity time.

(D) The number of foraging sites per night. Boxplots show median, quartiles, and whiskers extending to the most extreme data points not considered outliers (see MATLAB for outlier definition).

See also Figures S4.1–S4.3.

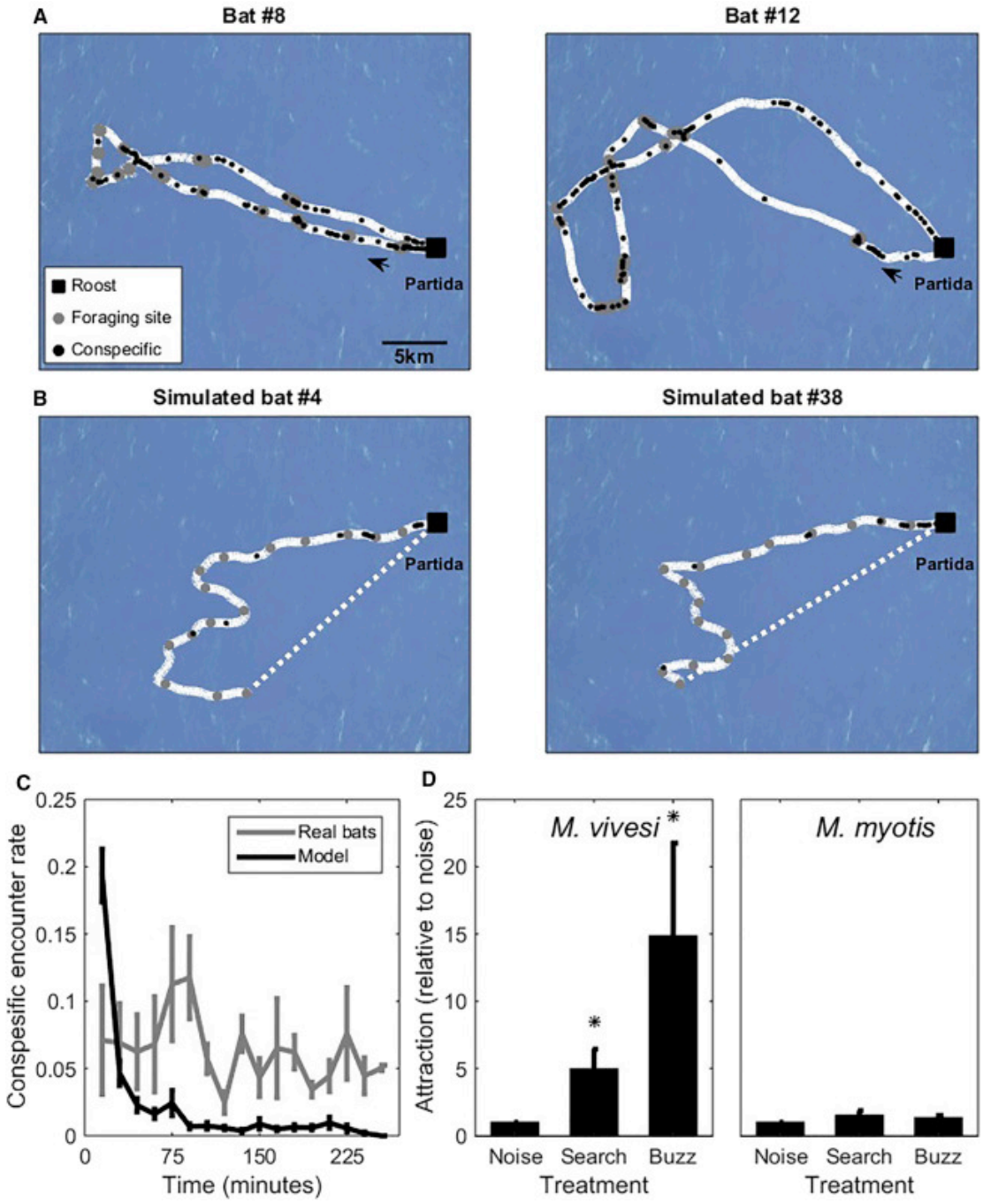

Figure 4. 2 Mexican Fish-Eating Bats Intentionally Aggregate to Search in a Group. (A and B) Two examples of nightly flight trajectories of real bats (A) and simulated bats (B), showing encounters with conspecifics (black circles) and detection of foraging sites (gray circles). The black arrows indicate the flight direction of the real bats. The scaling of all maps is equal. Note how the simulated bats encounter far

fewer conspecifics (black circles) and mostly at the beginning of the night (near the roost), whereas the real bats encounter conspecifics during the entire night. Real and simulated bats detected on average the same number of foraging sites). White dotted lines represent the return to the island, which we did not simulate because we stopped the simulation after the period of time observed in reality (STAR Methods).

(C) Encounter rate of conspecifics over time (15 min bins) in real fish-eating bats (gray) versus simulated independently moving fish-eating bats (black).

(D) Fish-eating bats are significantly attracted to playbacks of conspecific search and buzz echolocation calls, compared to the noise control, whereas mouse-eared bats are not attracted to any playback.

In (C) and (D), data are shown as means and SEs. See also Figure S4.4.

Appendix 1

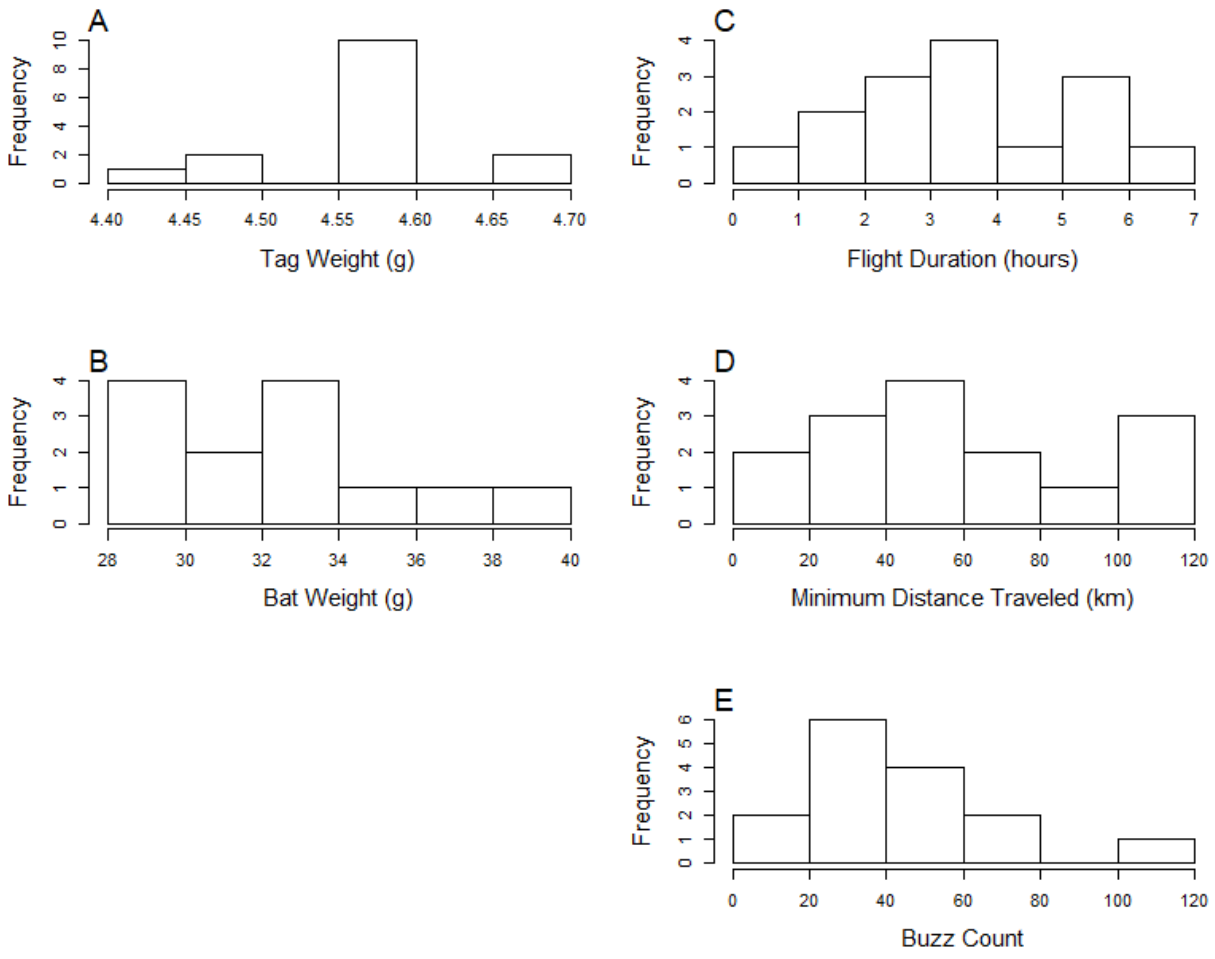

Figure S1. 1 Histograms of the flight parameters of foraging bats.

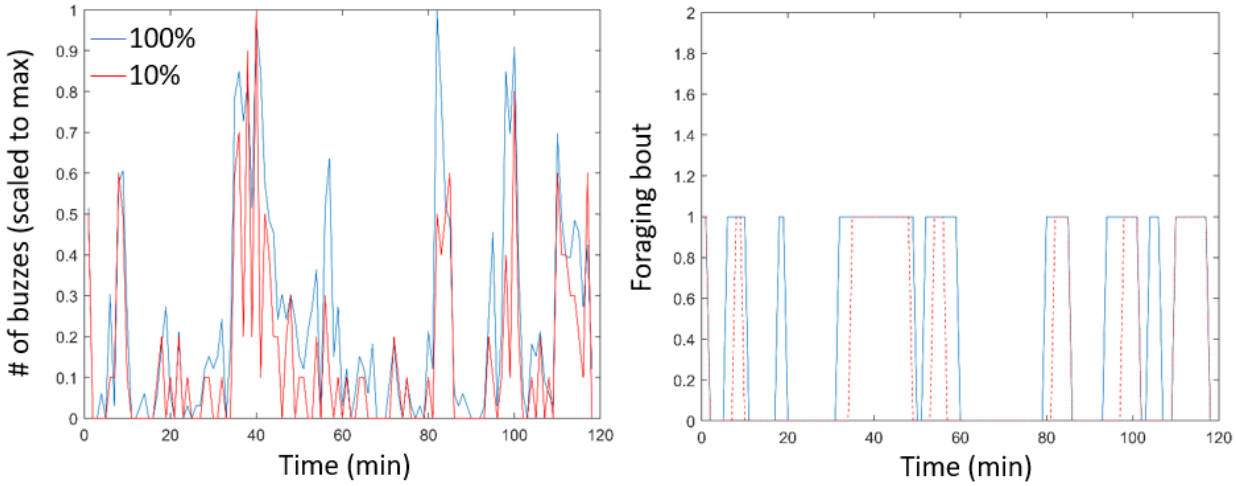

Figure S1. 2 Validation of audio sub-sampling

(A) Normalized buzzes per minute are presented for the 100% duty cycle (blue) and the 10% under-sampled (red) recordings. Both graphs were normalized relative to their maximum for comparison. The very strong correlation between the two graphs demonstrates how sub sampling still allows foraging bout detection. **(B)** Foraging bouts detected according to the buzzes (as a function of time) for the 100% duty cycle (blue) and the 10% under-sampled (red) data. Foraging bouts are depicted by values of '1'. Foraging bouts were defined as minutes in which the number of buzzes was above 20% relative to the max (bouts of 1 minute were removed and gaps of 1 minute were connected). This definition, relative to the max, allows a comparison between sampling strategies and as can be seen, 7 of the 9 bouts are detected in the under sampled data. Both A and B represent data of a single bat. In total, we repeated this analysis for three bats (see results in main text).

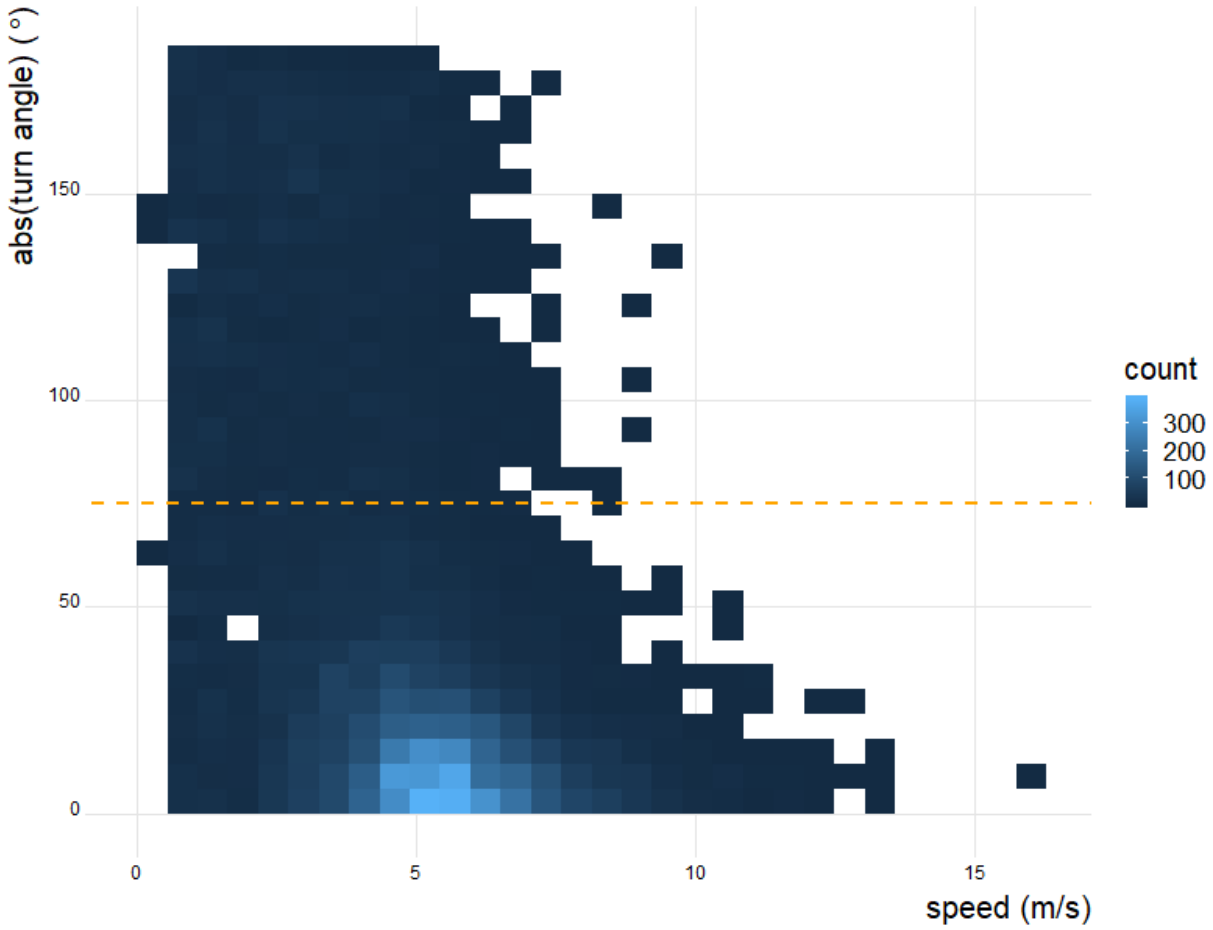

Figure S1. 3 Distribution of speed and absolute turn angle values for all GPS locations.

An orange dashed line indicates the boundary between k-mean states, with foraging occurring above 75º and commuting below 75º.

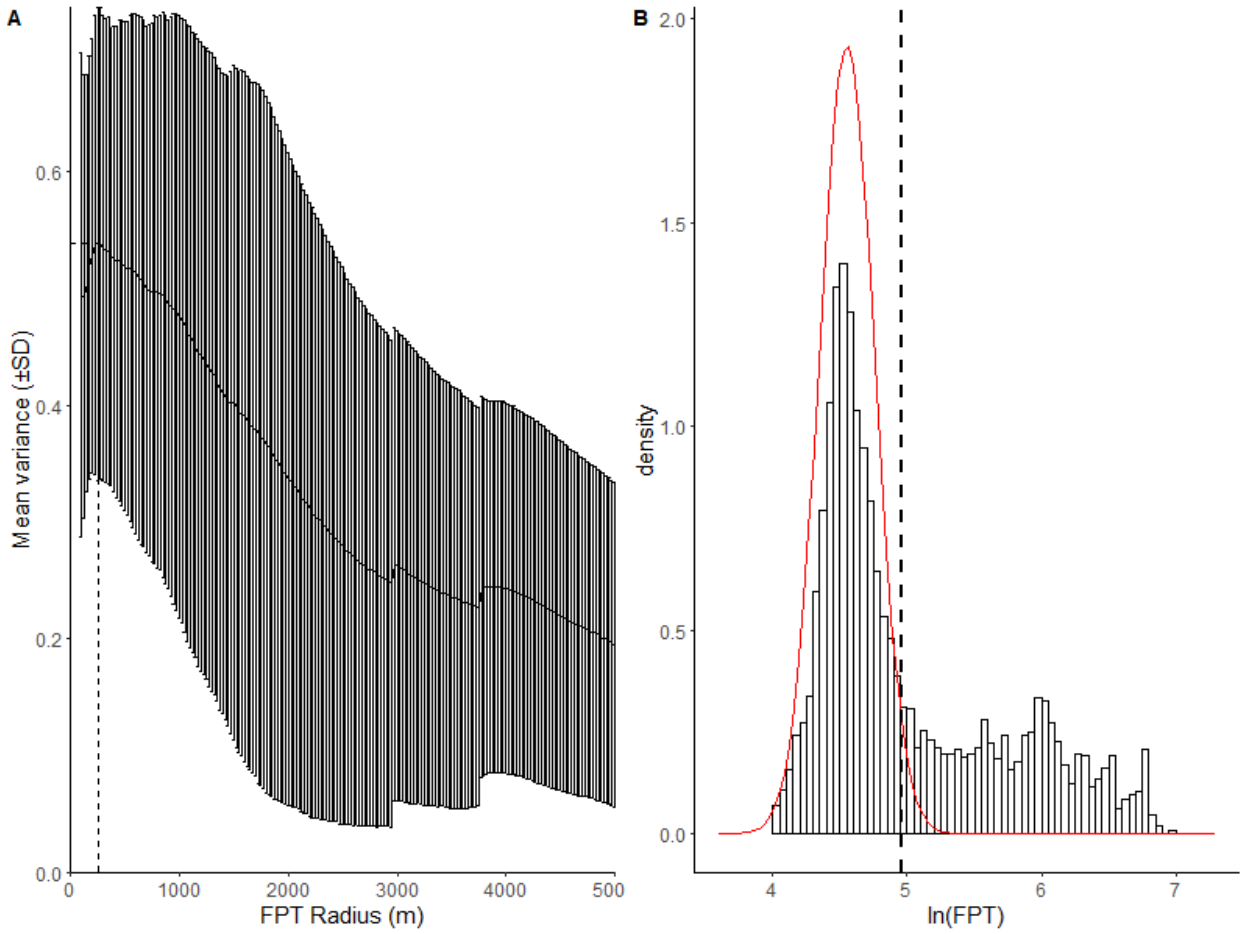

Figure S1. 4 First passage time radius and threshold.

(A) Whisker plots of mean variance of first-passage time values over a range of radii from 100 m to 5000 m. A dashed line is overlaid to represent the highest mean value, which occurs at a radius of 250 m. (B) Histogram of the natural log of first-passage time values calculated for all bats at a radius of 250 m. A threshold (dashed line) between high (commuting) and low (foraging) FPT values is selected at the upper 95% confidence interval of a gaussian curve fit to the lower peak at 142 s.

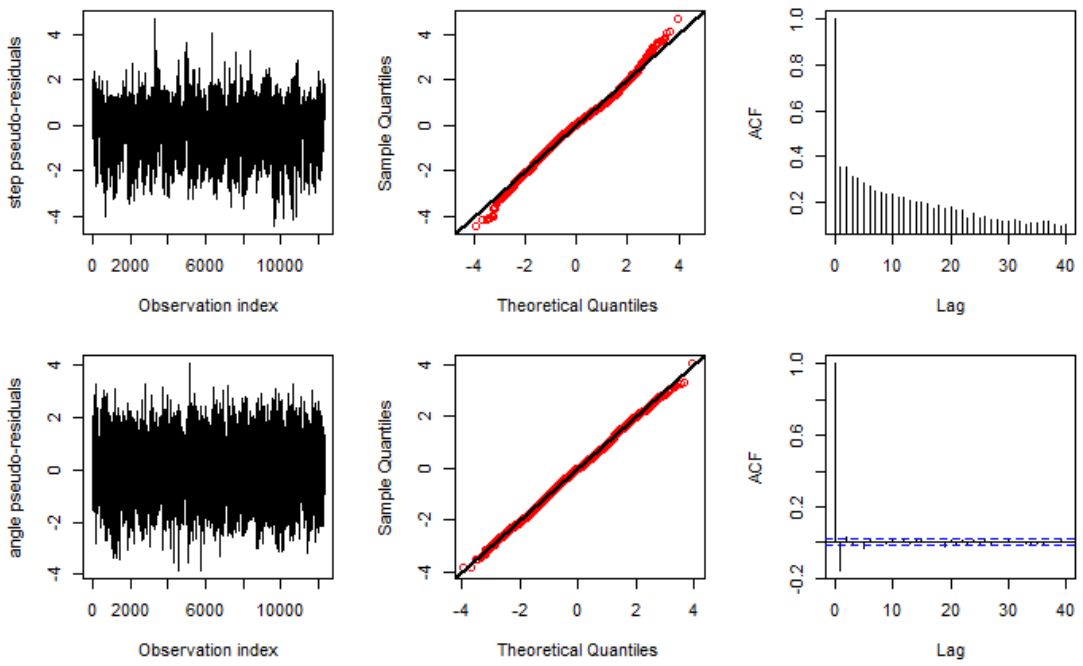

Figure S1. 5 Pseudo-residual, QQ, and autocorrelation function plots of step length and turn angle modeled by a two state HMM.

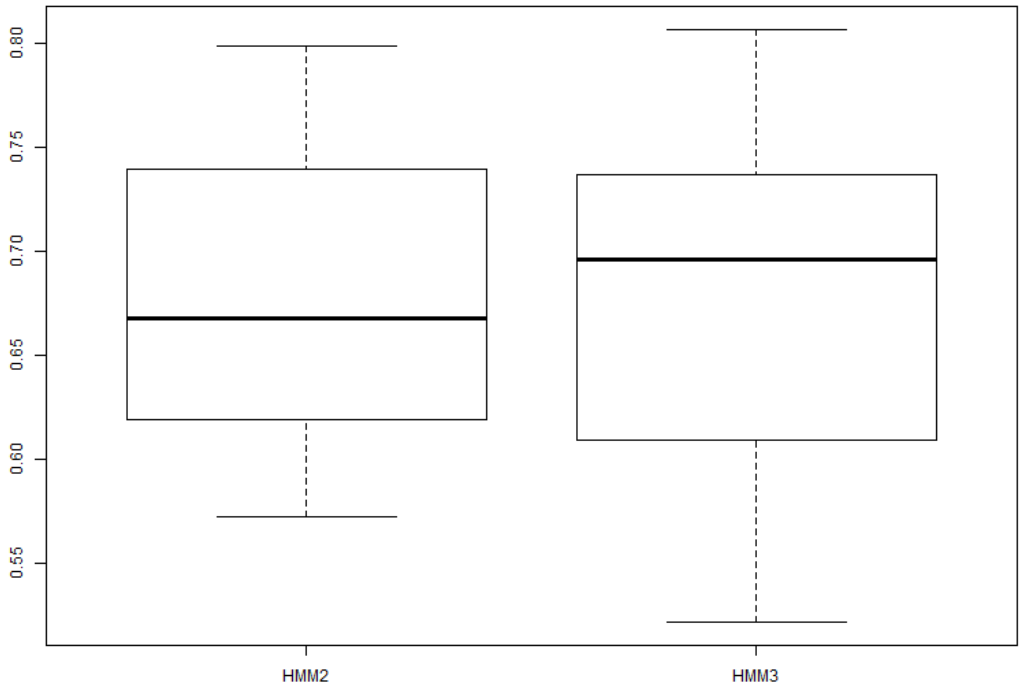

Figure S1. 6 Boxplot of the balanced accuracy for each bat flight (N = 15) for a two-state and three-state HMM.

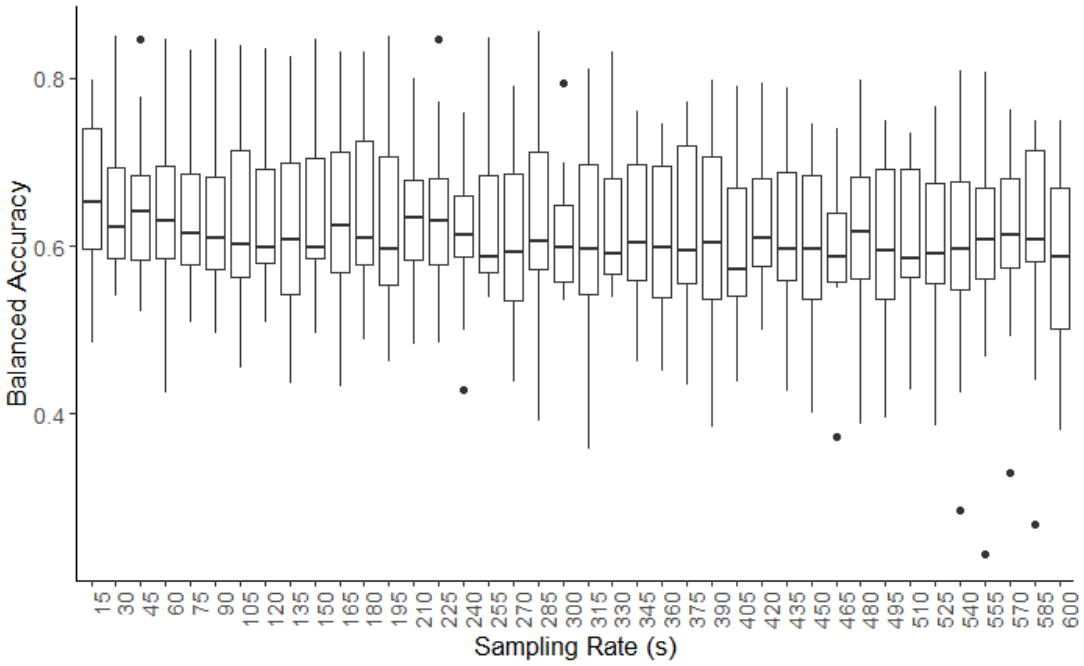

Figure S1. 7 Balanced accuracy of hidden Markov models run on all tracks subsampled at different sampling rates.

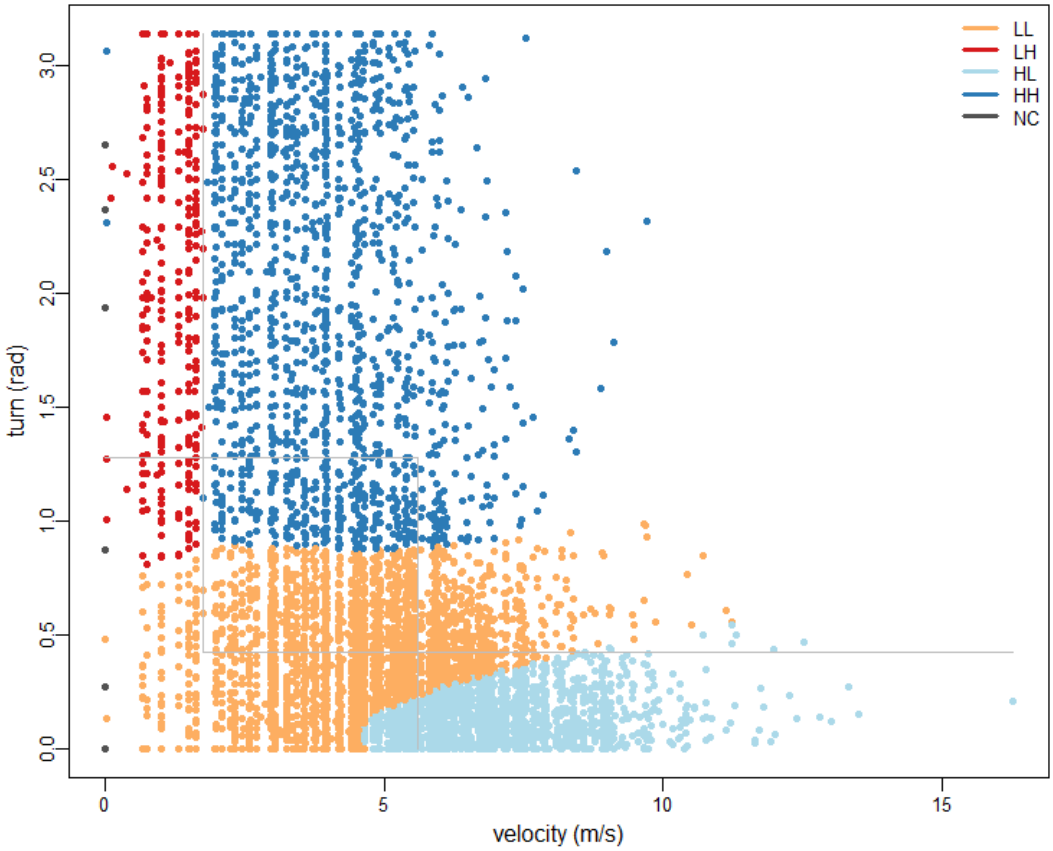

Figure S1. 8 Expectation-maximization and binary clustering output.

Colors correspond to the four categories of movement states defined by different clustering of the speed and turn angle.

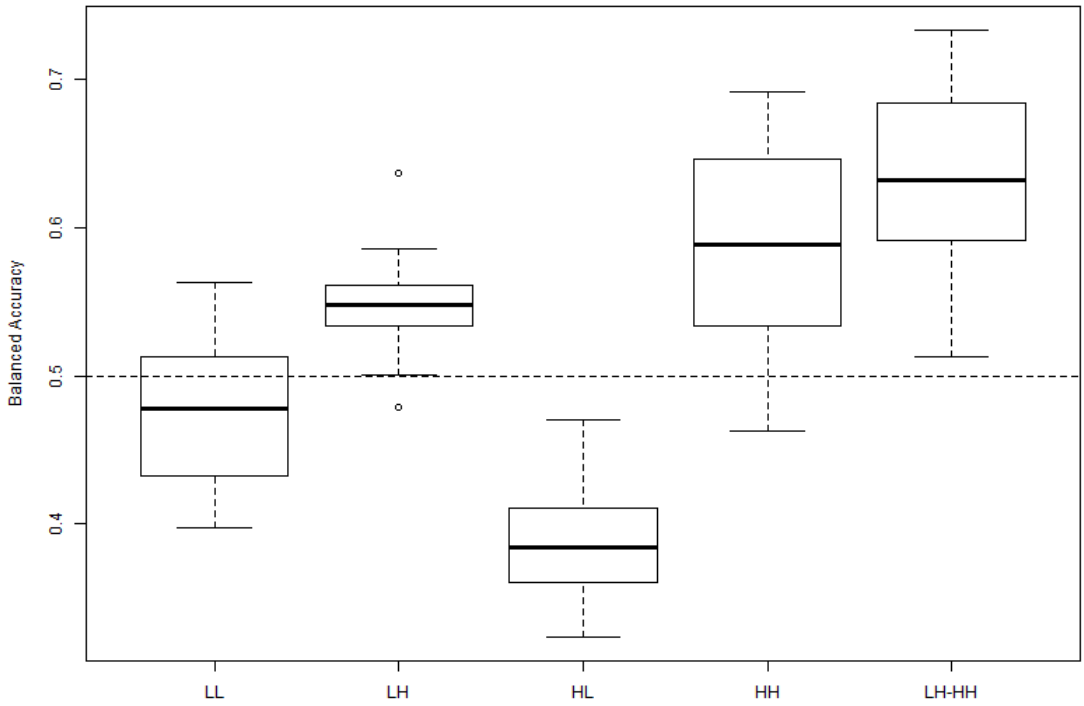

Figure S1. 9 Boxplot of the balanced accuracy of each flight path (N = 15) among all EMbC states and a combination of the two highest performing states, low speed-high turn angle and high speed-high turn angle.

This combination of states performed highest and was used as the foraging state for EMbC in the methodology comparison.

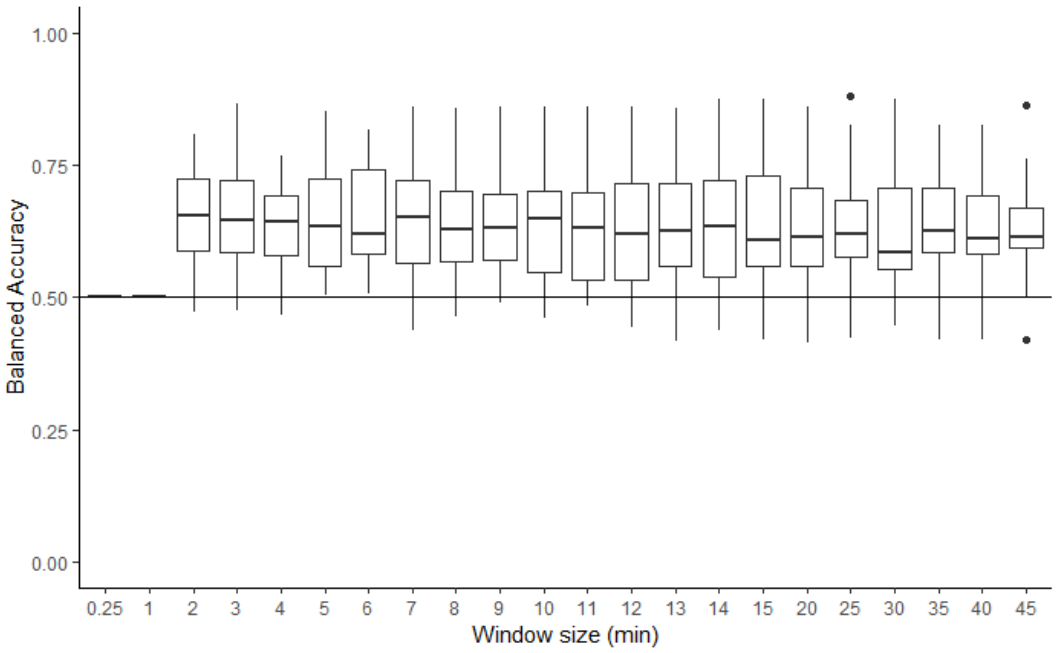

Figure S1. 10 Boxplots of balanced accuracy of each bat flight (N = 15) for CVCP across a range of window sizes.

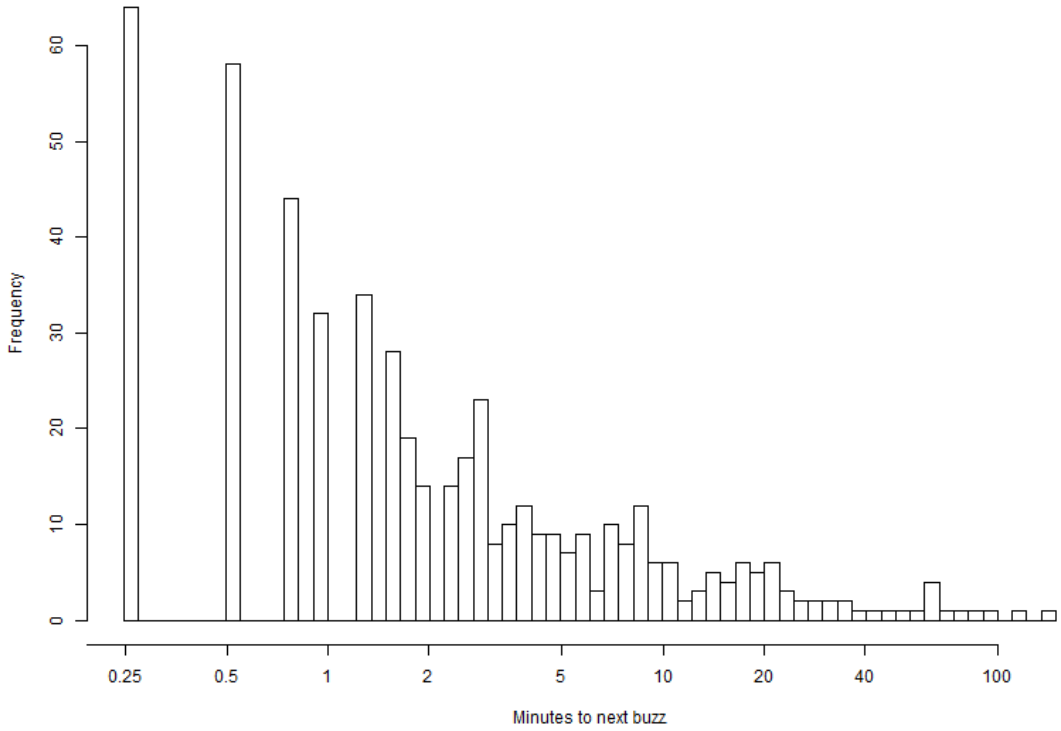

Figure S1. 11 Histogram of the time in minutes to the next location with a buzz recorded.

Table S1. 1 Summary of flight parameters of foraging bats.

ID	Capture weight (g)	Tag weight (g)	Flight	Departure Time (UTC-7)	Return Time (UTC-7)	Minimum Distance Traveled (km)	Duration (h)	Buzz Count	Audio files used (not filtered)	GPS fixes (not filtered)
5	29.5	4.4	1	5/27/2015 22:40	5/28/2015 1:58	34.28	3.3	78	2304	768
6	33.8	4.5	1	5/27/2015 22:16	5/28/2015 2:29	45.4	4.2	58	2967	989
6	NA	4.5	2	5/28/2015 21:54	5/29/2015 0:56	37.26	3.03	69	2112	704
8	33.8	4.6	1	5/29/2015 23:43	5/30/2015 2:47	30.5	3.07	35	2088	696
8	31.8	4.6	2	5/31/2015 21:08	6/1/2015 2:59	84.96	5.85	22	4134	1378
12	29.4	4.7	1	6/1/2015 20:48	6/1/2015 22:22	15.31	1.58	5	1140	380
12	29.4	4.7	2	6/2/2015 20:29	6/3/2015 1:34	51.19	5.07	49	3588	1196
14	36.1	4.6	1	5/30/2015 22:35	5/31/2015 2:29	54.25	3.9	25	2745	915
14	NA	4.6	2	5/31/2015 20:47	5/31/2015 21:38	6.79	0.85	10	615	205

15	33.3	4.6	1	5/31/2015 23:24	6/1/2015 2:06	46.77	2.7	34	1875	625
16	38.3	4.6	1	5/31/2015 21:02	6/1/2015 3:25	89.8	6.38	39	4509	1503
18	32.8	4.6	1	6/3/2015 20:25	6/4/2015 2:16	78.4	5.84	138	4134	1378
19	29.7	4.6	1	6/2/2015 20:57	6/2/2015 22:43	18.44	1.77	57	1278	426
21	34.2	4.6	1	6/2/2015 21:06	6/2/2015 22:11	15.2	1.1	24	792	264
24	30.1	4.6	1	6/5/2015 21:25	6/6/2015 0:02	29.82	2.63	45	1833	611

Table S1. 2 Summary of flight parameters of acoustically monitored foraging bats tagged with vesper tags.

ID	Capture weight (g)	Tag weight (g)	% body mass	Departure Time (UTC-7)	Return Time (UTC-7)	Duration (h)	Buzz Count	Recording Schedule
Mviv17_16	28.2	4.1	14.5	6/9/2017 21:20	6/10/2017 0:14	2.9	135	26 s/ 26 s
Mviv17_49	30.5	4.3	14.1	6/22/2017 21:19	6/23/2017 1:43	4.4	267	7.5 s/ 15 s
Mviv17_60	32.2	4.3	13.4	6/26/2017 20:47	6/27/2017 0:15	3.47	1624	35 s/ 35 s

Table S1. 3 HMM state transition probabilities provide the overall probability of transitioning from one state to another or remaining in the current state.

	State 1 – forage	**State 2 – commute**
State 1 – forage	93.1%	6.9%
State 2 – commute	4%	96%

Table S1. 4 Jarque Bera test of a three-state model

	Step	**Turn**
X^2	203.14	9.85
df	2	2
p-value	>0.001	0.007

Table S1. 5 Comparison of 2- and 3-state HMM models.

HMM	**State**	**Buzzes**	**Locations**	**TPR**	**Balanced Accuracy**	**AIC**	**dAIC**
2-state	1	450	4280	10.5%	Mean: 68.0%	133971	3398
	2	173	8043	2.2%	Median: 66.8%		
3-state	1	386	3380	11.4%	Mean: 67.8%	130573	
	2	201	4426	4.5%	Median: 69.6%		
	3	36	4567	0.7%			

Table S1. 6 EMbC states and a count of locations that correspond with buzzes and those that do not.

State	**Speed**	**Turn**	**Locations with buzz**	**Locations without buzz**
1	Low	Low	247	5321
2	Low	High	91	592
3	High	Low	46	3701
4	High	High	216	1817
5	NA	NA	0	7

Table S1. 7 Median and interquartile range of CVM parameter estimates.

	Root mean squared speed (m/s)	**Tau (s)**
UCVM (Foraging)	3.5, 2.7 – 4.9	17, 1 – 45
ACVM (Commuting)	5.3, 4.7 – 6.1	185, 91 – 308

Table S1. 8 Comparison of foraging and buzz identification across all segmentation methodologies**.**

ID	Flight	Segmentation methods									
		kmC		FPT		HMM		EMbC		CVCP	
		Foraging locations/ Total locations	Buzz hit/ total buzz	Foraging locations/ Total locations	Buzz hit/ total buzz	Foraging locations/ Total locations	Buzz hit/ total buzz	Foraging locations/ Total locations	Buzz hit/ total buzz	Foraging locations/ Total locations	Buzz hit/ total buzz
5	1	141/766	36/72	316/762	73/72	269/768	68/72	178/768	40/72	319/768	68/72
6	1	221/987	37/54	292/979	17/50	377/989	55/54	278/989	43/54	375/989	47/54
6	2	210/702	31/63	414/696	56/63	353/704	47/63	243/704	34/63	394/704	51/63
8	1	167/694	20/35	306/693	21/35	295/696	29/35	197/696	23/35	271/696	23/35
8	2	200/1376	11/21	409/1371	16/21	355/1378	15/21	235/1378	14/21	262/1378	11/21
12	1	50/378	2/5	116/374	43590	103/380	43560	63/380	2/5	62/380	3/5
12	2	226/1194	10/48	518/1189	32/48	453/1196	26/48	280/1196	14/48	479/1196	26/48

14	1	87/913	5/23	309/908	14/23	259/915	43822	123/915	43731	189/915	9/23
14	2	60/203	5/10	110/198	43687	98/205	43687	72/205	43595	114/205	8/10
15	1	58/623	17/20	129/618	27/20	135/625	25/20	94/625	21/20	76/625	25/20
16	1	192/1501	14/35	456/1492	25/35	428/1503	24/35	271/1503	18/35	409/1503	23/35
18	1	138/1376	46/94	482/1375	73/94	288/1378	78/94	204/1378	61/94	469/1378	69/94
19	1	148/424	33/54	313/419	56/54	297/426	55/54	181/426	36/54	289/426	53/54
21	1	91/262	43699	125/261	43821	193/264	21/22	126/264	13/22	159/264	20/22
24	1	140/609	15/44	269/604	27/44	270/611	31/44	171/611	21/44	320/611	31/44

Appendix 2

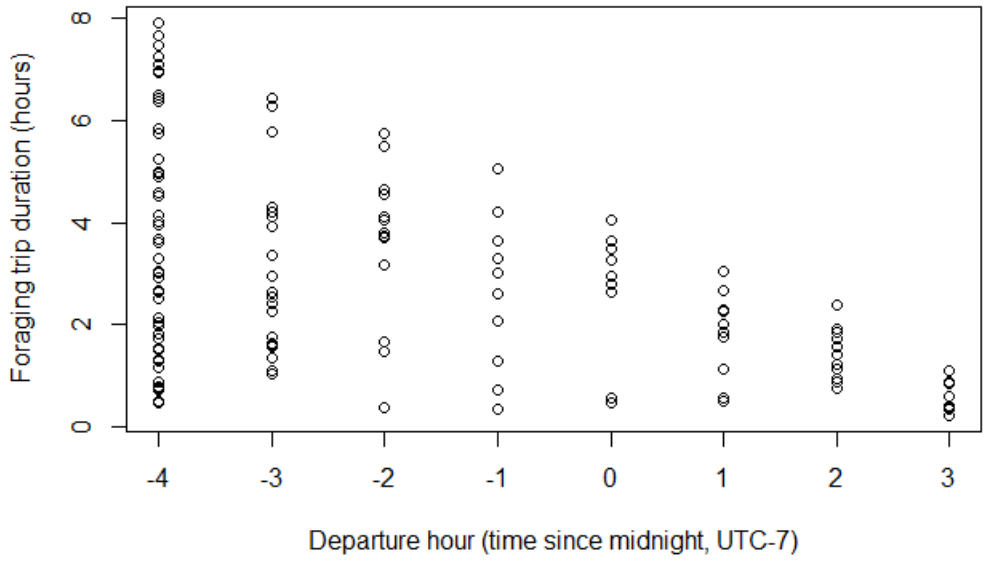

Figure S2. 1 Scatterplot of departure hour against foraging trip duration for all trips of tagged individuals (142 trips; 56 individuals).

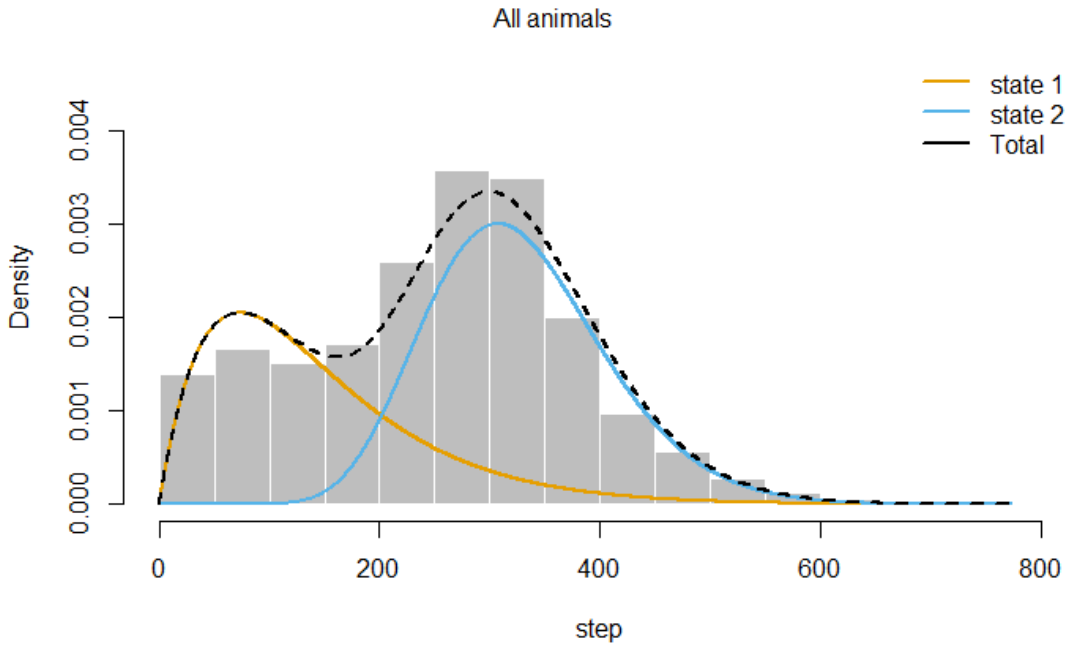
All animals
state 1
state 2
Total
Density
0.000
0.001
0.002
0.003
0.004
0
200
400
600
800
step

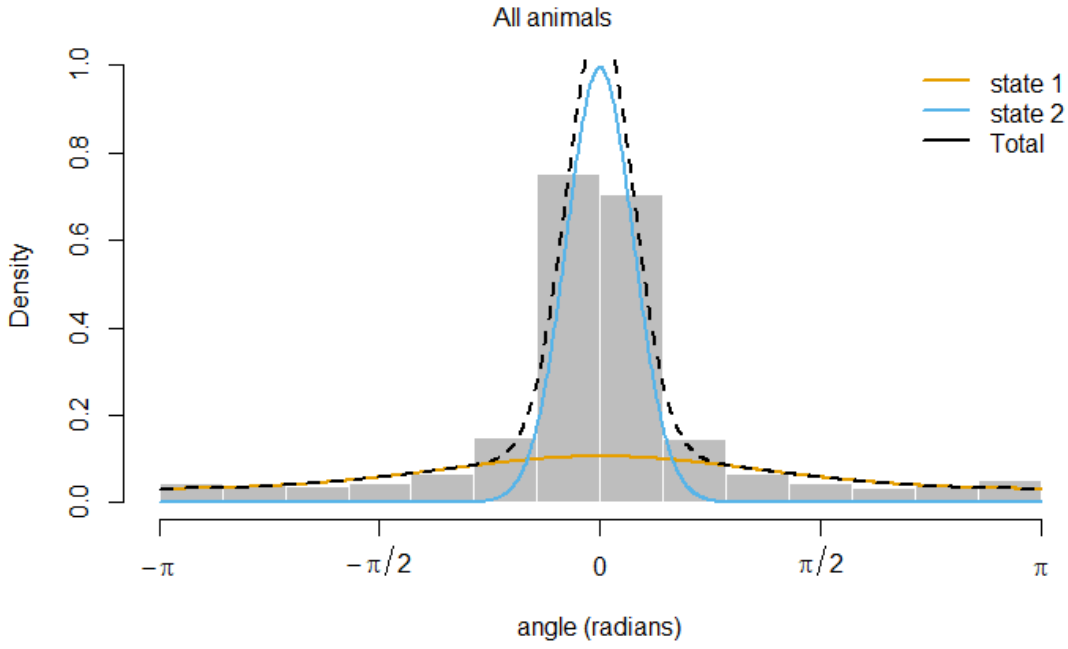
All animals
state 1
state 2
Total
Density
0.0
0.2
0.4
0.6
0.8
1.0
−π
−π/2
0
π/2
π
angle (radians)

Figure S2. 2 Histograms and density curves of the hidden Markov model fits for two behavioral states of all tracked bats.

Fits show the difference in distributions of (A) step length and (B) turn angle between state 1 (foraging) and state 2 (commuting).

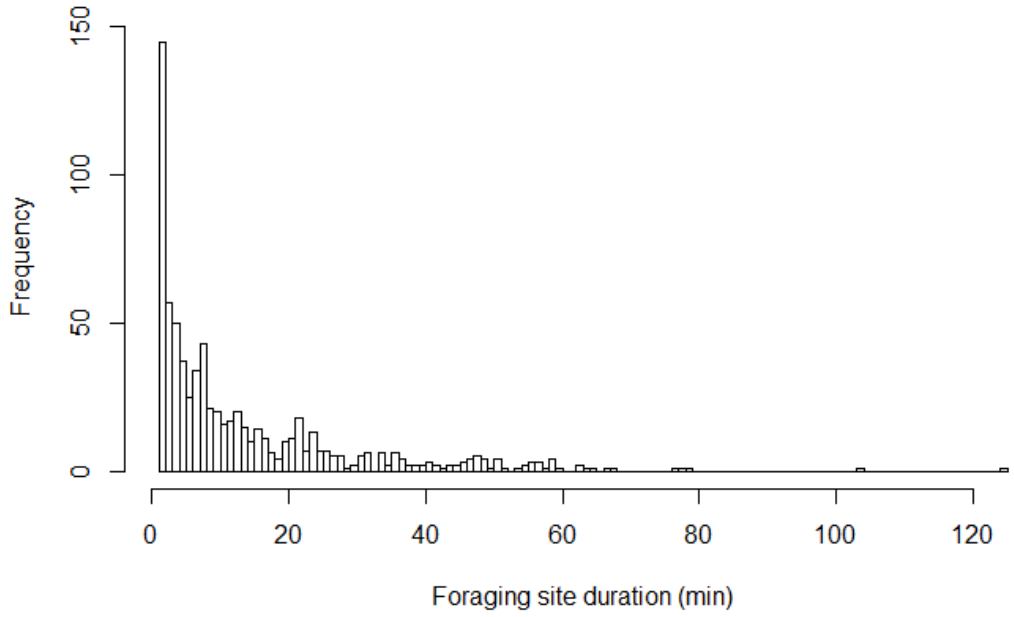

Figure S2. 3 Histogram of foraging site duration for all tagged bats.

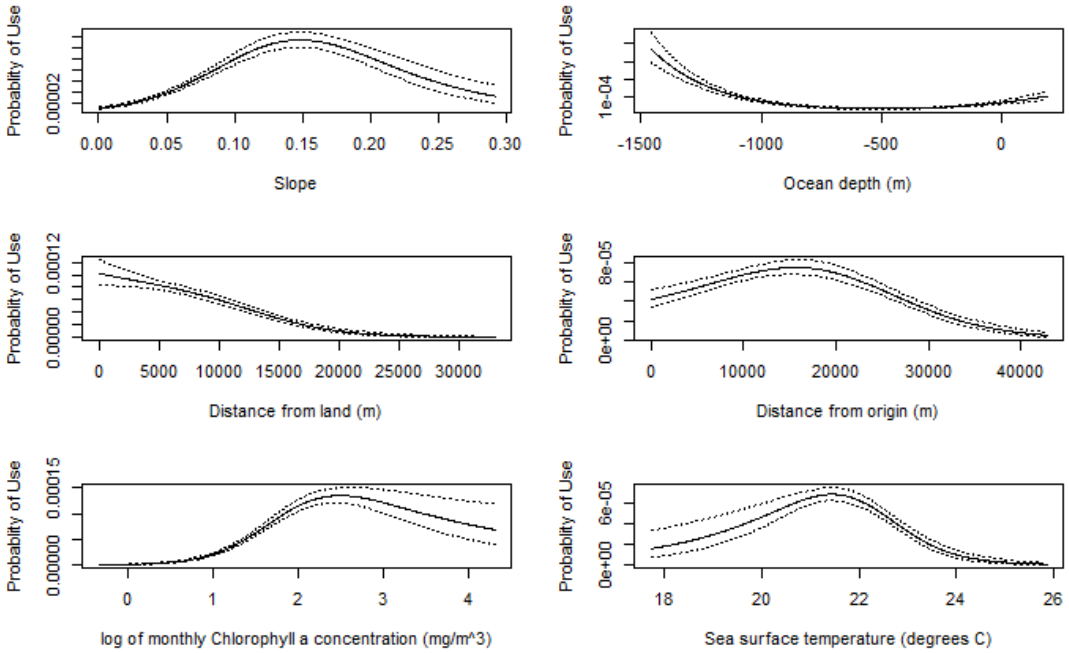

Figure S2. 4 Probability of use for individual fits of generalized additive mixed models of each covariate between foraging and available sites.

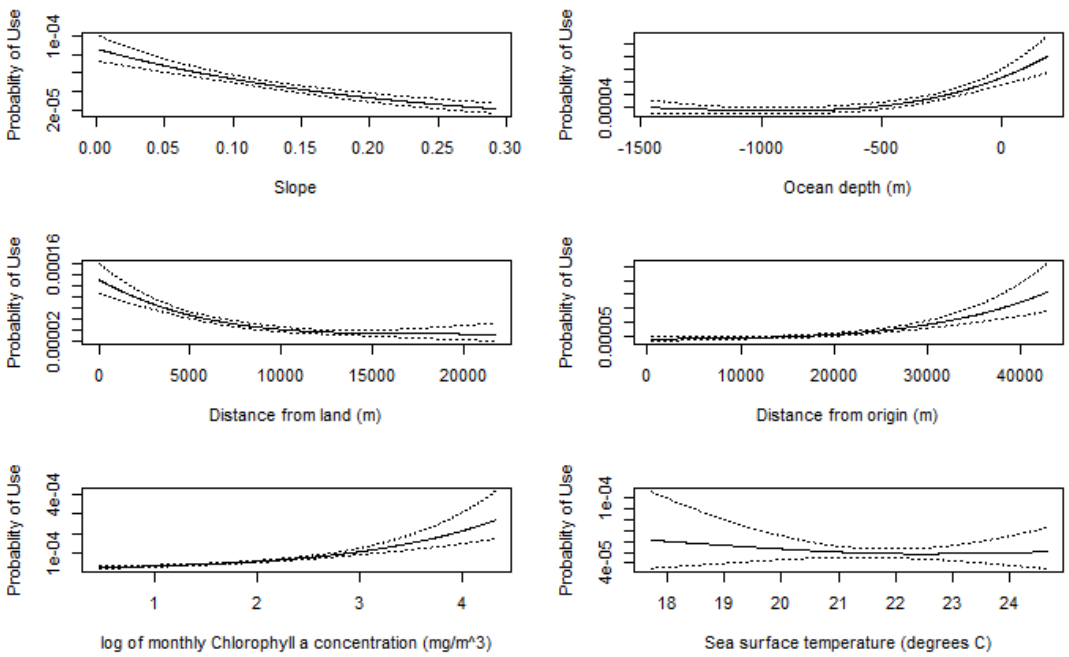

Figure S2. 5 Probability of use for individual fits of generalized additive mixed models of each covariate between foraging and simulated foraging sites.

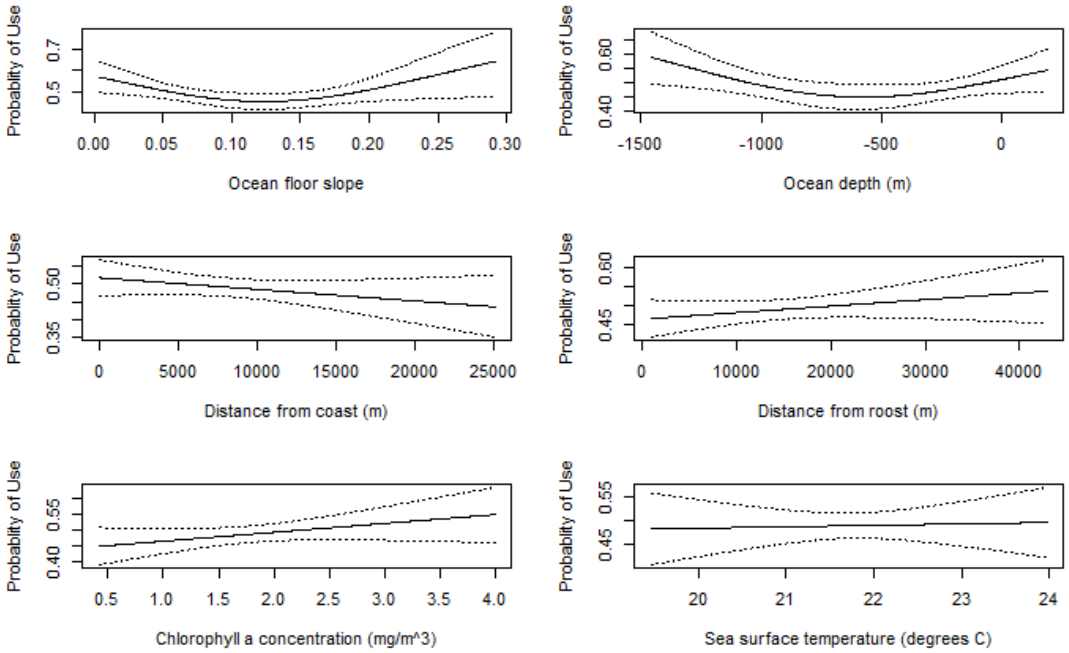

Figure S2. 6 Probability of use for individual fits of generalized additive mixed models of each covariate between foraging and commuting sites.

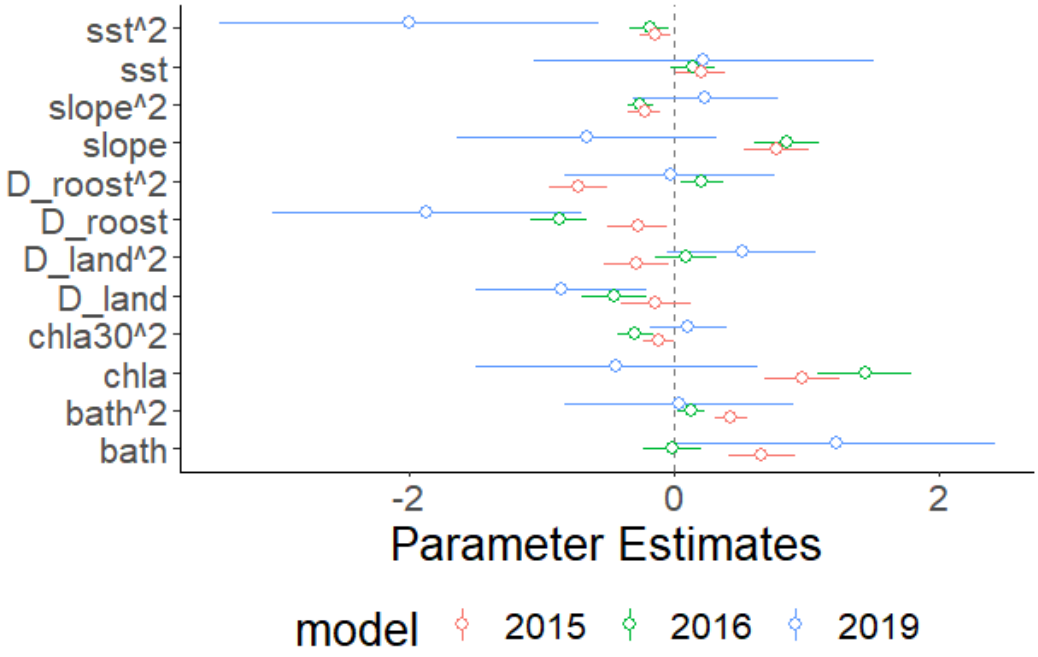

Figure S2. 7 Dot whisker plots show model parameter estimates and 95% confidence intervals for the combined static and dynamic model for available foraging site selection.

Table S2. 1 Models of Mexican fish-eating bat foraging site duration during lactation on Isla Partida Norte in 2015, 2016, and 2019.

Model	Parameters	K	AIC	ΔAIC	Marginal R^2	Conditional R^2	CV cor (SE)	CV AUC (SE)
Log(Duration at foraging site)								
Null	~ 1	3	2158	0	0	0.01	-	-
Dynamic	~ log(chla30) + year	8	2160	2	0.01	0.02	-	-
Static	~ bath + dist2coast + dist2roost + slope + year	9	2162	4	0.01	0.02	-	-
Combined	~ bath + log(chla30) + dist2coast + dist2roost + slope + year	11	2194	36	0.02	0.03	-	-

Appendix 3

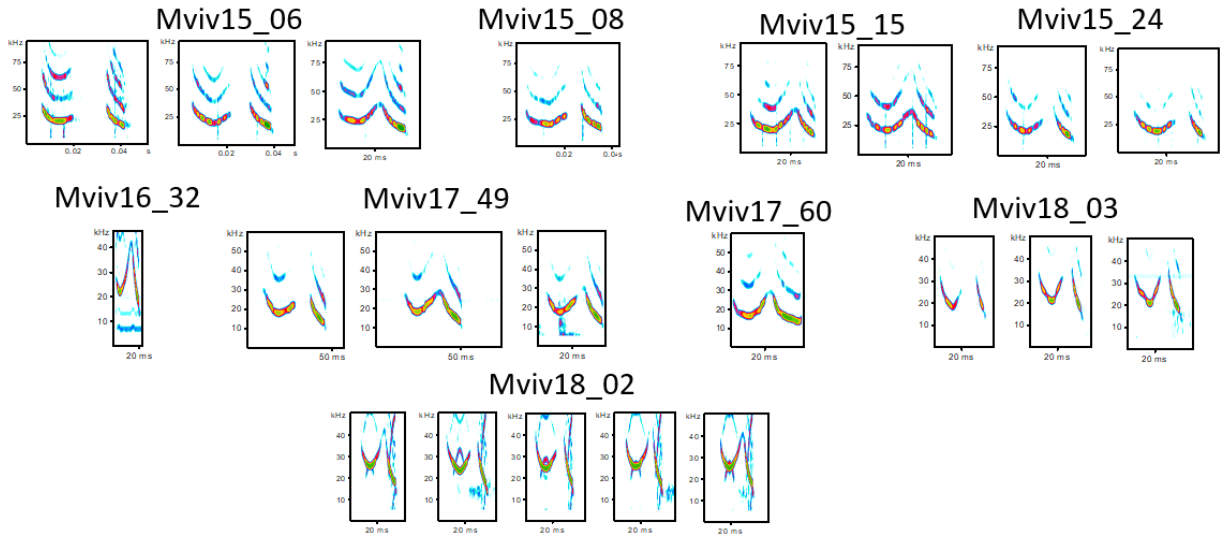

Figure S3. 1 Variation in in-flight social calls from several tagged bats.

Spectrogram recordings are positioned below bat IDs.

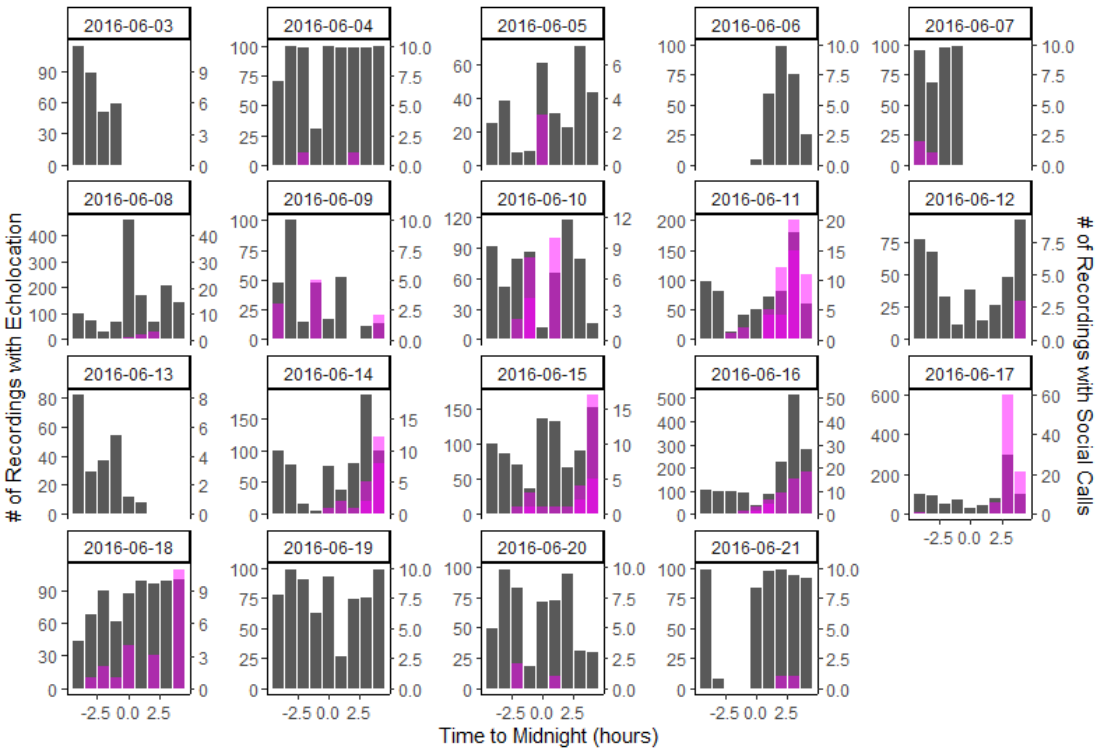

Figure S3. 2 Histograms of the number of recordings containing echolocation calls or social calls (dark grey or purple) each hour over the buoy sampling period.

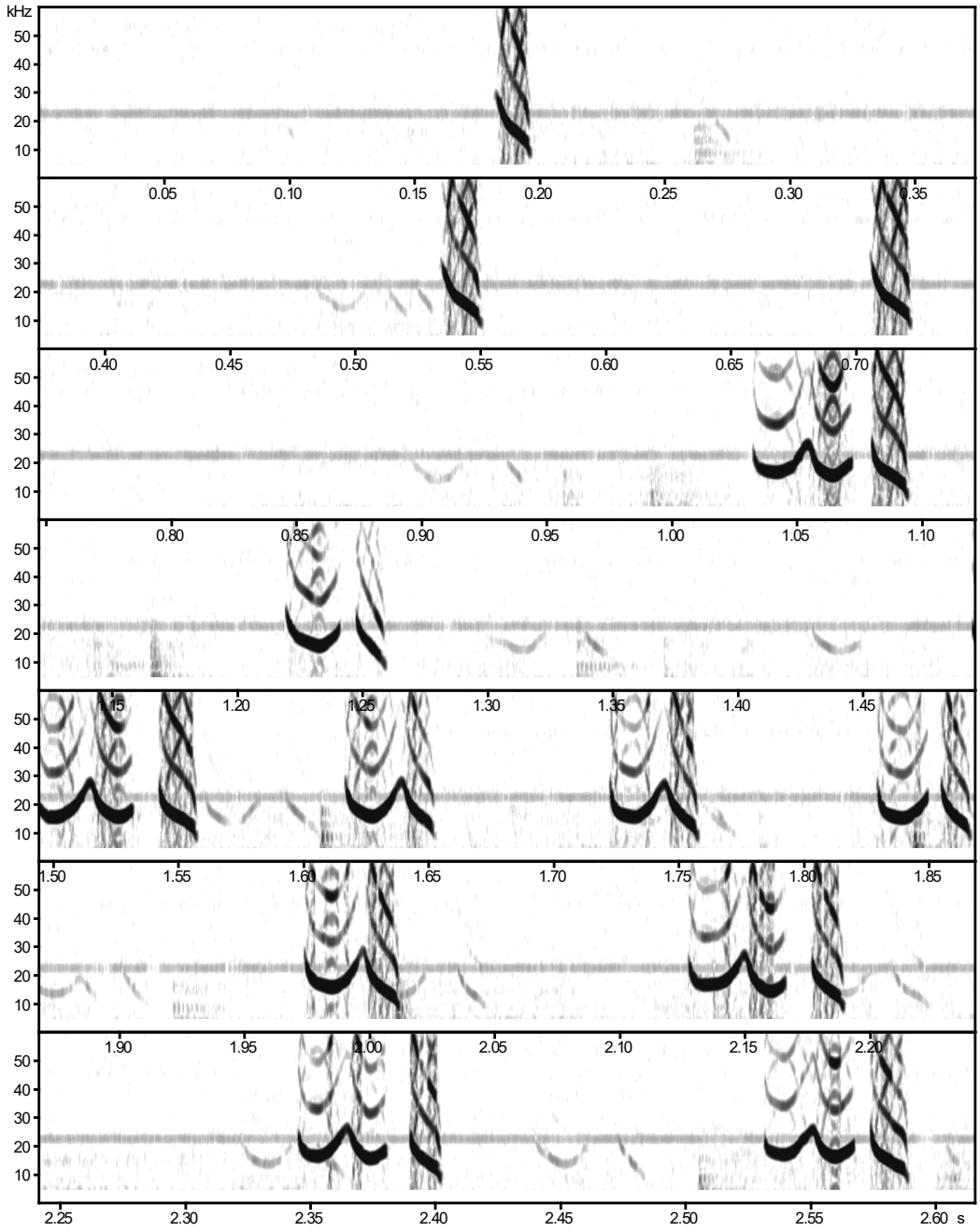

Figure S3. 3 Spectrogram sequence of social calls produced from a tagged bat (Mviv17_60) and conspecific social calls present in the background.

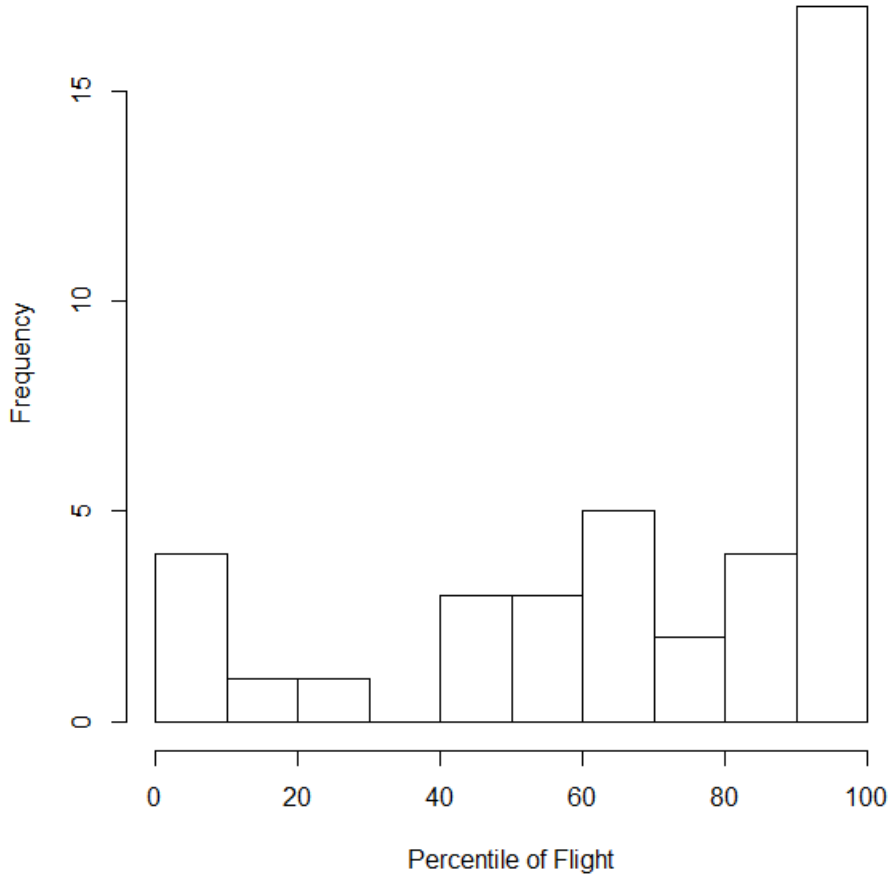

Figure S3. 4 Histogram of the median percentile of flight in which social calls occur.

Table S3. 1 Summary of on-board audio recordings for each tagged individual night.

ID	date	duration in flight (min)	raw number of social calls	trips	estimated pup age (days)	duty cycle	Duty cycle adjusted number of social calls	Proportion of flight with buzzes
Mviv15_05	5/27/2015	206.8	0	2	4.2	10%	0	0.02
Mviv15_06	5/27/2015	259.4	0	2	6.1	10%	0	0.02
Mviv15_06	5/28/2015	237.2	0	3	7	10%	0	0.03
Mviv15_06	5/29/2015	192.0	0	2	8	10%	0	0.01
Mviv15_06	5/30/2015	81.4	0	2	9	10%	0	0.01
Mviv15_06	5/31/2015	113.2	0	3	10	10%	0	0.04
Mviv15_06	6/1/2015	87.9	5	2	11	10%	4	0.01
Mviv15_08	5/29/2015	280.3	0	4	18	10%	0	0.02
Mviv15_08	5/30/2015	65.9	0	3	19	10%	0	0.00
Mviv15_08	5/31/2015	357.3	1	2	20	10%	1	0.01

Mviv15_12	6/1/2015	100.9	1	2	28	10%	1	0.00
Mviv15_12	6/2/2015	311.1	1	1	29	10%	1	0.02
Mviv15_14	5/30/2015	240.3	0	4	15	10%	0	0.01
Mviv15_14	5/31/2015	57.0	0	3	16	10%	0	0.01
Mviv15_15	5/30/2015	21.5	2	3	18	10%	2	0.02
Mviv15_15	5/31/2015	169.1	0	3	19	10%	0	0.02
Mviv15_16	5/30/2015	3.5	0	2	26	10%	0	0.00
Mviv15_16	5/31/2015	390.3	3	2	27	10%	2	0.01
Mviv15_18	6/3/2015	356.9	0	1	33*	10%	0	0.03
Mviv15_19	6/2/2015	124.8	6	2	29	10%	5	0.05
Mviv15_21	6/2/2015	78.3	0	3	34	10%	0	0.03
Mviv15_23	6/4/2015	74.7	3	7	38	10%	2	0.01
Mviv15_23	6/5/2015	212.2	21	1	39	10%	17	0.03
Mviv15_24	6/4/2015	57.4	0	7	28	10%	0	0.06
Mviv15_24	6/5/2015	170.4	4	6	29	10%	3	0.05
Mviv16_06	5/28/2016	59.0	0	3	5	8%	0	0.00
Mviv16_06	5/29/2016	327.0	0	1	6	8%	0	0.03
Mviv16_06	5/30/2016	235.0	0	1	7	8%	0	0.04

Mviv16_07	5/28/2016	175.0	0	3	5	8%	0	0.03
Mviv16_07	5/29/2016	165.0	0	2	6	8%	0	0.01
Mviv16_07	5/30/2016	313.0	0	2	7	8%	0	0.04
Mviv16_08	5/28/2016	171.0	0	2	19	8%	0	0.03
Mviv16_08	5/29/2016	122.0	0	1	20	8%	0	0.03
Mviv16_08	5/30/2016	404.0	0	1	21	8%	0	0.03
Mviv16_32	6/4/2016	109.0	44	8	22*	17%	22	0.00
Mviv16_32	6/5/2016	206.5	0	2	23*	17%	0	0.01
Mviv16_37	6/8/2016	1.5	0	1	27	17%	0	0.00
Mviv16_37	6/9/2016	249.0	0	1	28	17%	0	0.00
Mviv17_12	6/8/2017	16.6	0	1	18	100%	0	0.00
Mviv17_16	6/9/2017	174.0	0	1	12	100%	0	0.01
Mviv17_29	6/15/2017	304.3	0	2	22	50%	0	0.05
Mviv17_30	6/16/2017	215.3	2	1	23	50%	0	0.06
Mviv17_33	6/17/2017	405.5	0	2	21	50%	0	0.03
Mviv17_34	6/18/2017	277.8	64	1	19	50%	11	0.04
Mviv17_38	6/19/2017	362.1	2	6	29	50%	0	0.04
Mviv17_41	6/20/2017	15.7	2	9	22	50%	0	0.00

Mviv17_49	6/22/2017	264.4	26	4	24	50%	4	0.02
Mviv17_60	6/26/2017	215.6	197	3	29*	100%	16	0.05
Mviv18_02	6/5/2018	276.1	113	6	28	50%	19	0.04
Mviv18_03	6/6/2018	92.7	27	13	16*	50%	4	0.01
Mviv18_05	6/8/2018	28.8	0	2	12	50%	0	0.06
Mviv18_06	6/9/2018	247.4	0	1	23	50%	0	0.09

** Pup age estimated from population growth trends because of missing individual measurements.*

Table S3. 2 Repeatability of social call acoustic measurements. Repeatability was calculated using analyses of variance for all individuals.

Acoustic Parameter	*P values*	*F ratio (df)*	n_0	*Repeatability*
Duration 1st Syllable	< 0.001	50.5 (7,136)	20.6	0.71
Peak Frequency 1st Syllable	< 0.001	51.16 (7,136)	20.6	0.71
Peak Frequency 2nd Syllable	< 0.001	72.97 (7,136)	20.6	0.78
Break between Syllables	< 0.001	4.55 (7,136)	20.6	0.15
Difference in amplitude between syllables	< 0.001	10.25 (7,136)	20.6	0.31
Slope of start frequency to peak frequency of 1st syllable	< 0.001	17.51 (7,136)	20.6	0.45

Slope of peak frequency to end frequency of 1st syllable	< 0.001	7.71 (7,136)	20.6	0.25

Table S3. 3 LDA weightings for social call parameters.

	In-flight social calls *Training set*	
	LD1 (81.1%)	LD2 (8.5%)
Duration 1st Syllable	**-1.01**	-0.28
Peak Frequency 1st Syllable	**1.41**	**-1.00**
Peak Frequency 2nd Syllable	**1.32**	0.29
Break between Syllables	0.10	0.10
Difference in amplitude between syllables	0.44	**-0.83**
Slope of start frequency to peak frequency of 1st syllable	-0.48	**-0.66**
Slope of peak frequency to end frequency of 1st syllable	**0.67**	0.65

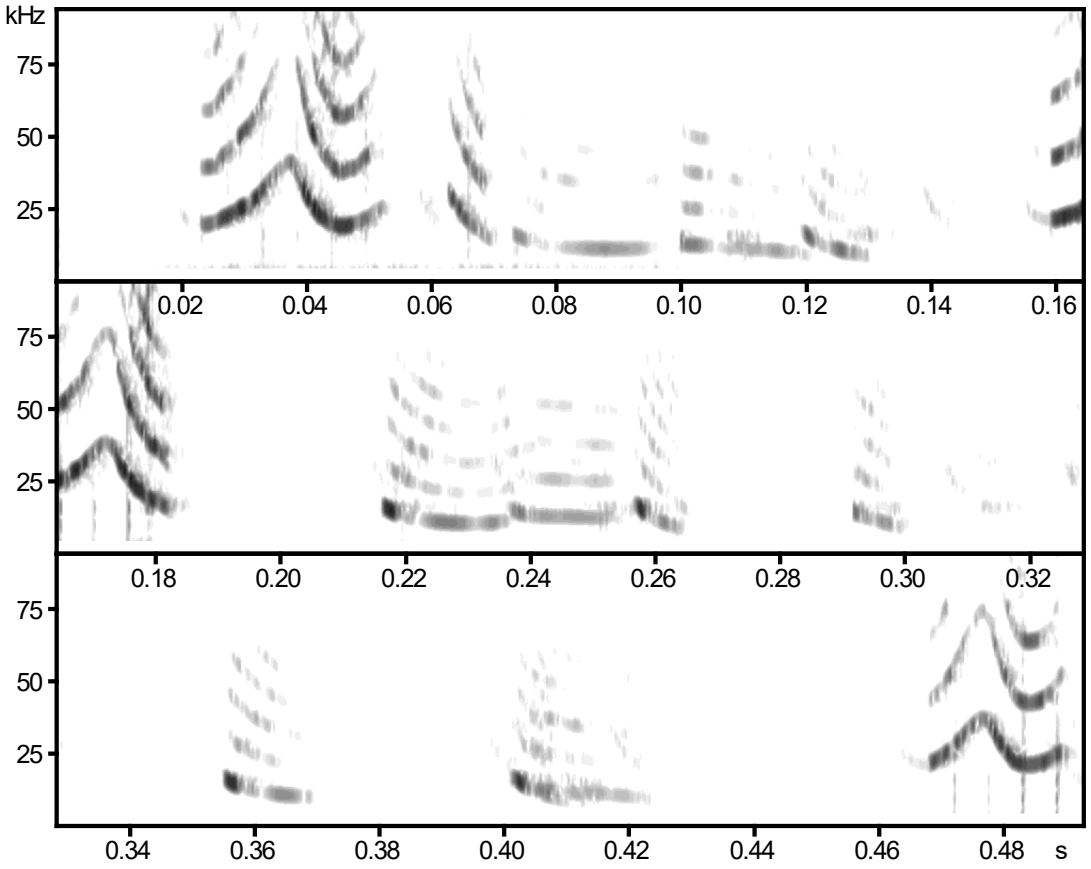

Figure S3. 5 Overlapping social calls produced in the roost.

This possible mother pup interaction was determined from the amplitude of multiple overlapping social calls in the roost audio from individual Mviv15_06. Frequencies with higher amplitudes in the spectrogram are darker. Further work is needed to determine if these calls are produced by pups or from nearby conspecifics, however, these calls are suggestive of pup calls given that most bat pups start out lower in frequency and longer in duration than adult social calls (Barclay 1982, Jin et al. 2012).

Appendix 4

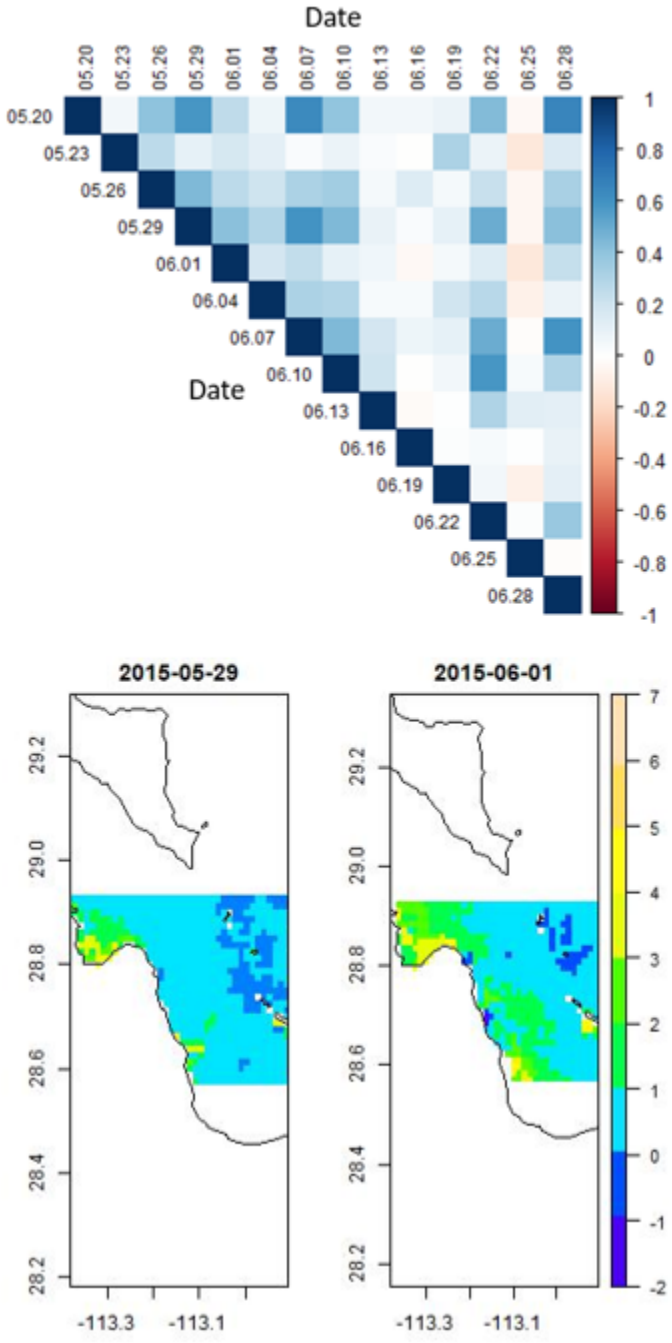
Date
05.20
05.23
05.26
05.29
06.01
06.04
06.07
06.10
06.13
06.16
06.19
06.22
06.25
06.28
Date
1
0.8
0.6
0.4
0.2
0
-0.2
-0.4
-0.6
-0.8
-1
2015-05-29
2015-06-01
29.2
29.0
28.8
28.6
28.4
28.2
-113.3
-113.1
7
6
5
4
3
2
1
0
-1
-2
Log Chla (mg/m^3)

Figure S4. 1 Food is difficult to predict in the foraging areas of the Fish-eating bats can be learnt from an analysis of ocean chlorophyll concentrations.

Related to Figure 4.1. Top - Two maps of chlorophyll concentrations (on May 29 and June 6) in the foraging area around Isla Partida Norte, between May 20 and June 30, 2015 (axes show dates). Each spatial map of chlorophyll concentration (mg/m^3) was generated for the foraging areas of our bats (X min: -113.3862, X max: -112.9022, Y min: 28.5709, Y max: 28.9277). Chlorophyll concentration strongly correlates with the concentration of plankton, which should predict the concentration of fish and crustaceans eaten by the bats. Bottom-Each cell in the matrix depicts the Pearson's correlation between the spatial distribution of chlorophyll concentrations on a pair of days (3-days apart). The dates are depicted on the axes (a total of 14 days were sampled). Chlorophyll concentration had low spatial correlation over time, suggesting that chlorophyll abundance and probably also fish abundance was spatially stochastic over the study period. Data was obtained from NOAA ERDDAP data server at 0.0125 degree (~1 km2) spatial resolution: (http://coastwatch.pfeg.noaa.gov/erddap/griddap/erdMWchla3day.graph).

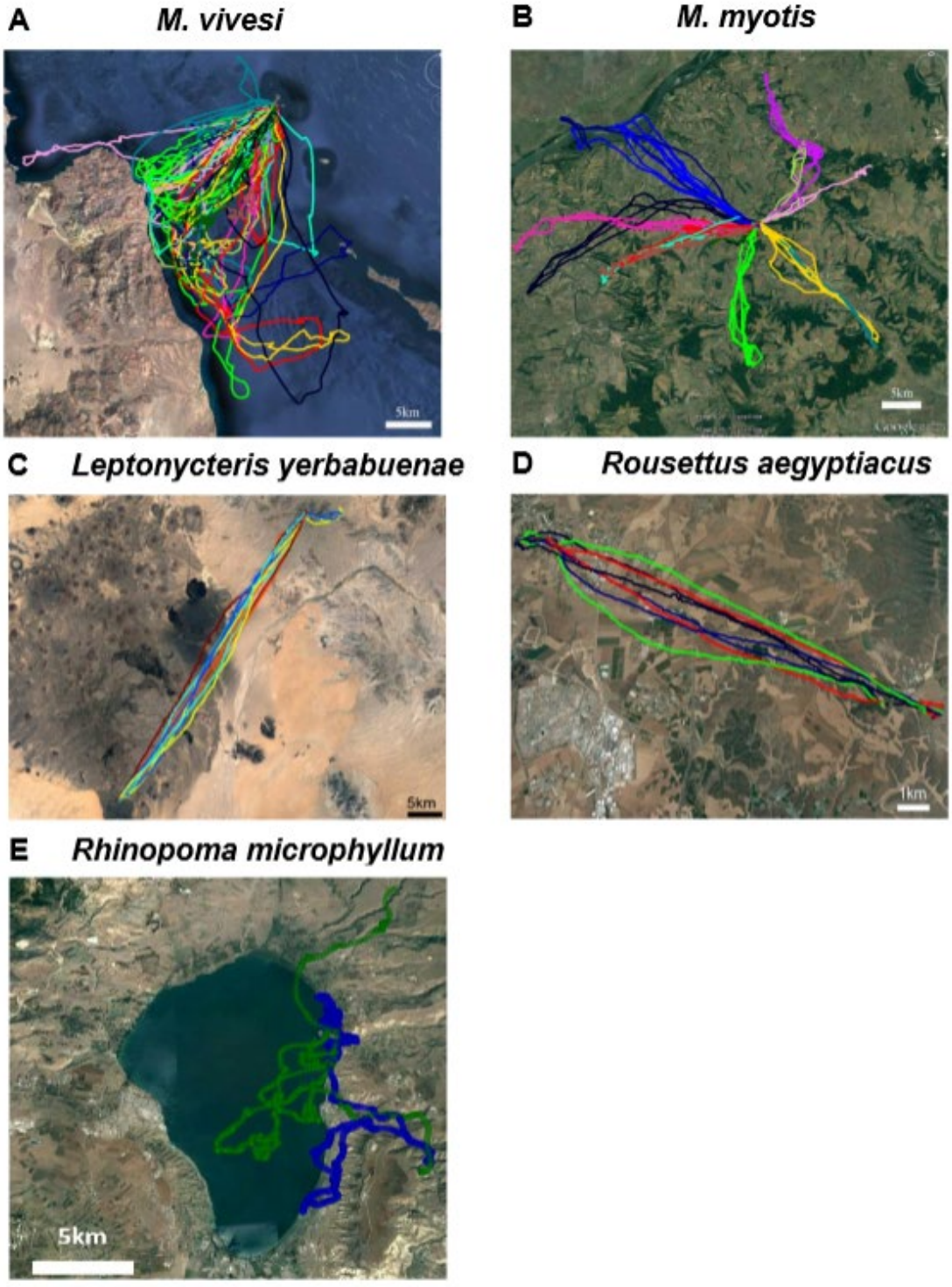
A
M. vivesi
5km
B
M. myotis
5km
C
Leptonycteris yerbabuenae
5km
D
Rousettus aegyptiacus
1km
E
Rhinopoma microphyllum
5km

Figure S4. 2 Flight trajectories of all five bat species.

Related to Figure 4.1. A-*M. vivesi*, B- *M. myotis*, C- *Leptonycteris yerbabuenae*, D-*Rousettus aegyptiacus* and E-*Rhinopoma microphyllum*. For *M. myotis* and *M. vivesi* the trajectories of different individuals (15 individuals per species) are presented indifferent colors (some individuals are masked by others). Note the straight flight trajectories of *M. myotis* bats vs. the wandering movement in *M. vivesi* bats. Several nights of one individual are presented for the other three species (C-E). In *Leptonycteris* nights are ordered: blue, turquoise, yellow, orange and brown. Rousettus nights are ordered: black, red, green and blue. *Rhinopoma* nights are ordered: blue, green. All maps in the supplementary figures are presented with the north pointing up.

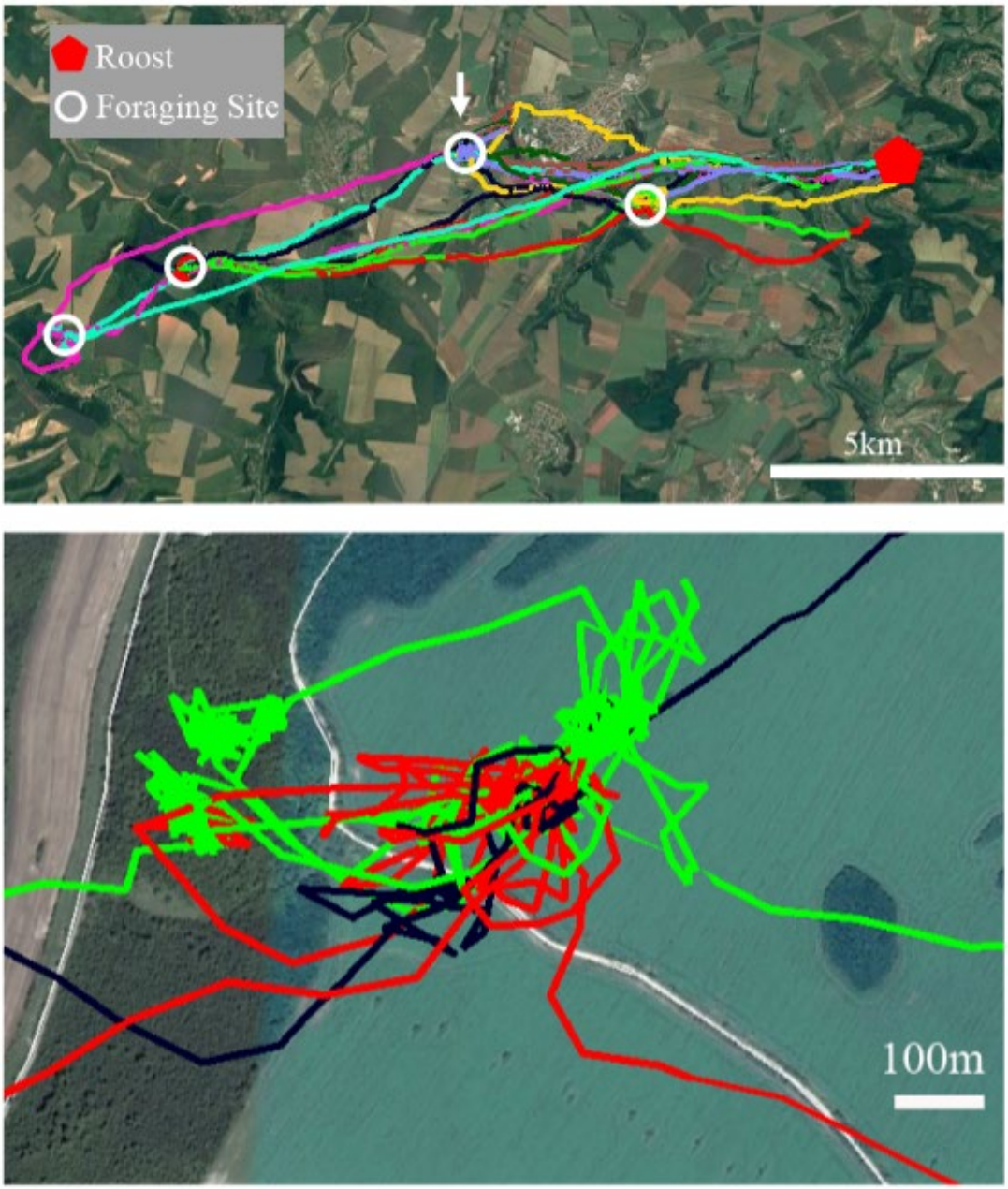

Figure S4. 3 Foraging trajectories of *M. myotis*.

Related to Figure 4.1. Top, the flight trajectories of a single *M. myotis* bat that visited 4 foraging sites (white circles) over a period of 9 nights (1-10/8/2015). Each color depicts a different night. All sites were visited for at least 3 nights consecutively, and the one most visited (white arrow) was visited on 7 nights in a row. Bottom, three

consecutive foraging nights (color coded) of one *M. myotis*. Note how in all three nights, the bat returned to the exact same patch in the field (note scale). In two of the nights (red and green) it also returned to the same patch in the nearby forest (to the left).

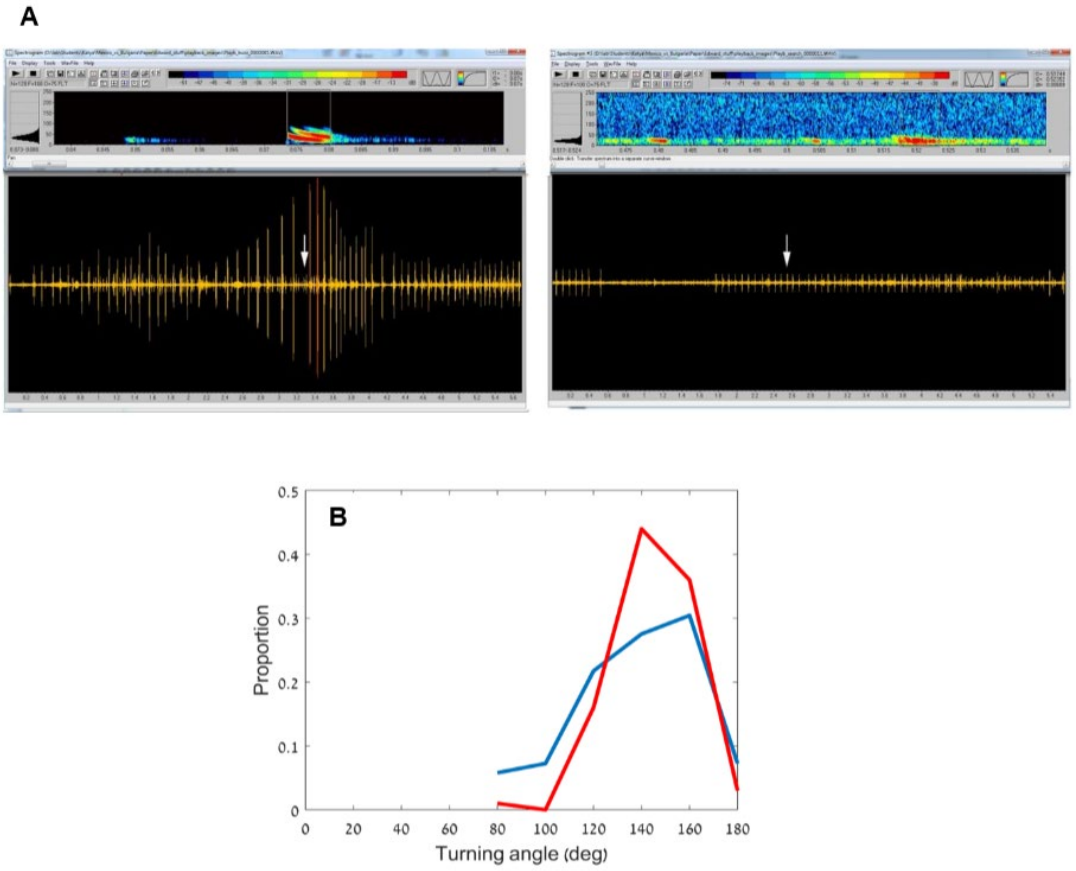

Figure S4. 4 Validation experiments.

Related to Figure 4.2. A - Recordings of playback experiments. Left –a recording of a *M. vivesi* bat that approached the speaker in response to a 'search' playback and was detected by our analysis. Right –a recording of a *M. vivesi* bat that passed above the system during the 'search' playback. Bottom panels show the time signals while the top ones show a spectrogram of a single call. Note the second harmonic that appears

in the call of the approaching bat (left) because its calls are directed towards the playback system (and microphone).This phenomenon allowed us to distinguish approaching bats from passing bats, and to detect the calls of approaching bats automatically. White arrows depict the playback signals. Playback signals are weak in the recordings because of the relative position of the speaker, which was behind the microphone. Screen shots are taken from Avisoft saslab. B- Turning angles of modeled bats (blue) and real bats (red). The turning angles were defined by three points – the turning points and two points at a distance of 1 km from the turning point (one before and one after the turn).

Bibliography

Aarts, G., J. Fieberg, and J. Matthiopoulos. 2012. Comparative interpretation of count, presence-absence and point methods for species distribution models. Methods in Ecology and Evolution 3:177–187.

Abrahms, B., N. R. Jordan, K. A. Golabek, J. W. McNutt, A. M. Wilson, and J. S. Brashares. 2016. Lessons from integrating behaviour and resource selection: activity-specific responses of African wild dogs to roads. Animal Conservation 19:247–255.

Ainley, D. G., K. D. Dugger, R. G. Ford, S. D. Pierce, D. C. Reese, R. D. Brodeur, C. T. Tynan, and J. A. Barth. 2009. Association of predators and prey at frontal features in the California Current: Competition, facilitation, and co-occurrence. Marine Ecology Progress Series 389:271–294.

Aizpurua, O., J. Aihartza, A. Alberdi, H. J. Baagoe, and I. Garin. 2014. Fine-tuned echolocation and capture-flight of Myotis capaccinii when facing different-sized insect and fish prey. Journal of Experimental Biology 217:3318–3325.

Aizpurua, O., and A. Alberdi. 2018. Ecology and evolutionary biology of fishing bats. Mammal Review 48:284–297.

Aizpurua, O., A. Alberdi, J. Aihartza, and I. Garin. 2015. Insight on how fishing bats discern prey and adjust their mechanic and sensorial features during the attack sequence. Scientific Reports 5:1–8.

Akamatsu, T., A. Matsuda, S. Suzuki, D. Wang, K. Wang, M. Suzuki, H. Muramoto, N. Sugiyama, and K. Oota. 2005. New stereo acoustic data logger for free-ranging dolphins and porpoises. Marine Technology Society Journal 39:3–9.

Álvarez-Borrego, S. 2012. Phytoplankton biomass and production in the Gulf of California: A review. Botanica Marina 55:119–128.

Arlettaz, R. 1999. Habitat selection as a major resource partitioning mechanism between the two sympatric sibling bat species Myotis myotis and Myotis blythii. Journal of Animal Ecology 68:460–471.

Arnold, B. D., and G. S. Wilkinson. 2011. Individual specific contact calls of pallid bats (Antrozous pallidus) attract conspecifics at roosting sites. Behavioral Ecology and Sociobiology 65:1581–1593.

Bailey, H., V. Lyubchich, J. Wingfield, A. Fandel, A. Garrod, and A. N. Rice. 2019. Empirical evidence that large marine predator foraging behavior is consistent with area-restricted search theory. Ecology 100:e02743.

Balcombe, J. P. 1990. Vocal recognition of pups by mother Mexican free-tailed bats, Tadarida brasiliensis mexicana. Animal Behaviour 39:960–966.

Barclay, R. M. R. 1982. Interindividual use of echolocation calls: Eavesdropping by bats. Behavioral Ecology and Sociobiology 10:271–275.

Barlow, K. E., and G. Jones. 1997. Function of pipistrelle social calls: Field data and a playback experiment. Animal Behaviour 53:991–999.

Bartón, K. 2019. Package MuMIn: Multi-Model Inference. R package version 1.43.6.

Bates, D., M. Mächler, B. Bolker, and S. Walker. 2015. Fitting Linear Mixed-Effects Models Using {lme4}. Journal of Statistical Software 67:1–48.

Becker, B. H., and S. R. Beissinger. 2003. Scale-dependent habitat selection by a nearshore seabird, the marbled murrelet, in a highly dynamic upwelling system. Marine Ecology Progress Series 256:243–255.

Bell, A. M., S. J. Hankison, and K. L. Laskowski. 2009. The repeatability of behaviour: a meta-analysis. Animal Behaviour 77:771–783.

Belviso, S., S. -K Kim, F. Rassoulzadegan, B. Krajka, B. C. Nguyen, N. Mihalopoulos, and P. Buat-Menard. 1990. Production of dimethylsulfonium propionate (DMSP) and dimethylsulfide (DMS) by a microbial food web. Limnology and Oceanography 35:1810–1821.

Bennison, A., S. Bearhop, T. W. Bodey, S. C. Votier, W. J. Grecian, E. D. Wakefield, K. C. Hamer, and M. Jessopp. 2018. Search and foraging behaviors from movement data: A comparison of methods. Ecology and Evolution 8:13–24.

Bestley, S., T. A. Patterson, M. A. Hindell, and J. S. Gunn. 2008. Feeding ecology of wild migratory tunas revealed by archival tag records of visceral warming. Journal of Animal Ecology 77:1223–1233.

Blood, B. R., and M. K. Clark. 1998. Myotis vivesi. Mammalian Species:1–5.

Bohn, K. M., and E. H. Gillam. 2018. In-flight social calls: A primer for biologists and managers studying echolocation. Canadian Journal of Zoology 96:787–800.

Bohn, K. M., C. F. Moss, and G. S. Wilkinson. 2009. Pup guarding by greater spear-nosed bats. Behavioral Ecology and Sociobiology 63:1693–1703.

Bohn, K. M., B. Schmidt-French, S. T. Ma, and G. D. Pollak. 2008. Syllable acoustics, temporal patterns, and call composition vary with behavioral context in Mexican free-tailed bats. The Journal of the Acoustical Society of America 124:1838–1848.

Bohn, K. M., G. S. Wilkinson, and C. F. Moss. 2007. Discrimination of infant isolation calls by female greater spear-nosed bats, Phyllostomus hastatus.

Animal Behaviour 73:423–432.

Börger, L. 2016. Stuck in motion? Reconnecting questions and tools in movement ecology. Journal of Animal Ecology 85:5–10.

Bost, C. A., C. Cotté, F. Bailleul, Y. Cherel, J. B. Charrassin, C. Guinet, D. G. Ainley, and H. Weimerskirch. 2009. The importance of oceanographic fronts to marine birds and mammals of the southern oceans. Journal of Marine Systems 78:363–376.

Boughman, J. W., and G. S. Wilkinson. 1998. Greater spear-nosed bats discriminate group mates by vocalizations. Animal Behaviour 55:1717–1732.

Boyce, M. S. 2006. Scale for resource selection functions. Diversity and Distributions 12:269–276.

Boyce, M. S., P. R. Vernier, S. E. Nielsen, and F. K. A. Schmiegelow. 2002. Evaluating resource selection functions. Ecological Modelling 157:281–300.

Bradbury, J. W., and S. L. Vehrencamp. 2011. Principles of Animal Communication, Second Edition literatury. Page Principles of Animal Communication, 2nd ed.

Brigham, R. M., J. E. Cebek, and M. B. C. Hickey. 1989. Intraspecific Variation in the Echolocation Calls of Two Species of Insectivorous Bats. Journal of Mammalogy 70:426–428.

Brodersen, K. H., C. S. Ong, K. E. Stephan, and J. M. Buhmann. 2010. The balanced accuracy and its posterior distribution. Proceedings - International Conference on Pattern Recognition:3121–3124.

Bumann, D., and J. Krause. 1993. Front individuals lead in shoals of three-spined sticklebacks (Gasterosteus aculeatus) and juvenile roach (Rutilus rutilus).

Behaviour 125:189–198.

Burgess, W. C. 2000. The bioacoustic probe: A general-purpose acoustic recording tag. The Journal of the Acoustical Society of America 108:2583.

Burkanov, V., E. Gurarie, A. Altukhov, E. Mamaev, P. Permyakov, A. Trukhin, J. Waite, and T. Gelatt. 2011. Environmental and biological factors influencing maternal attendance patterns of Steller sea lions (Eumetopias jubatus) in Russia. Journal of Mammalogy 92:352–366.

Cai, W., A. Santoso, G. Wang, S. W. Yeh, S. Il An, K. M. Cobb, M. Collins, E. Guilyardi, F. F. Jin, J. S. Kug, M. Lengaigne, M. J. Mcphaden, K. Takahashi, A. Timmermann, G. Vecchi, M. Watanabe, and L. Wu. 2015. ENSO and greenhouse warming. Nature Climate Change 5:849–859.

Calenge, C. 2006. The package "adehabitat" for the R software: A tool for the analysis of space and habitat use by animals. Ecological Modelling 197:516–519.

Caraco, T., and L. A. Giraldea. 1991. Social foraging: Producing and scrounging in a stochastic environment. Journal of Theoretical Biology 153:559–583.

Carroll, G., M. Cox, R. Harcourt, B. J. Pitcher, D. Slip, and I. Jonsen. 2017. Hierarchical influences of prey distribution on patterns of prey capture by a marine predator. Functional Ecology 31:1750–1760.

Carter, G. G., R. Logsdon, B. D. Arnold, A. Menchaca, and R. A. Medellin. 2012. Adult vampire bats produce contact calls when isolated: Acoustic variation by species, population, colony, and individual. PLoS ONE 7:e38791.

Castil, G., J. Minch, and R. P. Phillipa. 1980. The geology and ages of islands. Pages

13–25 *in* J. H. A. L. Carreño, editor. Island Biogeography in the Sea of Cortez. Oxford University Press, New York.

Charnov, E. L. 1976. Optimal foraging, the marginal value theorem. Theoretical Population Biology 9:129–136.

Chaverri, G., L. Ancillotto, and D. Russo. 2018. Social communication in bats. Biological Reviews 93:1938–1954.

Chaverri, G., E. H. Gillam, and M. J. Vonhof. 2010. Social calls used by a leaf-roosting bat to signal location. Biology Letters 6:441–444.

Chetkiewicz, C. L. B., and M. S. Boyce. 2009. Use of resource selection functions to identify conservation corridors. Journal of Applied Ecology 46:1036–1047.

Clark, C. W., and M. Mangel. 1986. The evolutionary advantages of group foraging. Theoretical Population Biology 30:45–75.

Codling, E. A., J. W. Pitchford, and S. D. Simpson. 2007. Group navigation and the "many-wrongs principle" in models of animal movement. Ecology 88:1864–1870.

Corcoran, A. J., and W. E. Conner. 2014. Bats jamming bats: Food competition through sonar interference. Science 346:745–747.

Cox, S. L., C. B. Embling, P. J. Hosegood, S. C. Votier, and S. N. Ingram. 2018. Oceanographic drivers of marine mammal and seabird habitat-use across shelf-seas: A guide to key features and recommendations for future research and conservation management. Estuarine, Coastal and Shelf Science 212:294–310.

Cox, S. L., B. E. Scott, and C. J. Camphuysen. 2013. Combined spatial and tidal processes identify links between pelagic prey species and seabirds. Marine

Ecology Progress Series 479:203–221.

Cvikel, N., K. Egert Berg, E. Levin, E. Hurme, I. Borissov, A. Boonman, E. Amichai, and Y. Yovel. 2015a. Bats aggregate to improve prey search but might be impaired when their density becomes too high. Current Biology 25:206–211.

Cvikel, N., E. Levin, E. Hurme, I. Borissov, A. Boonman, E. Amichai, and Y. Yovel. 2015b. On-board recordings reveal no jamming avoidance in wild bats. Proceedings of the Royal Society B: Biological Sciences 282:20142274.

Dall, S. R. X., L. A. Giraldeau, O. Olsson, J. M. McNamara, and D. W. Stephens. 2005. Information and its use by animals in evolutionary ecology. Trends in Ecology and Evolution 20:187–193.

Danchin, É., L. A. Giraldeau, T. J. Valone, and R. H. Wagner. 2004. Public information: From nosy neighbors to cultural evolution. Science 305:487–491.

Davis, A. J., B. F. J. Manly, L. L. McDonald, and D. L. Thomas. 2007. Resource Selection by Animals: Statistical Design and Analysis for Field Studies. Page Springer Science & Business Media.

Dechmann, D. K. N., S. L. Heucke, L. Giuggioli, K. Safi, C. C. Voigt, and M. Wikelski. 2009. Experimental evidence for group hunting via eavesdropping in echolocating bats. Proceedings of the Royal Society B: Biological Sciences 276:2721–2728.

Dechmann, D. K. N., B. Kranstauber, D. Gibbs, and M. Wikelski. 2010. Group hunting - A reason for sociality in molossid bats? PLoS ONE 5:e9012.

Denzinger, A., and H. U. Schnitzler. 2013. Bat guilds, a concept to classify the highly diverse foraging and echolocation behaviors of microchiropteran bats. Frontiers

in Physiology 4:164.

Deppe, J. L., M. P. Ward, R. T. Bolus, R. H. Diehl, A. Celis-Murillo, T. J. Zenzal, F. R. Moore, T. J. Benson, J. A. Smolinsky, L. N. Schofield, D. A. Enstrom, E. H. Paxton, G. Bohrer, T. A. Beveroth, A. Raim, R. L. Obringer, D. Delaney, and W. W. Cochran. 2015. Fat, weather, and date affect migratory songbirds' departure decisions, routes, and time it takes to cross the Gulf of Mexico. Proceedings of the National Academy of Sciences of the United States of America 112:E6331–E6338.

Dodge, S., G. Bohrer, R. Weinzierl, S. C. Davidson, R. Kays, D. Douglas, S. Cruz, J. Han, D. Brandes, and M. Wikelski. 2013. The environmental-data automated track annotation (Env-DATA) system: Linking animal tracks with environmental data. Movement Ecology 1:3.

Domalik, A. D., J. M. Hipfner, K. R. Studholme, G. T. Crossin, and D. J. Green. 2018. At-sea distribution and fine-scale habitat use patterns of zooplanktivorous Cassin's auklets during the chick-rearing period. Marine Biology 165:177.

Dragon, A. C., A. Bar-Hen, P. Monestiez, and C. Guinet. 2012. Comparative analysis of methods for inferring successful foraging areas from Argos and GPS tracking data. Marine Ecology Progress Series 452:253–267.

Edelhoff, H., J. Signer, and N. Balkenhol. 2016. Path segmentation for beginners: An overview of current methods for detecting changes in animal movement patterns. Movement Ecology 4:21.

Egert-Berg, K., E. R. Hurme, S. Greif, A. Goldstein, L. Harten, L. G. Herrera M., J. J. Flores-Martínez, A. T. Valdés, D. S. Johnston, O. Eitan, I. Borissov, J. R.

Shipley, R. A. Medellin, G. S. Wilkinson, H. R. Goerlitz, and Y. Yovel. 2018. Resource Ephemerality Drives Social Foraging in Bats. Current Biology 28:3667-3673.e5.

Escalante-Almazán, F. 2013. Temporal and spatial variation of sea surface temperature, chlorophyll a, and primary productivity in the Gulf of California. Ciencias Marinas 39:203–215.

Esser, K. -H, and U. Schmidt. 1989. Mother-Infant Communication in the Lesser Spear-nosed Bat Phyllostomus discolor (Chiroptera, Phyllostomidae) — Evidence for Acoustic Learning. Ethology 82:156–168.

De Fanis, E., and G. Jones. 1995. The role of odour in the discrimination of conspecifics by pipistrelle bats. Animal Behaviour 49:835–839.

Fauchald, P., and T. Tveraa. 2003. Using First-Passage Time in the Analysis of Area-Restricted Search and Habitat Selection. Ecology 84:282–288.

Fauchald, P., and T. Tveraa. 2006. Hierarchical patch dynamics and animal movement pattern. Oecologia 149:383–395.

Fenton, M. B., and G. P. Bell. 1981. Recognition of Species of Insectivorous Bats by Their Echolocation Calls. Journal of Mammalogy 62:233–243.

Field, C. B., M. J. Behrenfeld, J. T. Randerson, and P. Falkowski. 1998. Primary production of the biosphere: Integrating terrestrial and oceanic components. Science 281:237–240.

Fish, F. E., B. R. Blood, and B. D. Clark. 1991. Hydrodynamics of the feet of fish-catching bats: Influence of the water surface on drag and morphological design. Journal of Experimental Zoology 258:164–173.

Fithian, W., and T. Hastie. 2013. Finite-sample equivalence in statistical models for presence-only data. Annals of Applied Statistics 7:1917–1939.

Fleming, T. H., M. D. Tuttle, and M. A. Horner. 1996. Pollination biology and the relative importance of nocturnal and diurnal pollinators in three species of Sonoran desert columnar cacti. Southwestern Naturalist 41:257–269.

Flemming, S., P. Smith, N. Seymour, and R. Bancroft. 1992. Ospreys use local enhancement and flock foraging to locate prey. The Auk 109:649–654.

Flores-Martínez, J. J., C. H. Floyd, L. G. Herrera, and B. P. May. 2004. Genetic variation and population size of Myotis vivesi in Isla Partida. Pages 185–190 *in* V. S.-C. R. Medellín, editor. Contribuciones Mastozoológicas en Homenaje a Bernardo Villa. UniversidadNacional Autónoma de México, Mexico City, Mexico.

Fox, J., and S. Weisberg. 2019. An {R} Companion to Applied Regression. Third. Sage, Thousand Oaks {CA}.

Friedman, M. 2006. The use of ranks to avoid the assumption of normality implicit in the analysis of variance. Journal of the American Statistical Association 32:675.

Fryxell, J. M., M. Hazell, L. Borger, B. D. Dalziel, D. T. Haydon, J. M. Morales, T. McIntosh, and R. C. Rosatte. 2008. Multiple movement modes by large herbivores at multiple spatiotemporal scales. Proceedings of the National Academy of Sciences 105:19114–19119.

Galef, B. G., and L. A. Giraldeau. 2001. Social influences on foraging in vertebrates: Causal mechanisms and adaptive functions. Animal Behaviour 61:3–15.

Galef, B. G., and K. N. Laland. 2005. Social Learning in Animals: Empirical Studies

and Theoretical Models. BioScience 55:489–499.

Garriga, J., J. R. B. Palmer, A. Oltra, and F. Bartumeus. 2016. Expectation-maximization binary clustering for behavioural annotation. PLoS ONE 11:e0151984.

Geberl, C., S. Brinkløv, L. Wiegrebe, and A. Surlykke. 2015. Fast sensory–motor reactions in echolocating bats to sudden changes during the final buzz and prey intercept. Proceedings of the National Academy of Sciences 112:4122–4127.

Genin, A. 2004. Bio-physical coupling in the formation of zooplankton and fish aggregations over abrupt topographies. Journal of Marine Systems 50:3–20.

Gerber, B. D., and J. M. Northrup. 2019. Improving spatial predictions of animal resource selection to guide conservation decision making. Ecology 0:e02953.

Gillam, E. H. 2007. Eavesdropping by bats on the feeding buzzes of conspecifics. Canadian Journal of Zoology 85:795–801.

Giraldeau, L.-A., and T. Caraco. 2010. Social Foraging Theory. Page Princeton University Press.

Gittleman, J. L., and S. D. Thompson. 1988. Energy allocation in mammalian reproduction. Integrative and Comparative Biology 28:863–875.

Goldbogen, J. A., D. E. Cade, A. T. Boersma, J. Calambokidis, S. R. Kahane-Rapport, P. S. Segre, A. K. Stimpert, and A. S. Friedlaender. 2017. Using digital tags with integrated video and inertial sensors to study moving morphology and associated function in large aquatic vertebrates. Anatomical Record 300:1935–1941.

Gould, E., N. K. Woolf, and D. C. Turner. 1973. Double-Note Communication Calls

in Bats: Occurrence in Three Families. Journal of Mammalogy 54:998–1001.

Grecian, W. J., M. J. Witt, M. J. Attrill, S. Bearhop, P. H. Becker, C. Egevang, R. W. Furness, B. J. Godley, J. González-Solís, D. Grémillet, M. Kopp, A. Lescroël, J. Matthiopoulos, S. C. Patrick, H. U. Peter, R. A. Phillips, I. J. Stenhouse, and S. C. Votier. 2016. Seabird diversity hotspot linked to ocean productivity in the Canary Current Large Marine Ecosystem. Biology Letters 12:20160024.

Greif, S., and Y. Yovel. 2019. Using on-board sound recordings to infer behaviour of free-moving wild animals. The Journal of Experimental Biology 222:jeb184689.

Griffin, D. R., F. A. Webster, and C. R. Michael. 1960. The echolocation of flying insects by bats. Animal Behaviour 8:141–154.

Grünbaum, D., and R. R. Veit. 2003. Black-browed Albatrosses foraging on Antarctic krill: Density-dependence through local enhancement? Ecology 84:3265–3275.

Gurarie, E., R. D. Andrews, and K. L. Laidre. 2009. A novel method for identifying behavioural changes in animal movement data. Ecology Letters 12:395–408.

Gurarie, E., C. Bracis, M. Delgado, T. D. Meckley, I. Kojola, and C. M. Wagner. 2016. What is the animal doing? Tools for exploring behavioural structure in animal movements. Journal of Animal Ecology 85:69–84.

Gurarie, E., C. H. Fleming, W. F. Fagan, K. L. Laidre, J. Hernández-Pliego, and O. Ovaskainen. 2017. Correlated velocity models as a fundamental unit of animal movement: Synthesis and applications. Movement Ecology 5:13.

Gustin, M. K., and G. F. McCracken. 1987. Scent recognition between females and pups in the bat Tadarida brasiliensis mexicana. Animal Behaviour 35:13–19.

Hancock, P. A., E. J. Milner-Gulland, and M. J. Keeling. 2006. Modelling the many-

wrongs principle: The navigational advantages of aggregation in nomadic foragers. Journal of Theoretical Biology 240:302–310.

Harel, R., O. Spiegel, W. M. Getz, and R. Nathan. 2017. Social foraging and individual consistency in following behaviour: Testing the information centre hypothesis in free-ranging vultures. Proceedings of the Royal Society B: Biological Sciences 284:20162654.

Hartigan, J. A., and M. A. Wong. 2006. Algorithm AS 136: A K-Means Clustering Algorithm. Applied Statistics 28:100.

Hazen, E. L., R. M. Suryan, J. A. Santora, S. J. Bograd, Y. Watanuki, and R. P. Wilson. 2013. Scales and mechanisms of marine hotspot formation. Marine Ecology Progress Series 487:177–183.

Hedenstrom, A., and L. C. Johansson. 2015. Bat flight: aerodynamics, kinematics and flight morphology. Journal of Experimental Biology 218:653–663.

Hernández-Ayón, J. M., C. Chapa-Balcorta, F. Delgadillo-Hinojosa, V. F. Camacho-Ibar, M. A. Huerta-Díaz, E. Santamaría-del-Angel, S. Galindo-Bect, and J. A. Segovia-Zavala. 2013. Dinámica del carbono inorgánico disuelto en la región de las grandes islas del golfo de California: Influencia de las masas de agua. Ciencias Marinas 39:183–201.

Herrera M., L. G., J. J. Flores-Martínez, and V. Sánchez-Cordero. 2019. Geographical distribution and conservation status of an endemic insular mammal: The Vulnerable fish-eating bat Myotis vivesi. Oryx 53:388–393.

Hill, R. W., and J. W. H. Dacey. 2006. Metabolism of dimethylsulfoniopropionate (DMSP) by juvenile Atlantic menhaden Brevoortia tyrannus. Marine Ecology

Progress Series 322:239–248.

Hooker, S. K., T. Barychka, M. J. Jessopp, and I. J. Staniland. 2015. Images as proximity sensors: The incidence of conspecific foraging in Antarctic fur seals. Animal Biotelemetry 3:37.

Howard, R. 2014. Principles of Animal Communication. American Entomologist 45:126–126.

Howell, D. J. 1979. Flock Foraging in Nectar-Feeding Bats: Advantages to the Bats and to the Host Plants. The American Naturalist 114:23–49.

Hunt, G. L., R. W. Russell, K. O. Coyle, and T. Weingartner. 1998. Comparative foraging ecology of planktivorous auklets in relation to ocean physics and prey availability. Marine Ecology Progress Series 167:241–259.

Hurme, E., E. Gurarie, S. Greif, L. G. Herrera, J. J. Flores-Martínez, G. S. Wilkinson, and Y. Yovel. 2019. Acoustic evaluation of behavioral states predicted from GPS tracking: A case study of a marine fishing bat. Movement Ecology 7:21.

Hussey, N. E., S. T. Kessel, K. Aarestrup, S. J. Cooke, P. D. Cowley, A. T. Fisk, R. G. Harcourt, K. N. Holland, S. J. Iverson, J. F. Kocik, J. E. M. Flemming, and F. G. Whoriskey. 2015. Aquatic animal telemetry: A panoramic window into the underwater world. Science 348:1255642.

Jackson, A. L., G. D. Ruxton, and D. C. Houston. 2008. The effect of social facilitation on foraging success in vultures: A modelling study. Biology Letters 4:311–313.

Jain, A. K. 2010. Data clustering: 50 years beyond K-means. Pattern Recognition Letters 31:651–666.

Jin, L., J. Wang, Z. Zhang, K. Sun, J. S. Kanwal, and J. Feng. 2012. Postnatal development of morphological and vocal features in Asian particolored bat, Vespertilio sinensis. Mammalian Biology 77:339–344.

Johnson, A. R., J. A. Wiens, B. T. Milne, and T. O. Crist. 1992. Animal movements and population dynamics in heterogeneous landscapes. Landscape Ecology 7:63–75.

Johnson, D. H. 1980. The Comparison of Usage and Availability Measurements for Evaluating Resource Preference. Ecology 61:65–71.

Johnson, M. P., and P. L. Tyack. 2003. A digital acoustic recording tag for measuring the response of wild marine mammals to sound. IEEE Journal of Oceanic Engineering 28:3–12.

Jones, G., M. Morton, P. M. Hughes, and R. M. Budden. 1993. Echolocation, flight morphology and foraging strategies of some West African hipposiderid bats. Journal of Zoology 230:385–400.

Kahru, M., S. G. Marinone, S. E. Lluch-Cota, A. Parés-Sierra, and B. G. Mitchell. 2004. Ocean-color variability in the Gulf of California: Scales from days to ENSO. Deep-Sea Research Part II: Topical Studies in Oceanography 51:139–146.

Katsnelson, E., U. Motro, M. W. Feldman, and A. Lotem. 2008. Early experience affects producer-scrounger foraging tendencies in the house sparrow. Animal Behaviour 75:1465–1472.

Kays, R., M. C. Crofoot, W. Jetz, and M. Wikelski. 2015. Terrestrial animal tracking as an eye on life and planet. Science 348:aaa2478.

Ketchen Jr., D. J., and C. L. Shook. 2002. The application of cluster analysis in strategic management research: an analysis and critique. Strategic Management Journal 17:441–458.

Knörnschild, M., and O. von Helversen. 2008. Nonmutual vocal mother-pup recognition in the greater sac-winged bat. Animal Behaviour 76:1001–1009.

Knörnschild, M., K. Jung, M. Nagy, M. Metz, and E. Kalko. 2012. Bat echolocation calls facilitate social communication. Proceedings of the Royal Society B: Biological Sciences 279:4827–4835.

Kolodny, O., M. Weinberg, L. Reshef, L. Harten, A. Hefetz, U. Gophna, M. W. Feldman, and Y. Yovel. 2017. Who is the host of the host-associated microbiome? Colony-level dynamics overshadow individual-level characteristics in the fur microbiome of a social mammal, the Egyptian fruit-bat. bioRxiv.

Korine, C., I. Izhaki, and Z. Arad. 1999. Is the Egyptian fruit-bat Rousettus aegyptiacus a pest in Israel? An analysis of the bat's diet and implications for its conservation. Biological Conservation 88:301–306.

Krebs, J. R. 1974. Colonial nesting and social feeding as strategies for exploiting food resources in the Great Blue Heron (Ardea herodias). Behaviour 51:99–134.

Kunz, T. H. 1974. Reproduction, Growth, and Mortality of the Vespertilionid Bat, Eptesicus fuscus, in Kansas. Journal of Mammalogy 55:1–13.

Kunz, T. H. 1982. Roosting ecology of bats. Pages 1–55 *in* T. H. Kunz, editor. Ecology of bats. Springer, Boston, MA.

Kunz, T. H., J. O. Whitaker, and M. D. Wadanoli. 1995. Dietary energetics of the insectivorous Mexican free-tailed bat (Tadarida brasiliensis) during pregnancy

and lactation. Oecologia 101:407–415.

Lessells, C. M., and P. T. Boag. 1987. Unrepeatable Repeatabilities: A Common Mistake. The Auk 104:116–121.

Levin, E., Y. Yom-Tov, A. Hefetz, and N. Kronfeld-Schor. 2013. Changes in diet, body mass and fatty acid composition during pre-hibernation in a subtropical bat in relation to NPY and AgRP expression. Journal of Comparative Physiology B: Biochemical, Systemic, and Environmental Physiology 183:157–166.

López, M. E. J., D. M. Palacios, A. J. Legorreta, J. R. Urbán, and B. R. Mate. 2019. Fin whale movements in the Gulf of California, Mexico, from satellite telemetry. PLoS ONE 14:e0209324.

Loughry, W. J., and G. F. McCracken. 1991. Factors Influencing Female-Pup Scent Recognition in Mexican Free-Tailed Bats. Journal of Mammalogy 72:624–626.

Lynch, E., L. Angeloni, K. Fristrup, D. Joyce, and G. Wittemyer. 2013. The use of on-animal acoustical recording devices for studying animal behavior. Ecology and Evolution 3:2030–2037.

Marinone, S. G., J. I. González, and J. M. Figueroa. 2009. Prediction of currents and sea surface elevation in the Gulf of California from tidal to seasonal scales. Environmental Modelling and Software 24:140–143.

Marinovic, B. B., D. A. Croll, N. Gong, S. R. Benson, and F. P. Chavez. 2002. Effects of the 1997-1999 El Niño and La Niña events on zooplankton abundance and euphausiid community composition within the Monterey Bay coastal upwelling system. Progress in Oceanography 54:265–277.

Masters, W. M., K. A. S. Raver, and K. A. Kazial. 1995. Sonar signals of big brown

bats, Eptesicus fuscus, contain information about individual identity, age and family affiliation. Animal Behaviour 50:1243–1260.

Matthiopoulos, J. 2003. The use of space by animals as a function of accessibility and preference. Ecological Modelling 159:239–268.

Maya, J. 1968. The natural history of the fish-eating bat, Pizonyx vivesi. The University of Arizona.

Mayberry, H. W., and P. A. Faure. 2015. Morphological, olfactory, and vocal development in big brown bats. Biology Open 4:22–34.

Mayor, S. J., D. C. Schneider, J. A. Schaefer, and S. P. Mahoney. 2009. Habitat selection at multiple scales. Écoscience 16:238–247.

McClintock, B. T., and T. Michelot. 2018. momentuHMM: R package for generalized hidden Markov models of animal movement. Methods in Ecology and Evolution 9:1518–1530.

McCracken, G. F. 1993. Locational memory and female-pup reunions in Mexican free-tailed bat maternity colonies. Animal Behaviour 45:811–813.

McGarigal, K., H. Y. Wan, K. A. Zeller, B. C. Timm, and S. A. Cushman. 2016. Multi-scale habitat selection modeling: a review and outlook. Landscape Ecology 31:1161–1175.

McInnes, A. M., P. G. Ryan, M. Lacerda, J. Deshayes, W. S. Goschen, and L. Pichegru. 2017. Small pelagic fish responses to fine-scale oceanographic conditions: Implications for the endangered African penguin. Marine Ecology Progress Series 569:187–203.

Millán-Núñez, E., and C. M. Yentsch. 2000. El Canal de Ballenas, Baja California,

como ambiente favorable para el desarrollo del fitoplancton (The Ballenas Channel, Baja California, a favorable environment for the development of phytoplankton). Hidrobiológica 10:91–100.

Millar, J. S. 1977. Adaptive features of mammalian reproduction. Evolution 31:370–386.

Moll, R. J., J. J. Millspaugh, J. Beringer, J. Sartwell, and Z. He. 2007. A new "view" of ecology and conservation through animal-borne video systems. Trends in Ecology and Evolution 22:660–668.

Van Moorter, B., D. R. Visscher, C. L. Jerde, J. L. Frair, and E. H. Merrill. 2010. Identifying Movement States From Location Data Using Cluster Analysis. Journal of Wildlife Management 74:588–594.

Morales, J. M., D. T. Haydon, J. Frair, K. E. Holsinger, and J. M. Fryxell. 2004. Extracting more out of relocation data: Building movement models as mixtures of random walks. Ecology 85:2436–2445.

Moss, C. F., and A. Surlykke. 2010. Probing the natural scene by echolocation in bats. Frontiers in Behavioral Neuroscience 4:33.

Muff, S., J. Signer, and J. Fieberg. 2020. Accounting for individual-specific variation in habitat-selection studies: Efficient estimation of mixed-effects models using Bayesian or frequentist computation. Journal of Animal Ecology 89:80–92.

Nakagawa, S., and H. Schielzeth. 2013. A general and simple method for obtaining R2 from generalized linear mixed-effects models. Methods in Ecology and Evolution 4:133–142.

Nathan, R., W. M. Getz, E. Revilla, M. Holyoak, R. Kadmon, D. Saltz, and P. E.

Smouse. 2008. A movement ecology paradigm for unifying organismal movement research. Proceedings of the National Academy of Sciences of the United States of America 105:19052–9.

Neuweiler, G., W. Metzner, U. Heilmann, R. Rübsamen, M. Eckrich, and H. H. Costa. 1987. Foraging behaviour and echolocation in the rufous horseshoe bat (Rhinolophus rouxi) of Sri Lanka. Behavioral Ecology and Sociobiology 20:53–67.

Nevitt, G. A. 2008. Sensory ecology on the high seas: the odor world of the procellariiform seabirds. Journal of Experimental Biology 211:1706–1713.

O'Farrell, M. J., B. W. Miller, and W. L. Gannon. 1999. Qualitative Identification of Free-Flying Bats Using the Anabat Detector. Journal of Mammalogy 80:11–23.

O'Mara, T., M. Wikelski, and D. K. N. Dechmann. 2014. 50 years of bat tracking: Device attachment and future directions. Methods in Ecology and Evolution 5:311–319.

Obrist, M. K. 1995. Flexible bat echolocation: the influence of individual, habitat and conspecifics on sonar signal design. Behavioral Ecology and Sociobiology 36:207–219.

Oppel, S., A. Meirinho, I. Ramírez, B. Gardner, A. F. O'Connell, P. I. Miller, and M. Louzao. 2012. Comparison of five modelling techniques to predict the spatial distribution and abundance of seabirds. Biological Conservation 156:94–104.

Otálora-Ardila, A., L. G. Herrera M., J. J. Flores-Martínez, and C. C. Voigt. 2013. Marine and terrestrial food sources in the diet of the fish-eating myotis (Myotis vivesi). Journal of Mammalogy 94:1102–1110.

Paiva, V. H., P. Geraldes, I. Ramírez, S. Garthe, and J. A. Ramos. 2010. How area restricted search of a pelagic seabird changes while performing a dual foraging strategy. Oikos 119:1423–1434.

Paiva, V. H., P. Geraldes, I. Ramírez, A. Meirinho, S. Garthe, and J. A. Ramos. 2009. Foraging plasticity in a pelagic seabird species along a marine productivity gradient. Marine Ecology Progress Series 398:259–274.

Patterson, T. A., L. Thomas, C. Wilcox, O. Ovaskainen, and J. Matthiopoulos. 2008. State-space models of individual animal movement. Trends in Ecology and Evolution 23:87–94.

De Paz, O. 1986. Age estimation and postnatal growth of the Greater Mouse bat Myotis myotis (Borkhausen, 1797) in Guadalajara, Spain. Mammalia 50:243–252.

Peery, M. Z., S. H. Newman, C. D. Storlazzi, and S. R. Beissinger. 2009. Meeting reproductive demands in a dynamic upwelling system: Foraging strategies of a pursuit-diving seabird, the Marbled Murrelet. The Condor 111:120–134.

Péron, C., K. Delord, R. A. Phillips, Y. Charbonnier, C. Marteau, M. Louzao, and H. Weimerskirch. 2010. Seasonal variation in oceanographic habitat and behaviour of white-chinned petrels Procellaria aequinoctialis from Kerguelen Island. Marine Ecology Progress Series 416:267–284.

Pinaud, D. 2008. Quantifying search effort of moving animals at several spatial scales using first-passage time analysis: Effect of the structure of environment and tracking systems. Journal of Applied Ecology 45:91–99.

Postlethwaite, C. M., P. Brown, and T. E. Dennis. 2013. A new multi-scale measure

for analysing animal movement data. Journal of Theoretical Biology 317:175–185.

Powers, L. V., S. C. Kandarian, and T. H. Kunz. 1991. Ontogeny of flight in the little brown bat, Myotis lucifugus: behavior, morphology, and muscle histochemistry. Journal of Comparative Physiology A 168:675–685.

Prat, Y., L. Azoulay, R. Dor, and Y. Yovel. 2017. Crowd vocal learning induces vocal dialects in bats: Playback of conspecifics shapes fundamental frequency usage by pups. PLoS Biology 15:e2002556.

Prat, Y., M. Taub, and Y. Yovel. 2015. Vocal learning in a social mammal: Demonstrated by isolation and playback experiments in bats. Science Advances 1:e1500019.

Rainho, A., and J. M. Palmeirim. 2011. The importance of distance to resources in the spatial modelling of bat foraging habitat. PLoS ONE 6:e19227.

Ratcliffe, J. M., C. P. H. Elemans, L. Jakobsen, and A. Surlykke. 2013. How the bat got its buzz. Biology Letters 9:20121031.

Ripley, B., B. Venables, D. M. Bates, K. Hornik, A. Gebhardt, and D. Firth. 2019. Package 'MASS' (Version 7.3-51.4). Cran-R Project.

Ripperger, S., L. Günther, H. Wieser, N. Duda, M. Hierold, B. Cassens, R. Kapitza, A. Koelpin, and F. Mayer. 2019. Proximity sensors on common noctule bats reveal evidence that mothers guide juveniles to roosts but not food. Biology Letters 15:20180884.

Robinson, C. J., J. Gómez-Gutiérrez, U. Markaida, and W. F. Gilly. 2016. Prolonged decline of jumbo squid (Dosidicus gigas) landings in the Gulf of California is

associated with chronically low wind stress and decreased chlorophyll a after El Niño 2009-2010. Fisheries Research 173:128–138.

Robinson, P. W., D. P. Costa, D. E. Crocker, J. P. Gallo-Reynoso, C. D. Champagne, M. A. Fowler, C. Goetsch, K. T. Goetz, J. L. Hassrick, L. A. Hückstädt, C. E. Kuhn, J. L. Maresh, S. M. Maxwell, B. I. McDonald, S. H. Peterson, S. E. Simmons, N. M. Teutschel, S. Villegas-Amtmann, and K. Yoda. 2012. Foraging behavior and success of a mesopelagic predator in the northeast Pacific Ocean: insights from a data-rich species, the northern elephant seal. PloS one 7:e36728.

Rodríguez-Muñoz, R., A. Bretman, J. Slate, C. A. Walling, and T. Tregenza. 2010. Natural and sexual selection in a wild insect population. Science 328:1269–1272.

Rubio-Rodríguez, U., H. Villalobos, and M. O. Nevárez-Martínez. 2018. Acoustic observations of the vertical distribution and latitudinal range of small pelagic fish schools in the Midriff Islands Region, Gulf of California, Mexico. Latin American Journal of Aquatic Research 46:989–1000.

Russell, R. W., N. M. Harrison, and G. L. Hunt. 1999. Foraging at a front: Hydrography, zooplankton, and avian planktivory in the northern Bering Sea. Marine Ecology Progress Series 182:77–93.

Russell, R. W., G. L. Hunt, K. O. Coyle, and R. T. Cooney. 1992. Foraging in a fractal environment: Spatial patterns in a marine predator-prey system. Landscape Ecology 7:195–209.

Rutz, C., L. A. Bluff, A. A. S. Weir, and A. Kacelnik. 2007. Video cameras on wild birds. Science 318:765.

Rutz, C., and G. C. Hays. 2009. New frontiers in biologging science. Biology Letters 5:289–292.

Rutz, C., and J. Troscianko. 2013. Programmable, miniature video-loggers for deployment on wild birds and other wildlife. Methods in Ecology and Evolution 4:114–122.

Sánchez-Velasco, L., E. Beier, V. M. Godínez, E. D. Barton, E. Santamaría-del-Angel, S. P. A. Jiménez-Rosemberg, and S. G. Marinone. 2017. Hydrographic and fish larvae distribution during the "Godzilla El Niño 2015–2016" in the northern end of the shallow oxygen minimum zone of the Eastern Tropical Pacific Ocean. Journal of Geophysical Research: Oceans 122:2156–2170.

Sapir, N., N. Horvitz, D. K. N. Dechmann, J. Fahr, and M. Wikelski. 2014. Commuting fruit bats beneficially modulate their flight in relation to wind. Proceedings of the Royal Society B: Biological Sciences 281:20140018.

Scales, K. L., P. I. Miller, C. B. Embling, S. N. Ingram, E. Pirotta, and S. C. Votier. 2014. Mesoscale fronts as foraging habitats: Composite front mapping reveals oceanographic drivers of habitat use for a pelagic seabird. Journal of the Royal Society Interface 11:20140679.

Schaefer, J. A., and F. Messier. 1995. Habitat selection as a hierarchy: the spatial scales of winter foraging by muskoxen. Ecography 18:333–344.

Scherrer, J. A., and G. S. Wilkinson. 1993. Evening bat isolation calls provide evidence for heritable signatures. Animal Behaviour 46:847–860.

Schnitzler, H. U., E. K. V. Kalko, I. Kaipf, and A. D. Grinnell. 1994. Fishing and echolocation behavior of the greater bulldog bat, Noctilio leporinus, in the field.

Behavioral Ecology and Sociobiology 35:327–345.

Schnitzler, H. U., C. F. Moss, and A. Denzinger. 2003. From spatial orientation to food acquisition in echolocating bats. Trends in Ecology and Evolution 18:386–394.

Schoeman, M. C., and D. S. Jacobs. 2008. The relative influence of competition and prey defenses on the phenotypic structure of insectivorous bat ensembles in Southern Africa. PLoS ONE 3:e3715.

Smotherman, M., K. Bohn, K. Davis, K. Rogers, and C. P. Schwartz. 2016a. Daily and seasonal patterns of singing by the Mexican free-tailed bat, Tadarida brasiliensis. Pages 197–209 Sociality in Bats. Springer International Publishing.

Smotherman, M., M. Knörnschild, G. Smarsh, and K. Bohn. 2016b. The origins and diversity of bat songs. Journal of Comparative Physiology A: Neuroethology, Sensory, Neural, and Behavioral Physiology 202:535–554.

Springall, B. T., H. Li, and M. C. Kalcounis-Rueppell. 2019. The in-flight social calls of insectivorous bats: Species specific behaviors and contexts of social call production. Frontiers in Ecology and Evolution 7:1–16.

Stidsholt, L., M. Johnson, K. Beedholm, L. Jakobsen, K. Kugler, S. Brinkløv, A. Salles, C. F. Moss, and P. T. Madsen. 2019. A 2.6-g sound and movement tag for studying the acoustic scene and kinematics of echolocating bats. Methods in Ecology and Evolution 10:48–58.

Stockwell, D. R. B., and A. T. Peterson. 2002. Effects of sample size on accuracy of species distribution models. Ecological Modelling 148:1–13.

Stowell, D., E. Benetos, and L. F. Gill. 2017. On-bird sound recordings: Automatic

acoustic recognition of activities and contexts. IEEE/ACM Transactions on Audio Speech and Language Processing 25:1193–1206.

Strandburg-Peshkin, A., D. R. Farine, I. D. Couzin, and M. C. Crofoot. 2015. Shared decision-making drives collective movement in wild baboons. Science 348:1358–1361.

Sumpter, D. T. 2010. Collective animal behavior. Page Collective Animal Behavior. Princeton University Press, Princeton, NJ.

Suraci, J. P., L. G. Frank, A. Oriol-Cotterill, S. Ekwanga, T. M. Williams, and C. C. Wilmers. 2019. Behavior-specific habitat selection by African lions may promote their persistence in a human-dominated landscape. Ecology 100:e02644.

Suthers, R. A. 2006. Comparative echolocation by fishing bats. Journal of Mammalogy 48:79.

Tershy, B. R., D. Breese, and S. Alvarez-Borrego. 1991. Increase in cetacean and seabird numbers in the Canal de Ballenas during an El Nino-Southern Oscillation event. Marine Ecology Progress Series 79:299–302.

Tremblay, Y., A. Thiebault, R. Mullers, and P. Pistorius. 2014. Bird-borne video-cameras show that seabird movement patterns relate to previously unrevealed proximate environment, not prey. PLoS ONE 9:e88424.

Tsang, S. M., S. M. Tsang, A. L. Cirranello, N. B. Simmons, and P. J. J. Bates. 2016. The roles of taxonomy and systematics in bat conservation. Pages 503–538 *in* C. C. Voigt and T. Kingston, editors. Bats in the Anthropocene: Conservation of Bats in a Changing World. Springer.

Tuttle, M. D., and D. Stevenson. 1982. Growth and survival of bats. Pages 105–150 *in* T. H. Kunz, editor. Ecology of bats. Springer, Boston, MA.

Velarde, E., E. Ezcurra, M. A. Cisneros-Mata, and M. F. Lavín. 2004. Seabird ecology, El Niño anomalies, and prediction of sardine fisheries in the Gulf of California. Ecological Applications 14:607–615.

Voigt-Heucke, S. L., M. Taborsky, and D. K. N. Dechmann. 2010. A dual function of echolocation: Bats use echolocation calls to identify familiar and unfamiliar individuals. Animal Behaviour 80:59–67.

Ward, P., and A. Zahavi. 1973. The importance of certain assemblages of birds as "information-centres" for food-finding. Ibis 115:517–534.

Warton, D. I., and L. C. Shepherd. 2010. Poisson point process models solve the "pseudo-absence problem" for presence-only data in ecology. Annals of Applied Statistics.

Watanuki, Y., F. Daunt, A. Takahashi, M. Newell, S. Wanless, K. Sato, and N. Miyazaki. 2008. Microhabitat use and prey capture of a bottom-feeding top predator, the European shag, shown by camera loggers. Marine Ecology Progress Series 356:283–293.

Webb, N. F., M. Hebblewhite, and E. H. Merrill. 2008. Statistical methods for identifying wolf kill sites using global positioning system locations. Journal of Wildlife Management 72:798–807.

De Weerd, N., F. Van Langevelde, H. Van Oeveren, B. A. Nolet, A. Kölzsch, H. H. T. Prins, and W. F. De Boer. 2015. Deriving animal behaviour from high-frequency GPS: Tracking cows in open and forested habitat. PLoS ONE

10:e0129030.

Weimerskirch, H. 2007. Are seabirds foraging for unpredictable resources? Deep-Sea Research Part II: Topical Studies in Oceanography 54:211–223.

Weimerskirch, H., A. Gault, and Y. Cherel. 2005. Prey distribution and patchiness: Factors in foraging success and efficiency of Wandering Albatrosses. Ecology 86:2611–2622.

Weimerskirch, Pinaud, Frédéric Pawlowski, and Bost. 2017. Does prey capture induce area-restricted search? A fine-scale study using GPS in a marine predator, the Wandering Albatross. The American Naturalist 170:734.

Whitaker, J. S., T. M. Hamill, X. Wei, Y. Song, and Z. Toth. 2008. Ensemble data assimilation with the NCEP global forecast system. Monthly Weather Review 136:463–482.

Wiens, J. A. 1989. Spatial Scaling in Ecology. Functional Ecology 3:385.

Wiley, R. H., and D. G. Richards. 1978. Physical constraints on acoustic communication in the atmosphere: Implications for the evolution of animal vocalizations. Behavioral Ecology and Sociobiology 3:69–94.

Wilkinson, G. S. 1992a. Information transfer at evening bat colonies. Animal Behaviour 44:501–518.

Wilkinson, G. S. 1992b. Communal nursing in the evening bat, Nycticeius humeralis. Behavioral Ecology and Sociobiology 31:225–235.

Wilkinson, G. S. 2003. Social and vocal complexity in bats. Pages 322–341 *in* D. B. M. DeWaal and P. L. Tyack, editors. Animal Social Complexity: intelligence, culture, and individualized societies. Harvard University Press, Cambridge, MA.

Wilkinson, G. S., and J. W. Boughman. 1998. Social calls coordinate foraging in greater spear-nosed bats. Animal Behaviour 55:337–350.

Wilkinson, G. S., and J. W. Boughman. 1999. Social influences on foraging in bats. Pages 188–204 *in* H. O. Box and K. R. Gibson, editors. Mammalian social learing: Comparative and ecological perspectives. Cambridge University Press, Cambridge, MA.

Wilson, K., C. Littnan, P. Halpin, and A. Read. 2017. Integrating multiple technologies to understand the foraging behaviour of Hawaiian monk seals. Royal Society Open Science 4:160703.

Wood, S. N. 2011. Fast stable restricted maximum likelihood and marginal likelihood estimation of semiparametric generalized linear models. Journal of the Royal Statistical Society. Series B: Statistical Methodology 73:3–36.

Wright, G. S., C. Chiu, W. Xian, G. S. Wilkinson, and C. F. Moss. 2014. Social calls predict foraging success in big brown bats. Current Biology 24:885–889.

Yovel, Y., and S. Greif. 2018. Bats – Using sound to reveal cognition. Pages 31–59 *in* N. Bueno-Guerra and F. Amici, editors. Field and laboratory methods in animal cognition: A comparative guide. Cambridge University Press, Cambridge, MA.

Yovel, Y., M. L. Melcon, M. O. Franz, A. Denzinger, and H. U. Schnitzler. 2009. The voice of bats: How greater mouse-eared bats recognize individuals based on their echolocation calls. PLoS Computational Biology 5:e1000400.

Zar, J. H. 1976. Two-sample and multisample testing of circular data. Behavior Research Methods & Instrumentation 8:329–330.

Zuur, A. F., E. N. Ieno, and C. S. Elphick. 2010. A protocol for data exploration to

avoid common statistical problems. Methods in Ecology and Evolution 1:3–14.